Mechanism of GRASP65 Mediated Organelle Tethering and its Regulation

A thesis presented

by

Debrup Sengupta

to

Department of Biological Sciences

Carnegie Mellon University

4400 Fifth Avenue

Pittsburgh PA15213

in partial fulfillment of the requirements for the degree of Ph.D. in Biological Sciences

November 22, 2010

Thesis Advisor: Dr. Adam D. Linstedt

Abstract

In higher eukaryotes, the Golgi apparatus is organized into a single copy, ribbon-like membrane network. The ribbon-like structure is established by lateral homotypic interactions between analogous cisternae in adjacent ministacks. Lateral linking may involve homotypic tethering followed by membrane fusion. Indeed, ribbon formation is blocked by depletion of the membrane tethering proteins GRASP65 and GRASP55, which are localized to *cis* and *medial* Golgi cisternae, respectively. In this thesis we present a structure-function analysis of GRASP65 in order to further understand its mechanism of action and regulation in Golgi ribbon formation.

Because GRASP65 homo-oligomerizes *in vitro* we hypothesized that its self-interaction links cis cisternae prior to fusion. To test this model and determine the mechanism of GRASP65 self-interaction we developed a cell-based organelle-tethering assay. GRASP65 was targeted to the mitochondrial outer membrane allowing a quantitative visual assessment of induced mitochondrial tethering. We observed that GRASP65 interacts in *trans* to tether organellar membranes, and the tethering involves the binding groove of the first of two PDZ-like domains present at its N-terminus. Tethering also required membrane anchoring of the PDZ domain suggesting a mechanism that orientates the PDZ binding groove to favor interactions in *trans*. These results identify a homotypic PDZ interaction mediating organelle tethering in living cells.

GRASP65 self-interaction is regulated by mitotic phosphorylation but the mechanism is unclear. In fact, the known GRASP65 phosphorylation sites are outside the self-interacting N-terminal domain, and their mutation to mimic phosphorylation failed to block tethering. We identified a site phosphorylated by Polo-like kinase 1 (PLK1) in the GRASP65 N-terminal domain for which mutation to aspartic acid blocked tethering and alanine substitution prevented mitotic Golgi unlinking. Further, using interaction assays, we discovered an internal PDZ ligand adjacent to the PLK phosphorylation site that was required for tethering. These results reveal the mechanism of phospho-inhibition as direct inhibition by PLK1 of the PDZ ligand underlying the GRASP65 self-interaction.

Table of Contents

List of figures

ACKNOWLEDGEMENTS

I would like to extend my gratitude and sincere thanks to my advisor Dr. Adam D. Linstedt for his constant encouragement, support and great ideas. His faith in my abilities as a scientist has given me much needed confidence over the years. I would also like to thank him for keeping me focused.

I would like to thank my committee members, Drs. Tina Lee and John Woolford, for their insight and advice through out my graduate career. I thank Dr. Jeffrey Brodsky for being my external committee member for my thesis defense.

I would like to thank past and present member of my lab, Yusong Guo, Tim Feinstein, Steven Truschel, Collin Bachert, Simta Yadav, Somshuvra Mukhodhyay**,** Timothy Jarvela, Cassandra Priddy and Ritika Tewari for their support and great work environment. I would also like to thank members of the Lee lab, Jeanne Morin-Leisk, Kaitlyn Dykstra, Idil Ulengin and Simran Saini for sharing reagents and lab resources.

A word of thanks to Dr.Manojkumar Puthenveedu, for his advice and valuable scientific discussions.

Most importantly, I would like to thank my parents and friends for their support.

CHAPTER 1: Control of organelle size: the Golgi apparatus

In this chapter, we review functional and structural features of the mammalian Golgi, and discuss how these features correspond to changes in Golgi size. The chapter concludes with a brief description relating this review, which is submitted for publication, to the major body of the thesis that focuses on membrane tethering in Golgi ribbon formation.

The primary function of the mammalian Golgi apparatus is to process newly synthesized proteins and lipids moving through the secretory pathway. In addition, Golgi membranes are specialized for protein sorting and signaling functions and for Golgi-to-surface transport that supports the growth and composition of the plasma membrane. Although little is known, Golgi size is likely regulated to meet the demands of each of these functions. Because the organelle has distinct structural features comprising specialized subdomains, there is the potential for each to be differentially altered depending on physiological demand. Nevertheless, the primary changes observed to date are overall size increases by elongation of the Golgi ribbon-like network. This occurs during Golgi doubling for mitosis and in cells undergoing differentiation where secretory demand is upregulated. Signaling pathways regulating transport factors that impact the net balance of membrane influx and efflux at the Golgi have been described but little work directly addresses control of Golgi size. One hypothesis states that steady state Golgi size is set by the abundance of secretory cargo and Golgi components that, through interactions with vesicle coat complexes, drive vesicle coat formation to alter the Golgi influx and efflux pathways in which they traffic. While this hypothesis may adequately account for Golgi growth, much remains to be learned about the specialized changes in Golgi architecture that occur in diverse cell types including, but certainly not limited to, secretory, muscle and neuronal cells.

Functions of the Golgi apparatus

The Golgi apparatus is a multifunctional organelle. Its primary purpose is the processing of newly synthesized proteins and lipids moving through the secretory pathway. The major categories of processing taking place in the Golgi are glycosylation, sulfation and proteolytic processing. Modifications acquired in the Golgi apparatus play roles in protein localization, stability, activation, and specificity of interactions. A secondary function of the organelle is sorting. There are distinct exit routes from the Golgi for newly processed proteins and lipids depending on whether they are destined for constitutive or regulated secretion or trafficking towards lysosomes (Keller & Simons 1997). In polarized cells, additional exit routes target specialized membranes (Folsch et al 2009, Keller & Simons 1997, Weiss & Rodriguez-Boulan 2009). Another important aspect of sorting in the Golgi concerns retrieval of proteins to the ER to ensure their proper localization (Lee et al 2004). Golgi components themselves, such as the processing enzymes, are also subject to sorting to ensure their localization (Tu & Benfield 2010). A less frequently cited function of the Golgi apparatus that is particularly pertinent to a review of its size control is its role in supporting the plasma membrane (Gauthier et al 2009). Trafficking of lipid and protein from the Golgi to the plasma membrane and back is a significant factor in controlling both the surface area and the composition of the plasma membrane, especially in polarized cells. In growing cells, continuous exchange must be properly balanced to allow surface area doubling and the exchange must also be regulated to support dynamic changes in the plasma membrane (Novick & Schekman 1979). The Golgi apparatus is also involved in ion homeostasis (Missiaen et al 2007). Ions are actively pumped into the lumen, presumably for sequestration, and released to either the cytoplasm by channels for diverse purposes or to the extracellular space by secretion to reduce cellular levels. A final function is that membranes of the Golgi apparatus serve as a platform for various signaling pathways (Saini et al 2009). This makes sense given the general importance of membrane surfaces in the formation of signaling complexes and the central location of Golgi membranes in mammalian cells. Although several active signaling molecules transit or are recruited to the Golgi, the functional consequence of this localization still remains to be determined.

Golgi morphology in relation to size change

The Golgi apparatus is well known for its stacked morphology, which is evident in most eukaryotic cells. The stacks are comprised of flattened cisternal membranes. Although the number of cisternae per stack varies they are thought to comprise three functionally distinct compartments. These are termed *cis*, *medial* and *trans* Golgi compartments with *cis*-localized enzymes acting on cargo first followed by *medial* and then *trans* (Mellman & Simons 1992). The *trans* Golgi network represents a fourth compartment specialized for packaging cargo into carrier membranes as it leaves the Golgi apparatus (Griffiths et al 1985). In mammalian cells, the Golgi is present as a membrane network of stacked membranes termed the Golgi ribbon. At intervals along the ribbon network there are zones of fenestration where adjacent compact stacks appear to connect with each other through dynamic tubular contacts (Ladinsky et al 1999, Rambourg & Clermont 1990). Thus, the ribbon can be viewed as a collection of ministacks with lateral connections between adjacent analogous cisternae (i.e. cis with cis etc.) in the fenestrated zones. The integrity of these connections is dependent on microtubule-dependent inward movement of the membranes and this movement positions the ribbon near the microtubule organizing center, which is usually centrosome-based (Corthesy-Theulaz et al 1992, Thyberg & Moskalewski 1999). These morphological features of the Golgi allow for different modes of size change including changes to the volume of individual cisternae, the number of cisternae per stack or the number of ministacks in the ribbon (Figure 1-1).

Cisternal surface area and shape

Golgi cisternae are the smallest functional unit of the Golgi and their morphology strongly contributes to the overall morphology of the organelle. Critical features in cisternal size are surface area and shape.

The surface area of Golgi cisternae depends on the ratio of membrane input and output to the compartment along various trafficking routes. One example of this is a recent study showing that inhibition of Golgi-to-ER transport, a Golgi efflux pathway, increases Golgi size (Burman et al 2010). The total surface areas of *cis*, *medial* and *trans* cisternae are very similar (Ladinsky et al 1999) suggesting that net flux is uniform across the Golgi stack at steady state. In contrast, altered trafficking can dramatically and differentially change surface area of Golgi cisternae.

Pancreatic β-cells respond to glucose stimulation by altered trafficking and show an increase Golgi

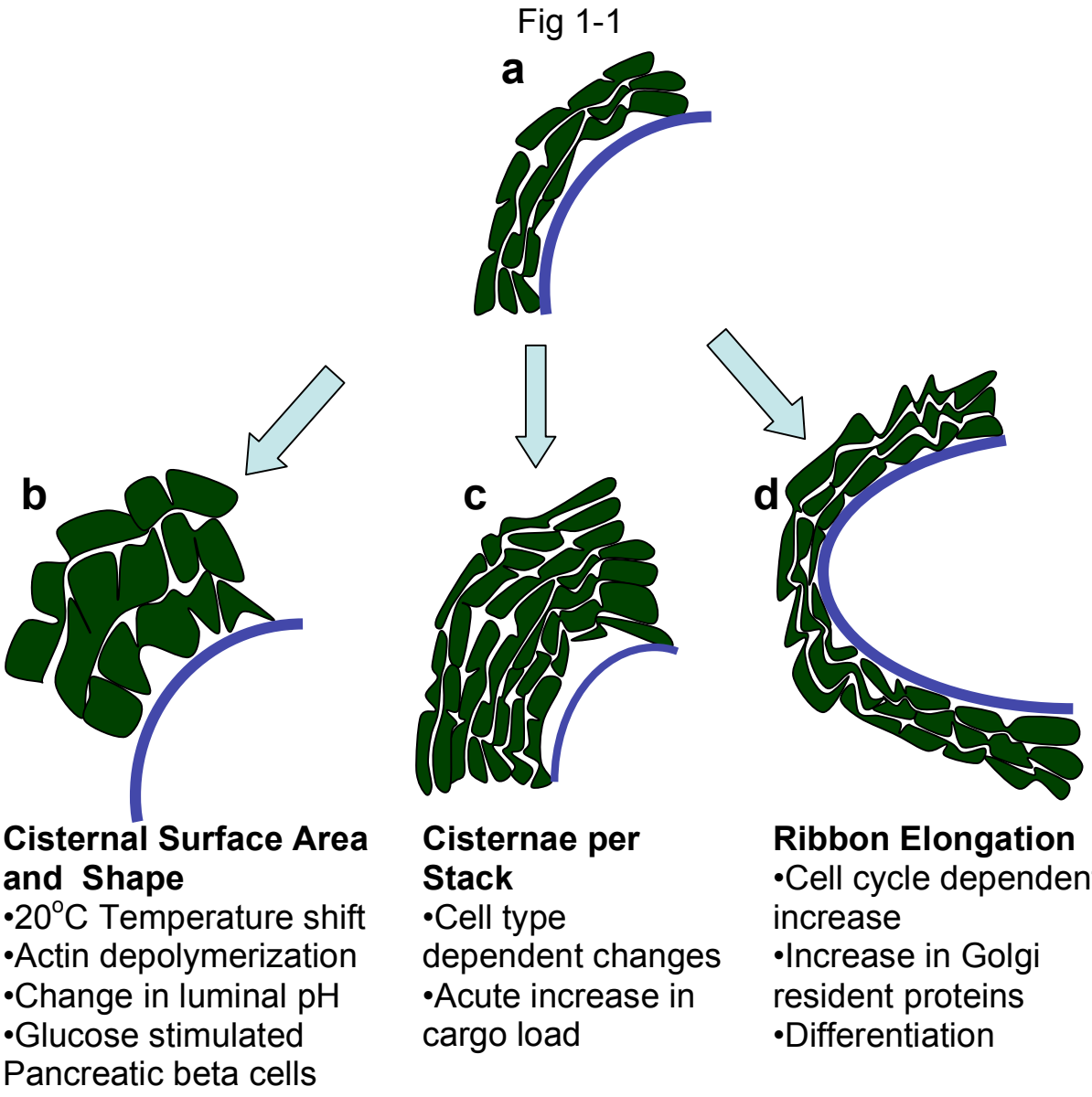

Figure 1-1 Changes in Golgi size in relation to Golgi morphology. (*a*) Schematic eukaryotic Golgi comprised of laterally linked stacked cisternae. (*b)* Cisternal volume can change in response to cellular stress and actin depolymerization. Cisternae surface area changes in response to altered membrane flux stimulated by cargo or temperature shift. (*c*) The number of cisternae per stack varies between cell types and can increase in response to a cargo pulse. (*d*) Elongation of the Golgi ribbon occurs by growth of additional ministacks in response to increased synthesis of Golgi constituents during cell growth and differentiation.

cisternae surface area (Noske et al 2008). A well-known example of differential change in surface area involves the *trans* Golgi network. Although this is not a cisternal compartment per se, these Golgi membranes selectively expand upon a trafficking block induced by 20°C incubation or when there is an increased cargo load in the Golgi (Clermont et al 1995, Griffiths et al 1989).

Cisternal shape refers largely to the degree that the membranes are flattened. Typical Golgi cisternae are flattened resulting in a high surface to volume ratio increasing the effective concentration of Golgi enzymes (Mellman & Simons 1992). Interestingly, medial cisternae are more compact than *cis* and *trans* cisternae even though the surface areas are similar (Ladinsky et al 1999), implying a greater degree of concentration in the center of Golgi stacks. Dilation of cisternae is observed under various pathological conditions including cancer and neutralization of the normally slightly acidic lumenal pH (Kellokumpu et al 2002, Maeda & Kinoshita 2008).

At least three mechanisms can be identified that conceivably contribute to cisternal flattening. The first is interactions between the luminal domains of enzymes or other components residing in Golgi cisternae. Binding in a *trans* configuration, i.e. one side of a cisternae binding to the other side, will hold the membranes in close contact thereby flattening the shape. Although we do not know if binding occurs in *trans* or whether it is required for cisternal flattening, Golgi-localized proteins do form hetero- and homo-oligomeric complexes within the cisternal lumen. One of the first identified interactions was between medial Golgi enzymes N-acetylglucosaminyltransferase I and mannosidase II (Hassinen et al 2010, Nilsson et al 1994) and others have since been observed (Hassinen et al, 2010; reviewed in (de Graffenried & Bertozzi 2004)).

A second mechanism depends on actin assembly at the Golgi. Actin depolymerization induces cisternal swelling (Egea et al 2006). Further, the *trans* Golgi localized protein GOLPH3/Vps74 links the Golgi membrane to an actin-based motor by simultaneously binding phosphoinositide-4-phosphate in the membrane and the unconventional myosin MYO18A (Dippold et al 2009). GOLPH3 depletion dilates Golgi cisternae suggesting that, via actin, the motor exerts pulling forces on Golgi membranes that contribute to their flattened morphology. Nevertheless, it is important to point out that the elongated morphology of Golgi cisternae persists when they are isolated from cells and free of such forces.

The third possible mechanism is induced membrane curvature. The edges of flattened Golgi cisternae are called the rims and these exhibit high membrane curvature. Energy imparted to the membranes to sustain this curvature could be, at least in part, from local changes in lipid composition or interaction with curvature-inducing proteins (Graham & Kozlov). Lipid modifying enzymes can induce membrane bending by generating lipid asymmetry. One class of proteins that generates bilayer asymmetry is the family of aminophospholipid translocases, which translocate specific lipid molecules across the lipid bilayer. In yeast, two of these enzymes, Drs2p and Neo1p, are Golgi-localized (Chen et al 1999, Hua et al 2002, Wicky et al 2004) and the trans Golgi network in *drs*2Δ yeast strains is notable for its lack of curvature (Chen et al 1999). Inactivation of Neo1p also causes accumulation of enlarged membranes (Wicky et al 2004). Although mammalian homologues of these proteins are known, their role in regulating cisternal morphology has not been tested (Lenoir et al 2007). The multifunctional small GTPase Arf1 could also contribute because it is Golgi-localized and it can generate membrane curvature by insertion of its N-terminal amphipathic helix into the outer leaflet of the lipid bilayer (Beck et al 2009, Lee et al 2005, Lundmark et al 2008). Membrane association of Arf1 depends on activation by Arf1GEF. Interestingly, Arf1GEF also activates the translocase activity of Drs2p (Natarajan et al 2009) suggesting dual contribution of Arf1-GEF to membrane deformation. The importance of dual contribution could stem from neither Arf1 nor Drs2p alone being sufficient. At least in the case of Arf1, it does not overcome the curvature defects of the *drs*2Δ yeast strain despite its normal activation.

Number of Cisternae per Stack

In addition to cisternal surface area and shape, the number of cisternae per stack contributes to Golgi size and is under regulation. The number of cisternae per stack also concerns the *cis*, *medial* and *trans* polarity of Golgi compartments. Typically a given cell type maintains a roughly constant number but distinct cell types can differ from one another. An average mammalian Golgi apparatus contains 5-8 cisternae per stack. The Golgi in the salivary Brunner's gland exhibits 9-11 cisternae per stack while epithelial cells of seminal vesicles contain Golgi formed by 2-3 cisternae per stack (Rambourg & Clement, 1997). Because *cis*, *medial* and *trans* Golgi enzymes overlap somewhat in their distribution across Golgi stacks it seems reasonable to conclude that a greater number of cisternae per stack ensures better compartmentalization within the Golgi. It is also arguable that if cargo molecules must transit a larger stack, processing will

achieve greater completion. Thus, cells carrying out greater extents of, or complexity in, Golgi processing may utilize greater numbers of cisternae. There is only correlative evidence to support this idea. Brunner's gland cells secrete copious mucous, which contains heavily O-glycosylated mucin as its major component (Van Halbeek et al 1983). A dramatic example of enlarged Golgi through increased cisternae per stack occurs in species of green algae that have more than 20 cisternae per stack (Becker & Melkonian 1996). These cells secrete large complex glycosylated scale proteins.

The mechanisms regulating the number of cisternae per stack are not known. When other parameters are constant, an increased number of cisternae imply more Golgi membrane and therefore a change in the input/output ratio at the Golgi. Indeed, a synchronized cargo pulse that increases membrane input to the Golgi transiently increases the number of cisternae per stack (Trucco et al 2004). Nevertheless, the increase in cisternal number is slight with more dramatic changes occurring in cisternal surface area and volume.

Another possibility involves regulation of Golgi stacking factors mediating inter-cisternal adhesion (Derganc et al 2006). Electron dense structures that appear to hold Golgi stacks together have been observed in electron micrographs of intact and isolated Golgi membranes (Cluett & Brown 1992, Mollenhauer 1965). In principle, regulation of the level, localization, or number of such factors could control the number of cisternae per stack. Unfortunately, the identity of Golgi stacking factors remains controversial.

Reassembly of mammalian Golgi membranes *in vitro* into a stacked structure depends on two related peripheral proteins, GRASP65 and GRASP55 (Barr et al 1997, Shorter et al 1999). These proteins are localized to cis and medial Golgi cisternae, respectively, and each self-interacts to bridge adjacent membranes (Wang et al 2005b, Xiang & Wang 2010). Although, they likely contribute to Golgi stacking it is unclear whether they are essential. Depletion of either alone fails to block Golgi stack formation, yet, as discussed below, it disrupts Golgi ribbon formation (Feinstein & Linstedt 2008, Puthenveedu et al 2006, Wang et al 2005b, Xiang & Wang 2010). In one report, simultaneous knockdown of both GRASPs perturbs both stacking and ribbon formation (Xiang & Wang 2010) but simpler eukaryotes express only one GRASP and its absence is not associated with defects in Golgi stacking (Kondylis et al 2005, Levi et al, 2010). Organisms that express a single GRASP do not have Golgi ribbons consistent with the idea that

expression of the dual isoforms relates to this feature of Golgi organization. In *S. cerevisiae*, which have neither ribbons nor stacks, loss of the single GRASP paralog leaves Golgi structurally and functionally intact (Behnia et al 2007, Levi et al 2010). Significantly, GRASP proteins in both mammals and simpler eukaryotes mediate trafficking of specific secretory cargo indicating multifunctional roles for the proteins (D'Angelo et al 2009, Kinseth et al 2007, Nickel & Rabouille 2009).

Another way in which Golgi cisternae may be linked into a stack is through golgins, elongated coil-coil proteins that associate with Golgi membranes. Certain golgins can simultaneously interact with two types of GTPase, Arf-like and Rab. The localization of the former to the *trans* Golgi network and the latter throughout Golgi cisternae raises the possibility that golgins anchored by these GTPases bridge cisternae (Hayes et al 2009, Sinka et al 2008). Because there are multiple golgins, most serving other functions related to Golgi integrity, it will be difficult to test whether golgins specifically mediate Golgi stacking. Another issue is that several golgins mediate vesicle tethering. A key difference between vesicle tethering and stacking is that the former facilitates membrane fusion, whereas the latter is largely, if not entirely, uncoupled from fusion.

Cisternal Linking

The most clearly regulated aspect of Golgi size control in mammalian cells is ribbon length, which is determined by the number of ministacks linked into the membrane network and probably relates the number and size of ER exit sites. The homotypic membrane linkages in the fenestrated zones are likely dynamic with repeated rounds of fusion and fission. Membrane tubules extend from one cisternae (Ladinsky et al 1999) and dock and fuse with an adjacent analogous cisternae. These contacts must persist long enough to account for the observed lumenal and membrane continuity that extends across all analogous cisternae in Golgi ribbons. The continuity confers uniform distribution of Golgi enzymes within analogous cisternae in the network allowing efficient cargo processing (Puthenveedu et al 2006, Feinstein, 2008). Linkage of ministacks into a ribbon also plays a role in controlling entry into mitosis (Colanzi et al 2007, Feinstein & Linstedt 2007) and reorientation of the Golgi and centrosomes in response to scratch wounding (Bisel et al 2008).

The dynamic nature of the linking reaction suggests that newly formed ministacks will readily form contacts with the pre-existing Golgi ribbon to elongate and enlarge the Golgi apparatus. Lengthening of the ribbon is clear during differentiation of neurons and muscle cells (Horton & Ehlers 2003, Lu et al 2001). Significantly, because growth by elongating the ribbon requires neither an increase in the size of individual ministack cisternae nor an increase in the number of cisternae per stack, this mechanism should allow expansion of the Golgi without imposing a limit on transport efficiency. The number and size of ER exit sites is increased by increased cargo load (Farhan et al 2008, Guo & Linstedt 2006). Individual ER exit sites each have a closely associated Golgi ministack in nocodazole-treated mammalian cells, a condition that prevents inward Golgi membrane movement to form the Golgi ribbon (Hammond & Glick 2000). A similar arrangement is seen in cells of many simpler eukaryotes where the Golgi does not undergo pericentrosomal positioning and ribbon formation (Bevis et al 2002). Thus, cargo-induced new ER exit site formation is coupled with formation of new ministacks. In the presence of inward motility of Golgi membranes this will lead to ribbon elongation by ministack addition.

Linking adjacent ministacks to form the Golgi ribbon requires the aforementioned GRASP proteins acting as organelle tethers (Feinstein & Linstedt 2008, Puthenveedu et al 2006). GM130, a golgin binding partner for GRASP65 is also required (Marra et al 2007, Puthenveedu et al 2006). Each GRASP protein contains a conserved domain at its N-terminus comprised of two predicted PDZ domains. The PDZ domain is a wide spread protein module involved in protein-protein interactions (Fan and Zhang, 2002; Harris and Lim, 2001; Hung and Sheng, 2002). The canonical structure consists of five to six β-strands (β1-6) and 2 α-helices (α1, α2) forming a groove such that a ligand inserts between β2 and α2 completing a sheet with β2 and β3 (Doyle et al., 1996; Hung and Sheng, 2002; Im et al., 2003a; Kang et al., 2003). Mutations in the predicted binding domain alpha helices of the GRASP65 PDZ1 and PDZ2 domains block GRASP65 self-interaction and GM130 binding, respectively (Bachert & Linstedt 2010, Sengupta et al 2009). These mutations helped establish that GRASP65 is targeted to cis cisternae by binding cis-localized GM130 and that GRASP65 uses an internal ligand and the PDZ1 binding groove to form a homotypic contact that bridges Golgi membranes for ribbon formation (Bachert & Linstedt 2010, Sengupta & Linstedt, 2010, Sengupta et al 2009). A parallel reaction involving GRASP55 on medial membranes is also likely (Feinstein & Linstedt 2008). It is logical that this homotypic fusion reaction is tethered by a homotypic protein interaction. The identity of the

fusion machinery is not known but might involve homotypic pairing of syntaxin 5-based SNARE complexes (Xu et al 2002).

In addition to tethers and fusases, the dynamic nature of linking depends on at least two other activities, membrane tubulation and membrane fission. In common with the rims from which they derive, the membrane tubules that bridge cisternae in the fenestrated zones have high curvature. Golgi-associated phospholipases may contribute by catalyzing the cleavage of acyl chains from the phospho-glycerol head groups creating bilayer asymmetry (Morikawa et al 2009, Schmidt & Brown 2009). Inhibition of one of these, PLA2, blocks Golgi ribbon formation (de Figueiredo et al 1998). Fission refers to the reaction that breaks the membranous contacts between cisternae. CtBP/BARS mediates membrane fission in vitro and in vivo and is required for Golgi unlinking in late G2 phase of the cell cycle (Hidalgo Carcedo et al 2004). Also, depletion of CtBP/BARS expands Golgi tubules in interphase cells. As discussed elsewhere other functions have also been suggested for CtBP/BARS (Corda et al 2006).

Why does the Golgi change size?

Growth for mitosis

The most basic need for growth of the Golgi apparatus is for mitosis. In proliferating cells the Golgi doubles in size as cells progress M-phase of the cell cycle (Kondylis et al 2007, Shima et al 1997, Shorter & Warren 2002). As for all cellular constituents, any consistent error in doubling rate will eventually lead to either loss or overgrowth. A cycle of mitotic disassembly, equal partitioning of Golgi membranes, and reassembly in daughter cells resets the Golgi size for another round of doubling. It can be assumed that doubling of the Golgi involves doubling of all its components and that this is achieved by rates of synthesis that exceed rates of degradation with the balance yielding doubling in the time of a cell cycle (Jackowski 1994, Yokoyama et al 1997). Presumably growth of the Golgi plays an important role in sustaining an ever-increasing amount of trafficking of proteins and lipids to the cell surface and other membranes for overall cellular growth. Growth during the cell cycle appears to involve elongation of the ribbon and number of ministacks while cisternae size in the ministacks and the number of cisternae per stack remains fairly constant (Tanaka et al 1998).

Growth for increased cargo processing

Another obvious need for Golgi growth is during differentiation of cell types that have increased processing demand. Simply put, Golgi expansion allows processing of more cargo. A few specific examples are provided below where differentiation is accompanied by dramatic alterations in Golgi size. Generally, increased Golgi size occurs while Golgi components and cargo are concomitantly upregulated, presumably by signaling pathways driving differentiation. Transcriptional events can alter processing capacity in at least thee ways. Changes in enzyme abundance are the most obvious and probably the most important, but enzyme localization and the availability of nucleotide donor substrates are also subject to regulation (Buckhaults et al 1997, Comelli et al 2006, Gill et al, Li et al 2002, Ohtsubo & Marth 2006, Varki 1998). Although signaling may simultaneously alter both enzymes and cargo there are ways in which cargo may drive enzyme changes. Transient increases in cargo load transiently increase Golgi size (Aridor et al 1999, Clermont et al 1993, Rambourg et al 1993, Trucco et al 2004), and reduced cargo load decreases size (Clermont et al 1993, Rambourg et al 1993). In anything but the most acute situations, such changes likely include altered enzyme expression to control Golgi processing capacity. It is not clear how altered cargo load might feedback on transcription of Golgi enzymes (Comelli et al 2006, Li et al 2002) but one possibility is that it occurs through the unfolded protein response pathway. As cargo is increased in the ER, this pathway triggers transcription of many genes including Golgi processing enzymes (Travers et al 2000).

Growth for enhanced sorting and signaling

Because of its role in other processes, such as protein sorting and signaling, there may be special circumstances where Golgi size changes are not a simple reflection of a need for increased processing capacity. Sorting depends on creation of membrane subdomains enriched with cargo to be packaged in transport carriers (De Matteis & Luini 2008). The surface area of the Golgi, or of Golgi subcompartments such as the trans Golgi network, might be expanded to accommodate increased sorting demands (Clermont et al 1995). In the absence of such changes, sorting efficiency might be decreased. Less surface area would yield higher concentrations of Golgi residents, which could increase their contamination of exit subdomains. An additional aspect by which Golgi changes might alter sorting ability is through altered lipid composition. Particular lipids play essential roles in sorting and their upregulation might also be part of Golgi size changes occurring under certain conditions (Schuck & Simons 2004, Simons & van Meer 1988).

Both Golgi surface area and lipid composition could also be regulated to meet the demands of Golgi participation in signaling. Subunits of certain trimeric G proteins translocate to the Golgi upon stimulation (Chisari et al 2007, Saini et al 2007). Ras proteins are localized to Golgi membranes and this localization is regulated by cycle of palmitoylation and depalmitoylation (Goodwin et al 2005, Rocks et al 2005). Components of the mTOR signaling pathway are Golgi and ER-associated (Drenan et al 2004, Liu & Zheng 2007). Kinases in the Src family are also on Golgi membranes and depend on lipid modifications for this localization (Sato et al 2009). The thought that Golgi membranes provide a surface for signaling suggests that Golgi surface area may be regulated as signaling is taking place.

Mechanisms of Golgi size control

There are few studies that directly address the mechanisms of size control for the Golgi apparatus. One that does, proposes a mechanism based on the influence of cargo and, especially, Golgi resident abundance on fundamental properties of vesicle formation (Guo & Linstedt 2006). Most other studies focus on mechanisms modifying transport factors, which is relevant as such regulation impacts the membrane influx/efflux ratio at the Golgi. Control by resident abundance and modification of transport factors are not mutually exclusive. It is also likely that other mechanisms await discovery.

Cargo/resident coat-interaction controls input/output ratio

The hypothesis by Guo and Linstedt derives from considering rate-determining factors likely to impact the balance of membrane influx and efflux at the Golgi apparatus. Because of the paucity of transport vesicles under normal steady state conditions it can be argued that vesicle formation, rather than consumption, is rate limiting. Thus, regulation of vesicle formation rates in pathways driving influx and efflux at the Golgi would have the greatest impact (Figure 1-2). Exit from the ER and trans Golgi network are clearly critical paths for influx and efflux, respectively, as are input from endosomes and output by recycling paths back to the ER (Bonifacino & Rojas 2006, De Matteis & Luini 2008, Lee et al 2004). The authors focused on COPII mediated ER export because its mechanism is well understood and because, among the budding events that most contribute to membrane flux in the Golgi, ER exit is first to be impacted by transcription-induced changes in abundance of cargo and Golgi residents (Guo & Linstedt 2006). Cargo and residents

are synthesized on ER membranes and have a chance to interact with the COPII coat complex during exit (Giraudo & Maccioni 2003, Mancias & Goldberg 2008, Miller et al 2003, Mossessova et al 2003). Cargo interactions with vesicle coat components contribute to coat recruitment by increasing the avidity of the interaction between coat and membrane. Indeed, expression of a commonly used model membrane protein, VSVG, containing a di-acidic COPII interaction motif increases COPII assembly into ER exit sites. Further, expression of Golgi proteins with a di-basic motif that binds the COPII Sar1 GTPase increases both the size and number of COPII-positive ER exit sites (Aridor et al 1999, Farhan et al 2008, Guo & Linstedt 2006). These results imply that cargo and Golgi residents increase membrane input to the Golgi. Indeed, each condition increases Golgi size (Guo & Linstedt 2006).

Thus, the idea is that coat interactions by cargo and residents control the magnitude of membrane movement in a given pathway providing a link between expression level and compartment size. It is interesting to compare the effects of cargo versus resident expression. Cargo transits the Golgi en route to other destinations. In the case of VSVG, it exits the Golgi en route to the plasma membrane. This means that by the hypothesis, VSVG should drive both input to and exit from the Golgi. Indeed, Golgi size increases induced by a bolus of VSVG are transient with Golgi size decreasing back to starting values as the VSVG leaves the Golgi (Guo & Linstedt 2006). In contrast, Golgi residents remain Golgi localized even as they recycle locally among Golgi cisternae. Therefore, increases in Golgi membrane induced by a bolus of Golgi resident expression should be sustained in relation to the half-life of the expressed proteins. Expression of Golgi residents does cause stable Golgi size changes with magnitudes that correlate with expression level and these changes are blocked by inhibition of Golgi enzyme binding to the COPII Sar1 GTPase (Guo & Linstedt 2006). In sum, this mechanism has the advantage that cargo and especially residents intrinsically set compartment size. For a cell to increase Golgi size and processing capacity it need only increase expression of Golgi components. Because there is no significant reservoir of Golgi enzymes in the ER this will not work for acute changes. A further limitation of the hypothesis is that it does not provide mechanistic insight into differential regulation of Golgi morphology.

Fig 1-2

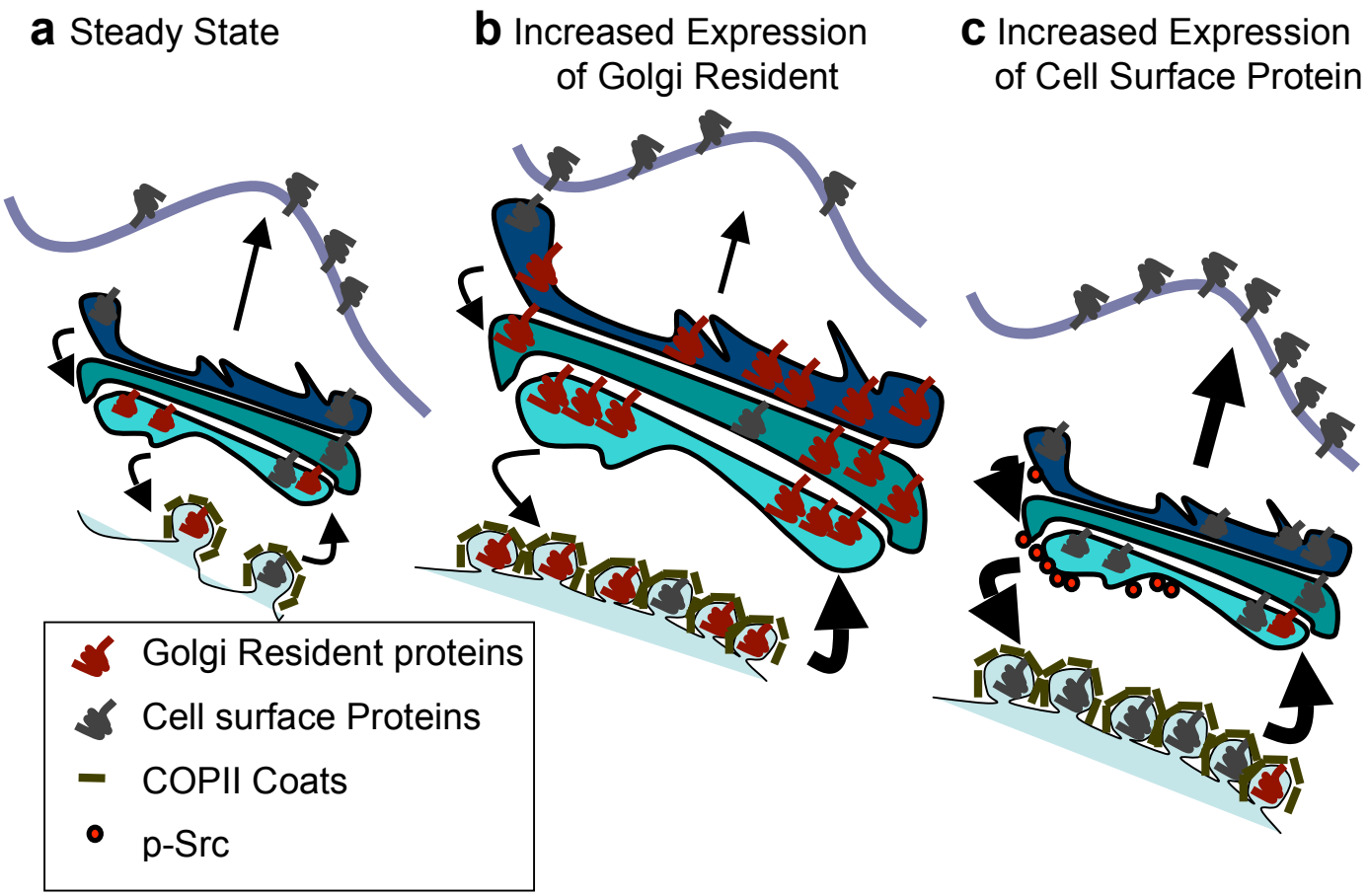

Figure 1-2 Hypothetical mechanisms of Golgi size control. (*a*) At steady state, membrane output balances membrane input. (*b*) In response to increased expression of Golgi residents, COPII-mediated membrane input exceeds rate of membrane output. During exit from the ER, Golgi residents bind Sar1 to upregulate COPII vesicle formation. (*c*) In response to increased expression of cell surface cargo, both the rate of COPII-mediated membrane input and the rate of output increase. Cargo coat interactions upregulate vesicle formation at the ER and trans Golgi network and activation of Src kinase increases Golgi to ER trafficking.

Regulation of transport factors affecting the Golgi influx/efflux ratio

Numerous studies have indicated that factors controlling vesicle formation, vesicle movement, and vesicle fusion are regulated, but few have been carried out in the context of compartment size changes. Nevertheless, modifications of transport factors that influence activity such that the membrane influx/efflux ratio is changed at the Golgi are expected to alter Golgi size (Sallese et al 2006). It should be noted, however, that such changes are unlikely to increase processing capacity in the Golgi unless they are accompanied by an increase in Golgi resident abundance or activity.

One example is the modification of Sec16 by growth factor signaling. Sec16 plays a role in ER exit site formation (Connerly et al 2005, Ivan et al 2008, Watson et al 2006). Activation of MAPK signaling increases ER exit sites and leads to phosphorylation of Sec16 and a change in its dynamic membrane association (Farhan et al 2010). One possibility suggested by Farhan and colleagues is that Sec16 is altered to enhance ER-to-Golgi traffic in order to handle increased amounts of cargo being upregulated by growth factor signaling (Pierce et al 1997).

Another example is the activation of intra-Golgi transport and Golgi-to-ER transport by the Src family of kinases. Pulvirenti and colleagues observed activation of Src during a pulse of cargo in the Golgi (Pulvirenti et al 2008). The activation is indirect as it involves escaped ER proteins using their KDEL retrieval motif to bind KDEL receptors, which then use their cytosolic domains to bind Src. Inhibition of Src family kinases arrests cargo transit in the Golgi suggesting Src activation by cargo load enhances Golgi trafficking. Interestingly, Src activation causes redistribution to the ER of both KDEL receptor (Bard et al 2003) and certain Golgi enzymes (Gill et al). This indicates that Src also controls Golgi-to-ER retrieval, which makes sense given that escaped ER residents accumulating in the Golgi activate it. Thus, Src controls an adaptive response to changes in cargo loads and sorting. Given these activities it is likely to influence Golgi size and, indeed, cells lacking Src family kinases exhibit dilated Golgi cisternae (Bard et al 2003).

A final example is control of trans Golgi network exit by protein kinase D (PKD), which may also be part of a cargo-stimulated adaptive response to increase trafficking capacity of the Golgi. Inhibition of PKD by expression of inactive versions arrests cargo exit in tubules protruding

from the trans Golgi network (Liljedahl et al 2001). Golgi association of PKD requires diacyl-glycerol (Baron & Malhotra 2002) and protein kinase Cη (Diaz Anel & Malhotra 2005). Protein kinase Cη is recruited to the Golgi by subunits of a heterotrimic G-protein (Diaz Anel & Malhotra 2005). One possibility is that secretory cargo binds a Golgi localized G-protein coupled receptor and promotes the formation of PKD-dependent transport carriers (Bard & Malhotra 2006). PKD facilitates Golgi recruitment of a lipid kinase (Hausser et al 2006, Hausser et al 2005) to generate phosphoinositol-4-phosphate, which is a known mediator of TGN exit for constitutive secretion (Audhya et al 2000, Hama et al 1999, Walch-Solimena & Novick 1999). Phosphoinositol-4-phosphate likely acts by recruiting export machinery including FAPP2 (Godi et al 2004). Thus, in an adaptive response involving PKD and phosphoinositol-4-phosphate, cargo stimulates TGN exit. Inhibiting synthesis of phosphoinositol-4-phosphate enlarges the TGN (Wang et al 2003) showing the potential of this pathway to alter Golgi size.

Specific examples of Golgi size change

Cell cycle entry and exit

Transition of a eukaryotic cell from a non-proliferative state (G0) to a proliferative state (G1) begins an increase in the levels of Golgi components allowing for doubling every cell cycle. Consistent with this, Golgi and ER proteins are expressed at higher levels in proliferating cancerous tissue and developing brain (Silvestre et al 2009). Further, phosphatidylcholine synthesis and glycosyltransferase activity are increased when cells arrested in G0 by serum starvation are induced to enter the cell cycle by growth factor addition (Guo et al 2000, Jackowski 1994, Pierce et al 1997, Pouncey et al 1991). Growth of the Golgi involves extending ribbon length, presumably by a doubling of the number of ministacks, rather than enlargement of cisternae or the number of cisternae per stack, as observed in lower eukaryotes (Kondylis et al 2007, Pelletier, 2002 #547). As mentioned above, Golgi ministacks are in communication with ER exit sites and ER exit sites increase in number and total mass during the cell cycle (Hammond & Glick 2000). Increases in Golgi components may not be uniform throughout the cell cycle as phosphatidylcholine levels double during S-phase (Jackowski 1994), glycosylceramide and sphingomyelin increase during G2-phase (Yokoyama et al 1997), and beta1-4-galactosyltransferase increases during S-phase (Pouncey et al 1991). Interestingly, however, cell cycle regulation of cell growth is not strictly controlled as cells arrested in S-phase

continue to grow (and increase their Golgi size and number of ministack) even past the doubling size (Shorter & Warren 2002). If one assumes that Golgi components continue to be made during the S-phase block, the mechanism of Golgi size change could simply reflect the intrinsic ability of Golgi components to set Golgi size (Guo & Linstedt 2006).

Mitosis

Partitioning of Golgi components during mitosis determines Golgi size in the daughter cells. Mitotic Golgi disassembly starts with unlinking of the Golgi ribbon in G2 phase of the cell cycle and by metaphase Golgi membranes are mostly dispersed vesicles with some vesicle clusters (Jesch et al 2001, Shima et al 1999). The mitotic kinases, CDK1, ERK/MEK and PLK1, phosphorylate Golgi localized structural proteins and promote mitotic Golgi fragmentation. CDK1 is active during M-phase Golgi fragmentation, where as ERK/MEK and PLK1 promotes late G2 Golgi unlinking (Colanzi and Corda, 2007; Feinstein and Linstedt, 2007; Sengupta and Linstedt, 2010). PLK family of kinases initially bind substrate and become activated through their Polo box domains. The Polo box domain binds to a phospho-serine/threonine motif that includes proline, S-[pS/pT]-P, and then the kinase can phosphorylate distant sites (Elia *et al.*, 2003; Barr *et al.*, 2004; Lowery *et al.*, 2005). The interphase Golgi is reformed after cytokinesis (Shima, et al 1997), and the cytokinetic furrow separates the membranes. Whether partitioning is active or passive is not known. A passive mechanism seems plausible given that the number and dispersed state of the Golgi elements can account for the observed accuracy of partitioning, which is close to perfect (Lucocq & Warren 1987, Jesch 2001). Asymmetric division resulting in different sized daughter cells presents an interesting test case. The stochastic model predicts that partitioning and the ensuing Golgi size solely depends on the position of the cleavage furrow, whereas an active process might yield inheritance less tightly coupled to daughter cell size.

Secretory cells

A hallmark of specialized secretory cells is the presence of the regulated secretory pathway. In these cells, membranes of the Golgi are often exaggerated in size and the trans Golgi network is prominent due its role in forming dense core secretory granules (Clermont et al 1995). The key distinguishing feature of these cell types is that cargo in the regulated pathway is stored in dense core vesicles until a stimulus triggers their fusion with the plasma membrane. It is reasonably

clear that cell types that continuously secrete large amounts of cargo, such as mucous secreting cells, have extensive processing demands at steady state that correlate with enlarged Golgi size (Forstner 1995). Further, secretory cells can increase Golgi size after a stimulus, presumably to replenish the storage pool of cargo in dense core granules (Rambourg & Clermont 1990). One example is prolactin-secreting cells. In unstimulated animals, these cells lack identifiable intact Golgi, but large Golgi stacks are clearly evident upon stimulation (Rambourg et al 1993). Another example is antigen stimulation of B-cells where Golgi size increases 3-fold as the cells differentiate and upregulate secretion of immunoglobulin (Kirk et al 2010). Golgi size is also increased after stimulation of parathyroid acinar cells and pancreatic beta cells (Clermont et al 1993, Noske et al 2008, Oliver & Hand 1983). The latter have been studied in detail using 3D EM tomography (Marsh et al 2004, Noske et al 2008). Beta cells secrete insulin in response to glucose stimulation, which causes up to a 1.5-fold increase in Golgi volume and surface area, thus, suggesting increased membrane input. The size change correlates with the extent of degranulation suggesting coupling of exocytosis and Golgi morphology (Noske et al 2008).

Such coupling may involve signaling cascades regulating transport factors and/or upregulated expression of secretory molecules and Golgi enzymes. Upregulation of secretory cargo for the purpose of replenishment is known (Jamieson & Palade 1971, Lillie & Han 1973). Proinsulin synthesis is upregulated by glucose stimulation as is the expression of proteins required for insulin processing and secretion (Martens & Pipeleers 2009, Permutt & Kipnis 1972). Part of the increase could be due to the unfolded protein response, at least in the case of chronic glucose exposure, which activated this response (Wang et al 2005a).

Muscle cells

Muscle fuse during development to form multinucleated syncytia filled with dense actinomyosin networks. Unlike the single Golgi ribbon network in most other mammalian cells, the Golgi in skeletal myotubes is present as multiple ministacks dispersed around each nucleus (Ralston 1993). Interestingly, as myoblasts differentiate into myotubes, centrosomal material also redistributes to a circumnuclear belt and ER exit sites occupy positions adjacent to the Golgi ministacks (Lu et al 2001, Ralston 1993, Tassin et al 1985). Thus, a dramatic reorganization accompanies muscle differentiation including altered Golgi position and size. Further specialization is also evident. In fast twitch muscle, Golgi membranes are mostly in the core of

the muscle fiber, whereas Golgi membranes are closer to the cell surface in slow twitch muscle (Ralston et al 2001). In heart muscle, the Golgi is also circumnuclear but it remains an intact ribbon (Kronebusch & Singer 1987). The purpose of the changes in Golgi organization are unknown but it is noteworthy that dystroglycan is a heavily O-glycosylated and defects in its glycosylation cause congenital muscular dystrophy (Barresi & Campbell 2006). The spectrin-repeat protein syne-1 may play a role in muscle Golgi organization because it binds nuclear and Golgi membranes and its inhibition disrupts Golgi morphology in myotubes (Gough et al 2003). Interestingly, cardiac myocytes express a splice variant of syne-1, GSRP-56, that causes Golgi enlargement when expressed in non-muscle cells (Kobayashi et al 2006). Whether the isoform differences relate to the differences in Golgi ribbon integrity remains to be determined.

Neuronal Cells

Neuronal morphology and function present special challenges to the secretory system. Their surface/volume ratio can be 1000 times that of non-neuronal cells due to branched dendrites and extended axons. Dendritic and axonal membranes are dynamic in composition and morphology and their changes are driven by neuronal activity (Kasai et al 2010). The Golgi can be present in neurons as a fairly typical ribbon-like network next to the nucleus, but there are also Golgi elements present in dendrites called Golgi outposts (Gardiol et al 1999, Horton & Ehlers 2003, Pierce et al 2001). Golgi outposts presumably augment the processing and secretory capacity of the cell. Loss of these structures via laser ablation or knockdown of key supporting components causes loss of dendritic branching (Horton et al 2005, Ye et al 2007). It is believed that the presence of Golgi outposts reflects highly localized miniature versions of the secretory pathway. ER exit sites are present (Aridor et al 2004) and certain cargos have been visualized moving from ER exit sites to Golgi outposts (Horton & Ehlers 2003, Jeyifous et al 2009). Furthermore, isolated dendrites carry out glycosylation (Torre & Steward 1996).

The mechanism that drives the expansion of the neuronal Golgi and the biogenesis of Golgi outposts is not known. Upregulation likely reflects increased processing demand such as for gangliosides, which are glycolipids modified in the Golgi and produced during brain development (Yu et al 2004). Golgi outposts may derive de novo or from the pre-existing juxtanuclear Golgi. Evidence for the latter is that differentiation of neuroblasts triggers Golgi

expansion and fragmentation with some of the Golgi fragments moving to become outposts (Horton & Ehlers 2003). Golgi movement in Drosophila neurons requires the protein Lava Lamp to connect Golgi membranes to the dynein motor, and Lava Lamp knockdown blocks Golgi outpost formation (Ye et al 2007). Evidence for the former is that isolated dendrites separated from the soma, can support the Golgi outpost and process newly synthesized cargo, at least 4hr post scission (Torre & Steward 1996).

Concluding remarks

In summary, it must be stated that there is much to be done if we are to achieve an understanding of homeostasis and growth control of the Golgi apparatus. In terms of what is needed, it is arguable that model systems are the first and foremost requirement. A tractable model in which Golgi size is acutely or stably altered due to a physiologically meaningful condition will provide a path to rapid progress. Quantitative analysis of Golgi size changes at the level of its key subdomains, akin to that carried out by Marsh and colleagues for pancreatic beta cells (Marsh et al 2004, Noske et al 2008), will also be important and allow correlation of structure changes with their functional consequences. Similarly, a quantitative time course of Golgi component abundance is needed. Ultimately, descriptions at the molecular level will define causal changes in pathways leading to altered Golgi size and function.

As emphasized in this chapter, ribbon elongation involving cisternal linking is arguably the most important mechanism driving Golgi size increase. Moreover, this linkage reaction is regulated under physiological conditions such as cell cycle, cell migration and growth factor stimulation (Colanzi et al 2007, Feinstein & Linstedt 2007, Bisel et al 2008, Yoshimura *et al.*, 2005). Therefore, the work presented in this thesis has the goal of understanding the mechanism of action and regulation of GRASP65, which is a key factor involved in linking of Golgi cisternae to form the ribbon-like membrane network.

CHAPTER 2: Organelle tethering by a homotypic PDZ interaction underlies formation of the Golgi membrane network

Abstract

Formation of the ribbon-like membrane network of the Golgi apparatus depends on GM130 and GRASP65 but the mechanism is unknown. We developed an in vivo organelle tethering assaying in which GRASP65 was targeted to the mitochondrial outer membrane either directly or via binding to GM130. Mitochondria bearing GRASP65 became tethered to one another and this depended on a GRASP65 PDZ domain that was also required for GRASP65 self-interaction. Point mutation within the predicted binding groove of the GRASP65 PDZ domain blocked both tethering and, in a gene replacement assay, Golgi ribbon formation. Tethering also required proximate membrane anchoring of the PDZ domain suggesting a mechanism that orientates the PDZ binding groove to favor interactions in *trans*. Thus, a homotypic PDZ interaction mediates organelle tethering in living cells.

Introduction

Intracellular organelles form membrane networks through fusion and fission events, which must be tightly regulated to preserve organelle identity and morphology (Voeltz and Prinz, 2007). In mammals the Golgi apparatus forms a ribbon-like network comprised of laterally linked stacked cisternae, or ministacks. Each ministack is comprised of subcompartments that carry out ordered processing reactions on cargo passing through the organelle (Pfeffer, 2007; Puthenveedu and Linstedt, 2005). The lateral linkages that connect adjacent ministacks are homotypic and dynamic. That is, analogous cisternal subcompartments are linked with each other and both fusion and fission occur at the sites of contact (Colanzi and Corda, 2007). Disruption of the lateral connections is associated with increased deviation in enzyme distribution among ministacks and processing deficiencies (Puthenveedu et al., 2006). The linkages also appear to act as a control point in cell cycle progression as a MAP kinase pathway (Acharya et al., 1998; Yoshimura et al., 2005; Shaul and Seger, 2006) triggers unlinking of the Golgi ribbon in late G2 phase of the cell cycle and blockade of this event delays entry into M-phase (Feinstein and Linstedt, 2007). Lateral linkage of the Golgi ribbon may also be regulated to allow repositioning of the Golgi apparatus to face the wound edge during the cellular response to a scratch wound (Bisel et al., 2008).

Two of the identified factors required for ribbon formation are the golgin GM130 and its binding partner GRASP65 (Marra et al., 2007; Puthenveedu et al., 2006), which is also required for reassembly of Golgi stacks in an in vitro assay (Barr et al., 1997; Wang et al., 2003). In the absence of GM130 or GRASP65 the Golgi apparatus is fragmented into ministacks that nevertheless mostly retain their juxtanuclear positioning and transport competence (Kodani and Sutterlin, 2008; Puthenveedu et al., 2006; Sutterlin et al., 2005). Significantly, whereas knockdown of GRASP65 leaves GM130 properly localized on the Golgi (Puthenveedu et al., 2006; Sutterlin et al., 2005), knockdown of GM130 causes loss of GRASP65 (Kodani and Sutterlin, 2008; Puthenveedu et al., 2006). Further, GM130 function requires its ability to bind GRASP65 (Puthenveedu et al., 2006). Based on these findings and the demonstrated ability of the GRASP65 N-terminus, which contains a tandem array of PDZ-like domains (Barr et al., 1998; Kuo et al., 2000), to form homo-oligomeric structures (Wang et al., 2005; Wang et al., 2003), we hypothesized that GM130 recruits GRASP65 to the Golgi membrane and that

GRASP65 mediates homotypic tethering of adjacent cis cisternae via oligomeric interactions in *trans* (Puthenveedu et al., 2006).

However, evidence that the GM130/GRASP65 complex plays a direct role in organelle tethering is lacking, as is a detailed understanding of how it might work. The finding that GRASP65 oligomerizes forming complexes in *trans* was carried out with protein purified from bacteria (Wang et al., 2005; Wang et al., 2003). These preparations were not myristoylated, were studied in the absence of membranes, and formed large polydisperse complexes leaving the physiological context of a key aspect of the hypothesis that GRASP65 oligomers bridge membranes an open question. Further, although oligomerization activity mapped to the N-terminal region containing PDZ-like domains, it is not clear whether either or both of these domains mediate the interaction, whether the interaction involves a bone fide PDZ domain interaction or whether these domains even form PDZ domains at all. Finally, the validity of the model in which GM130/GRASP65 complexes bridge membranes to mediate Golgi ribbon formation is further complicated by recent findings that implicate the proteins in non-classical secretion occurring outside the Golgi apparatus at specific points of development of two non-vertebrates (Kinseth et al., 2007; Schotman et al., 2008).

Thus, to investigate their sufficiency in organelle tethering in a physiological context, GM130 and GRASP65 constructs were expressed on the mitochondrial outer membrane of mammalian cells containing or lacking endogenous mitochondrial tethering factors. Paralleling its activity at the Golgi, GM130 recruited GRASP65 and GRASP65 was necessary and sufficient for mitochondrial tethering. Tethering depended on the predicted ligand-binding groove of a self-interacting GRASP65 PDZ domain and mutation of this predicted groove to block tethering also blocked Golgi ribbon formation. The combined results indicate that, after recruitment by GM130, GRASP65 homotypic PDZ-type interactions mediate organelle tethering.

Results

Organelle clustering induced by GRASP65

As a test of the hypothesis that GRASP65 directly crossbridges membranes we expressed in HeLa cells a modified version of GRASP65 containing a C-terminal membrane anchor sequence specifying targeting to the mitochondrial outer membrane. The mitochondrial-targeting signal, derived from the ActA protein of *Listeria monocytogens* (Pistor et al., 1994), was placed after an inserted green fluorescent protein (GFP) coding sequence at the C-terminus of GRASP65 to yield a cytoplasmically disposed G65-GFP-ActA construct (Fig 2-1A). GFP-ActA, which lacked the GRASP65 sequence but was otherwise identical, served as a control.

The control GFP-ActA was targeted to mitochondria as indicated by its colocalization with Mitotracker™ and it altered neither mitochondrial nor Golgi morphology (Fig 2-1B-I). G65-GFP-ActA also colocalized with Mitotracker™ staining indicating mitochondrial targeting but, in striking contrast with GFP-ActA, G65-GFP-ActA expression had a profound effect on mitochondrial location and appearance (Fig 2-1J-M). The mitochondria became clustered in the juxtanuclear region of the cells with little or no mitochondrial staining remaining elsewhere in the cytoplasm. The Golgi apparatus, which appeared intermingled with the clustered mitochondria, was fragmented in these cells. The mitochondrial clusters were strikingly similar to those induced by overexpression of the mitofusin proteins that normally tether mitochondria (Chen et al., 2003; Koshiba et al., 2004) suggesting that G65-GFP-ActA was tethering the membranes to one another.

To exclude the possibility that the juxtanuclear clustering induced by G65-GFP-ActA depended on interaction with Golgi membranes, cells expressing GFP-ActA or G65-GFP-ActA were treated with brefeldin A (BFA). As expected, BFA induced Golgi collapse in control cells (Fig 2-1N-Q) and in cells expressing G65-GFP-ActA (Fig 2-1R-U) and mitochondrial clusters persisted in the latter. In fact, the clusters frequently appeared tighter suggesting that, in the absence of BFA, the Golgi membranes partially constrained, or otherwise limited, interactions between the clustered mitochondria.

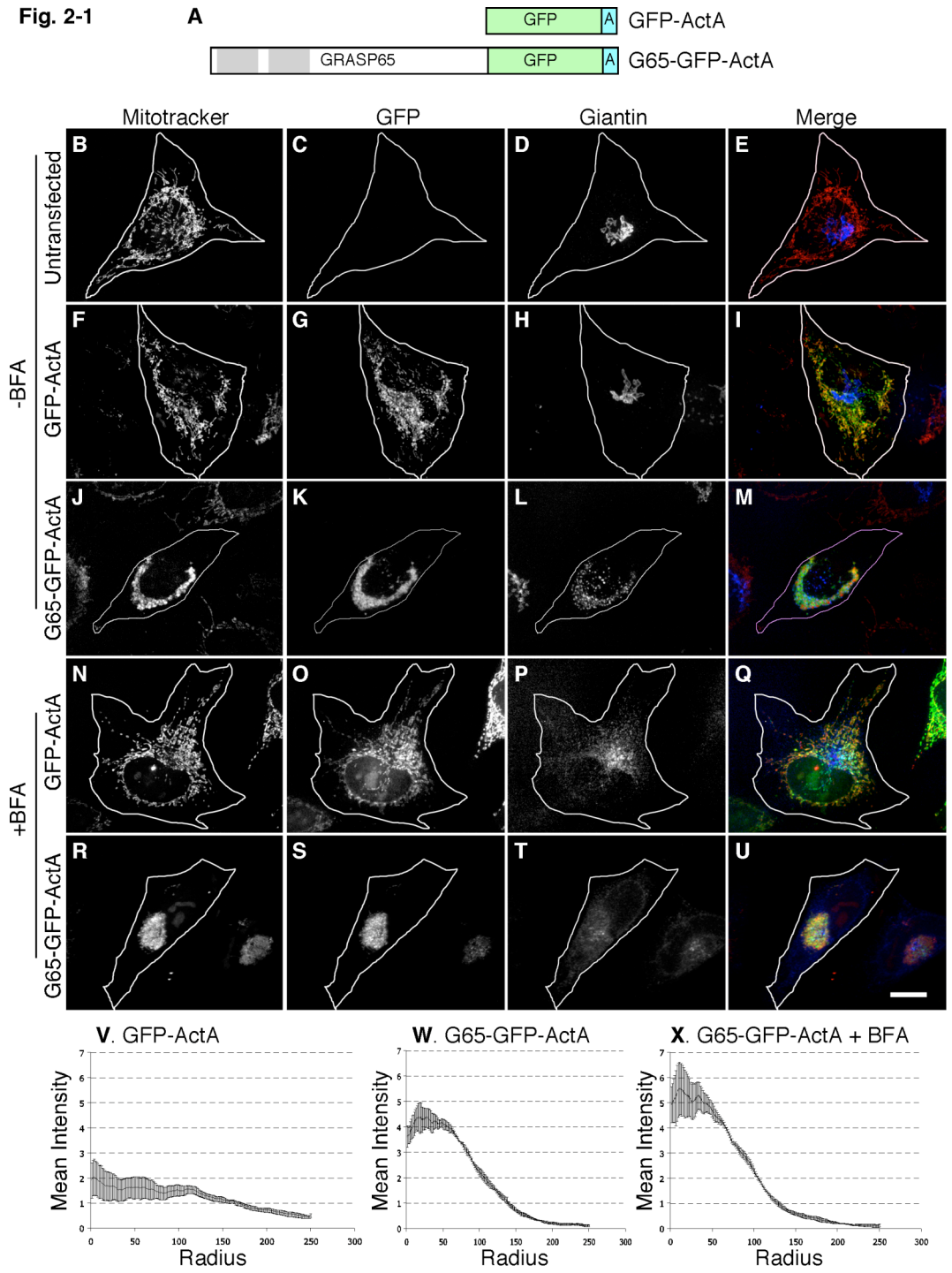

Figure 2-1 Mitochondrial clustering by GRASP65 Schematic diagram of the constructs (A). Untransfected HeLa cells (B-E) or cells expressing GFP-ActA (F-I) or G65-GFP-ActA (J-M) were analyzed 24 h post-transfection using Mitotracker (red) to stain mitochondria, GFP fluorescence (green) to localize the transfected proteins, and giantin (blue) staining to image the Golgi apparatus. An identical analysis was carried out after a 30 min BFA treatment on cells expressing GFP-ActA (N-Q) or G65-GFP-ActA (R-U). Bar=10 μm. Radial profile plots show the spread of mitochondrial fluorescence starting from the centroid and extending to the cell periphery for cells expressing GFP-ActA (V), G65-GFP-ActA (W), or BFA-treated cells expressing G65-GFP-ActA (X). Values are averages corresponding to the fraction of total fluorescence present in each concentric circle drawn from the centroid (n=3, ±SEM, >15 cells/experiment).

To obtain a quantitative measure of the extent of mitochondrial spread in the transfected cells a radial profile algorithm was used. For each cell, the algorithm measured the mean signal intensity for a series of concentric circles emanating from the calculated centroid of the fluorescent signal. Average values from many cells over multiple experiments were then used to generate radial profile plots in which the fraction of total mean intensity is expressed as a function of distance from the centroid. The radial profile plot for cells expressing the GFP-ActA control construct was essentially flat reflecting the uniform spread of the mitochondria throughout the cytoplasm (Fig 2-1V). In contrast, a clearly significant clustering was evident in cells expressing G65-GFP-ActA (Fig 2-1W) and this was slightly accentuated in G65-GFP-ActA expressing cells treated with BFA (Fig 2-1X). These results indicate that GRASP65 when targeted to the mitochondrial outer membrane is sufficient to induce organelle clustering.

Nocodazole-induced microtubule disassembly was used to test whether clustering depended on an intact microtubule network. Untreated cells expressing the GFP-ActA control construct exhibited filamentous tubulin staining and filamentous mitochondria and nocodazole converted the tubulin pattern from filamentous to diffuse and this reduced the filamentous appearance of mitochondria, which, nevertheless, remained dispersed throughout the cytoplasm (Fig 2-2A-D). Significantly, nocodazole had no effect on mitochondrial morphology or distribution in G65-GFP-ActA expressing cells. That is, mitochondria were found in juxtanuclear clusters in cells lacking microtubules (Fig 2-2E-H). Thus, in contrast to nocodazole-sensitive mitochondrial clustering involving recruitment of motor and/or mictrotubule binding activity (Hoogenraad et al., 2003; Rios et al., 2004), the microtubule independence GRASP65-mediated clustering argues that it is likely a direct effect of crossbridging the mitochondrial membranes and forming a large structure that, for steric reasons, occupies the juxtanuclear area.

Next, electron microscopy was carried out on the BFA-treated transfected cells to assess the ultrastructure of the clustered mitochondria. In untransfected cells, and in cells transfected with the GFP-ActA control plasmid, mitochondria were evident throughout the entire cytoplasm and were frequently well separated from each other (Fig 2-3A-B). As expected, the filamentous aspect apparent using fluorescence microscopy was not evident, presumably due to the low probability of obtaining thin sections with longitudinal profiles of membrane tubules. In contrast, cells transfected with G65-GFP-ActA had prominent clusters of mitochondria in the juxtanuclear region and the remaining cytoplasm was essentially devoid of mitochondria (Fig 2-

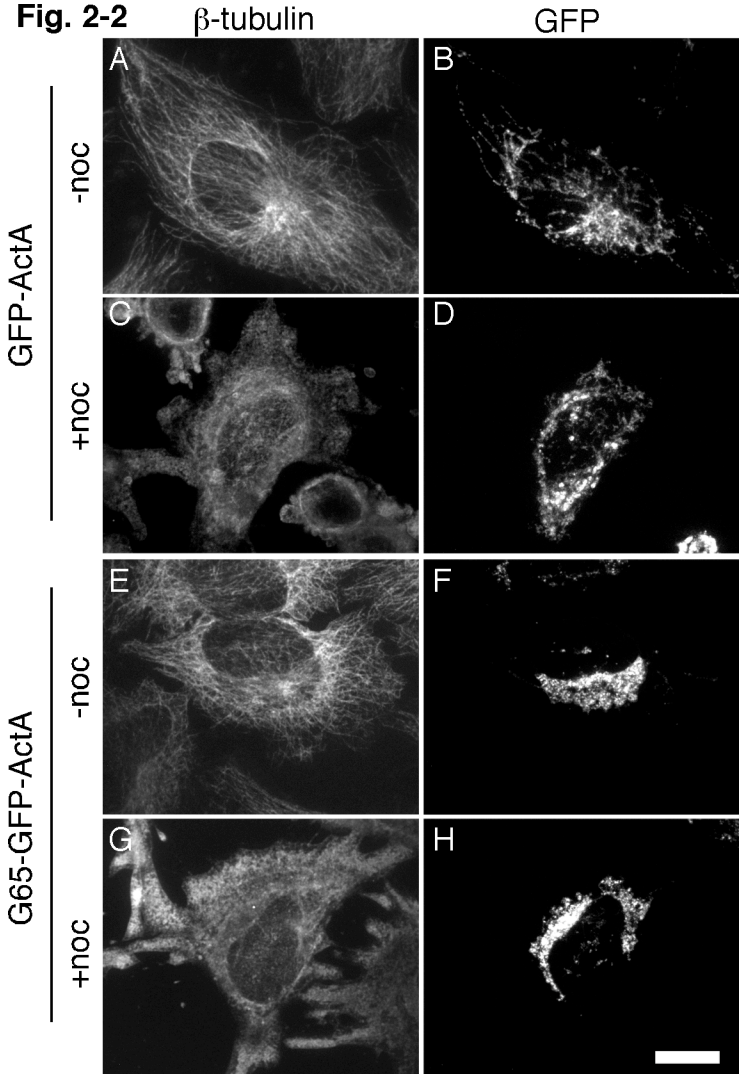

Figure 2-2 Clustering persists in the absence of microtubules. A-H. HeLa cells (not BFA-treated) expressing GFP-ActA (A-D) or G65-GFP-ActA (E-H) were either untreated (A,B,E,F) or nocodazole-treated to depolymerize microtubules (C,D,G,H) and then stained and imaged to reveal beta-tubulin and GFP patterns. Bar=10 μm.

3C-D). Unlike Golgi stacks, which have extended zones of apposition with uniform gap widths, the mitochondria in the clusters were apposed mostly at discrete sites and at a greater distance. Other membranes may be present within the clusters. Nevertheless, an immunofluorescence assay (not shown) failed to reveal any accumulation in the clusters of calnexin, an ER marker, or ERGIC53, a marker of the intermediate compartment that accumulates in BFA remnants (Seemann et al., 2000). Interestingly, the outer membranes of individual mitochondria appeared distinct from neighboring outer membranes suggesting maintenance of mitochondrial integrity within the cluster. Absence of syncytia formation was further supported by fluorescence recovery after photobleaching experiments. Cells expressing the control construct, GFP-ActA, exhibited an extended mitochondrial network and when a small region of the network was bleached, fluorescence was rapidly recovered in the bleached structures (Fig 2-3E-H). This is the expected behavior for a contiguous membrane network established by membrane fusion. In contrast, cells expressing the G65-GFP-ActA construct exhibited a juxtanuclear cluster of mitochondria and there was no recovery of fluorescence observed after photobleaching small portions of the clustered membranes (Fig 2-3I-L).

Mitofusins form homotypic interactions in *trans* thereby crossbridging mitochondria (Chen and Chan, 2005; Griffin et al., 2006). To test whether mitofusins were involved, GFP-ActA and G65-GFP-ActA were expressed in *mfn*-/- cells, which are homozygous for deletions in each of the mitofusin genes and contain mitochondria that are incompetent to dock and fuse (Chen et al., 2003; Koshiba et al., 2004). Mitochondria were detected using DsRed fused to pre-sequence of subunit IV of cytochrome C oxidase (COX-IV-DsRed), which is localized to the matrix of mitochondria (Koshiba et al., 2004). The cells were also treated with BFA to disperse Golgi membranes. The GFP-ActA control colocalized with COX-IV-DsRed and the mitochondria appeared as discrete punctate structures distributed throughout the cytoplasm (Fig 2-3M-O). Expression of G65-GFP-ActA caused clustering of the mitochondria in *mfn*-/- cells (Fig 2-3P-R). Further, because COX-IV-DsRed and G65-GFP-ActA were localized to the matrix and the outer membrane, respectively, it was possible to distinguish individual mitochondria in the clusters after acquiring single optical sections by confocal microscopy. This analysis provided strong evidence that, instead of undergoing fusion to form syncytia, mitochondria remained intact as

Fig. 2-3

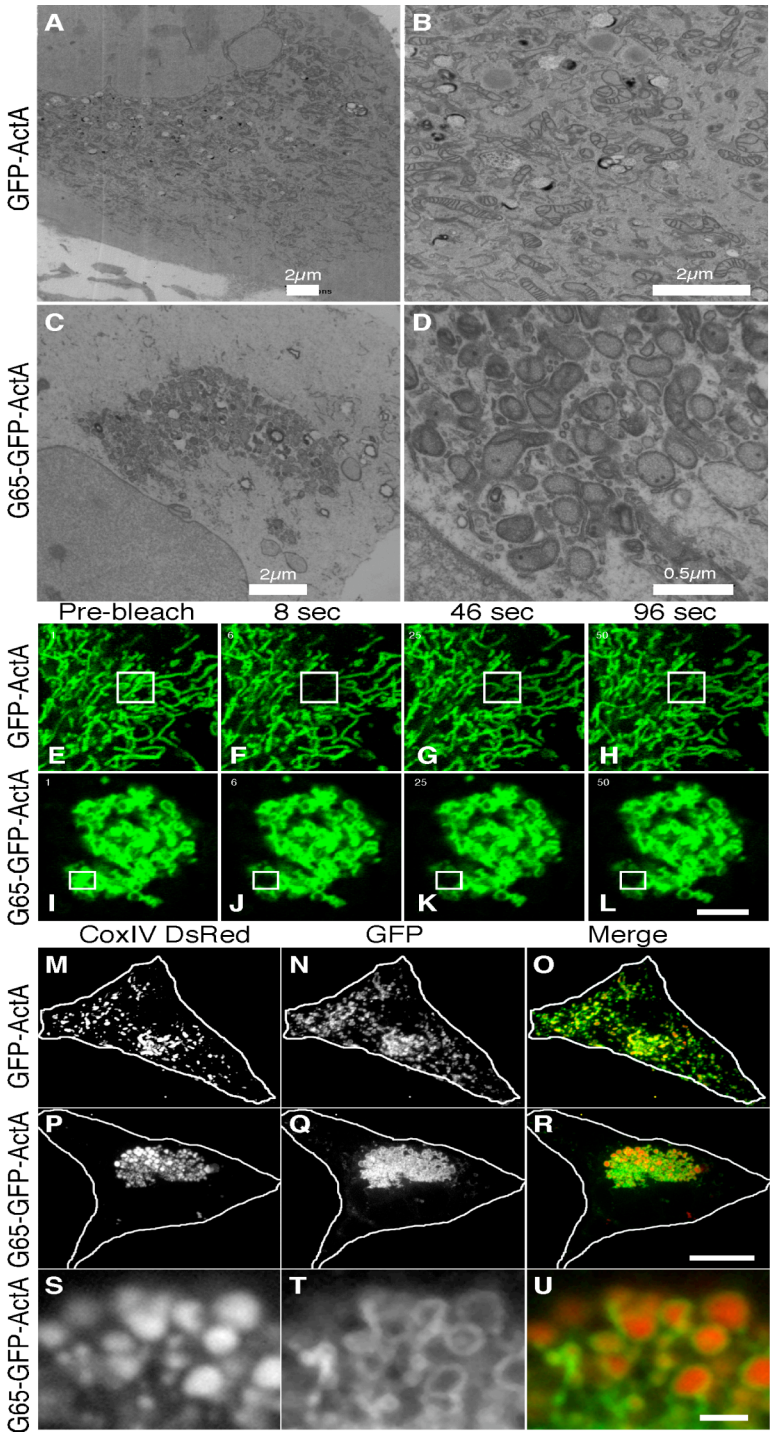

Figure 2-3 Mitochondria are tethered and not fused into syncytia. GFP-ActA (A-B) or G65-GFP-ActA (C-D) transfected HeLa cells were BFA-treated, processed for electron microscopy and shown at 2 magnifications. GFP-ActA (E-H) or G65-GFP-ActA (I-L) transfected cells were imaged live using a scanning laser microscope. A region of interest (marked in figure) was selected and bleached and recovery was monitored in subsequent frames at 2 sec intervals. Bar=2μm. Mouse embryonic fibroblasts lacking mitofusin-1/2 and expressing the matrix marker COX-IV-DsRed were transfected with GFP-ActA (M-O) or G65-GFP-ActA (P-R), BFA-treated, and processed to reveal mitochondria (red), and the expressed proteins (green). Bar=10 μm. An enlarged view of a single optical section is also shown (S-U). Bar=1 μm.

discrete entities each containing an outer membrane compartment surrounding a matrix compartment (Fig 2-3S-U).

The experiments in this section argue that G65-GFP-ActA tethers adjacent mitochondria to generate juxtanuclear clusters. To verify that interactions in *trans* mediated mitochondrial clustering, HeLa cells expressing G65-GFP-ActA were fused to HeLa cells expressing either mCherry-ActA or G65-mCherry-ActA. Cycloheximide was used to prevent new protein synthesis and the mitochondria in the resulting heterokaryons were analyzed. Importantly, mitochondria bearing the control construct mCherry-ActA mostly remained strikingly distinct from mitochondria bearing G65-GFP-ActA in that the former retained the filamentous morphology characteristic of control mitochondria whereas the latter remained clustered (Fig 2-4A-C). Further, the mitochondria bearing G65-mCherry-ActA coalesced with mitochondria bearing G65-GFP-ActA into single clusters (Fig 2-4D-F). Thus, clustering depended on GRASP65 being present in both membranes. Due to a low transfection frequency, we were unable to achieve dual labeled heterokaryons with *mfn*-/- cells, thus the apparent mixing of the two markers in HeLa cells could be attributed to mitofusin-dependent membrane fusion (Legros et al., 2002) or membrane transfer (Neuspiel et al., 2008) in the 3 h following cell fusion.

GM130 tethers membranes by recruiting GRASP65

As mentioned above, GM130 is required for Golgi ribbon formation and for targeting of GRASP65 to Golgi membranes. Therefore a strong prediction is that targeting of GM130 to mitochondria would also induce mitochondrial clustering, but in a manner dependent on its ability to recruit GRASP65. To test this idea, we targeted the GM130 C-terminus, which contains the GRASP65 binding site, to mitochondria. One technical challenge was that targeting GM130 to mitochondria required a distinct strategy because GM130 uses its C-terminus to interact with GRASP65 (Barr et al., 1998) and the ActA C-terminal membrane anchor was likely to interfere with this interaction. Fortunately, a search for outer membrane targeting sequences that could be used at the N-terminus yielded a sequence in TOM20, a component of the outer membrane translocator complex. The N-terminal 40 amino acids of TOM20 contains a membrane anchoring domain that orients such that the C-terminal hydrophilic sequences are exposed to the cytosol (Waizenegger et al., 2003) and this domain is sufficient for mitochondrial targeting (Kanaji et al., 2000). Thus, we generated the constructs diagrammed (Fig 2-5A)

Fig. 2-4

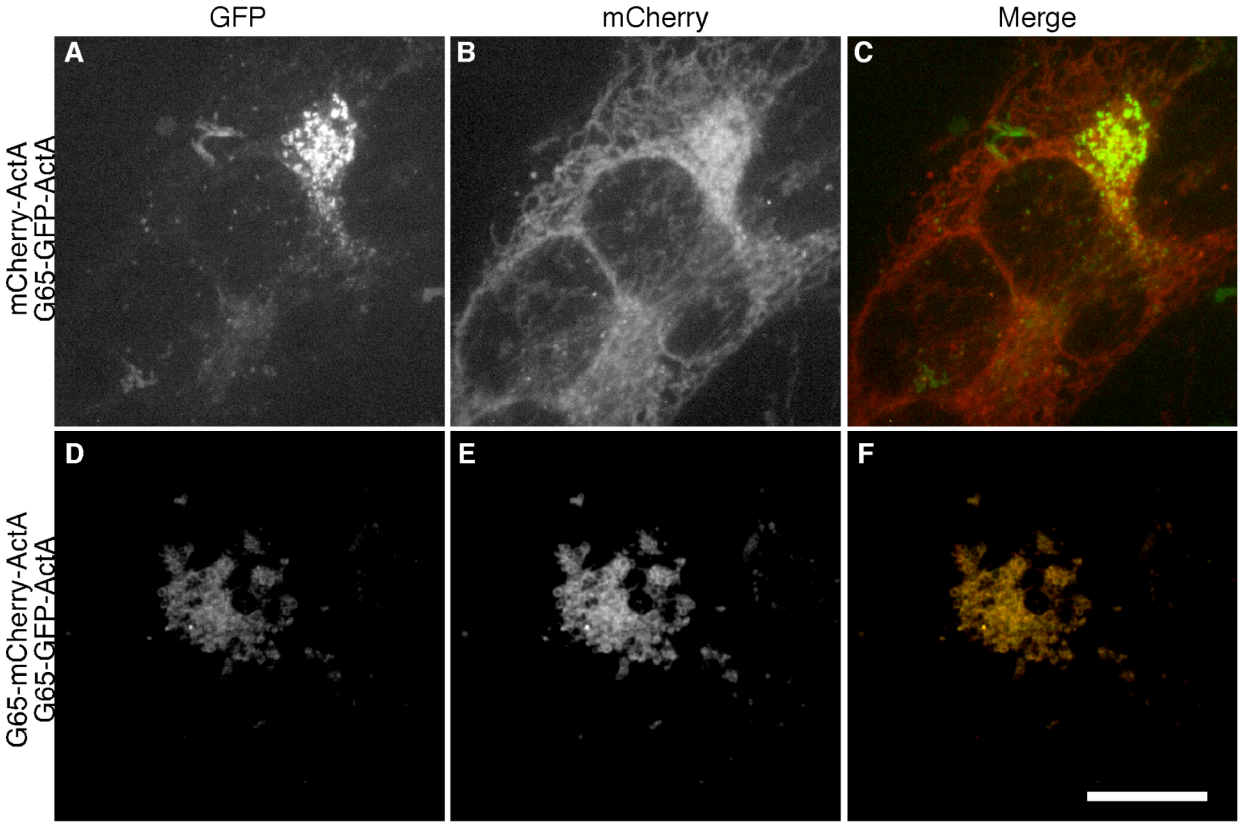

Figure 2-4 Clustering persists in the absence of microtubules. A-H. HeLa cells (not BFA-treated) expressing GFP-ActA (A-D) or G65-GFP-ActA (E-H) were either untreated (A,B,E,F) or nocodazole-treated to depolymerize microtubules (C,D,G,H) and then stained and imaged to reveal beta-tubulin and GFP patterns. Bar=10 μm.

containing the TOM20 signal anchor followed by GFP alone (T20-GFP) or by GFP and the C-terminal 100 amino acids of GM130 (T20-GFP-GM130^{Cterm}). As a further control, we also constructed T20-GFP-GM130$^{C\Delta10}$ which lacked 10 amino acids required for both GRASP65 binding (Barr et al., 1998) and for GM130 function in Golgi linking (Puthenveedu et al., 2006). BFA was used to carry out the assays in the absence of an intact Golgi apparatus.

T20-GFP was targeted to the mitochondria as indicated by colocalization with Mitotracker^{TM} staining (Fig 2-5B-E). T20-GFP-GM130^{Cterm} was also targeted to mitochondria but it induced mitochondrial clustering in the juxtanuclear region (Fig 2-5F-I). Mitochondrial clustering was not evident in cells expressing T20-GFP-GM130$^{C\Delta10}$ despite its evident targeting to mitochondrial membranes (Fig 2-5J-M). These results were quantified using the radial profiling analysis (Fig 2-5N-P) and were also observed in cells not treated with BFA (Fig 2-6A-L). Further, T20-GFP-GM130^{Cterm} induced mitochondrial clustering in *mfn*-/- cells (Fig 2-6M-R) where, similar to the case for G65-GFP-ActA, the integrity of the GFP-labeled outer membranes surrounding their DsRed-labeled matrices appeared intact suggesting that the mitochondria were clustered by crossbridging rather than fusion (Fig 2-6S-U).

The absence of clustering by T20-GFP-GM130$^{C\Delta10}$ strongly suggests that T20-GFP-GM130^{Cterm} clusters mitochondria by recruiting endogenous GRASP65. As a test, GRASP65 localization was determined. In BFA treated cells GRASP65 is known to be principally associated with remnant membrane structures localized adjacent to distributed ER exit sites (Seemann et al., 2000; Ward et al., 2001). Consistent with this localization, GRASP65 was present in dispersed punctate structures in cells expressing T20-GFP, which itself was localized to filamentous mitochondria (Fig 2-7A-D). In striking contrast, GRASP65 localization was largely juxtanuclear in cells expressing T20-GFP-GM130^{Cterm} and it was clearly evident on the clustered mitochondria (Fig 2-7E-H). In the case of cells expressing T20-GFP-GM130$^{C\Delta10}$, GRASP65 retained the control BFA remnant pattern and was distinct from the filamentous mitochondria (Fig 2-7J-M). GRASP65 coincidence with the GFP constructs was analyzed on a pixel-by-pixel basis and the quantified results indicated significant specific recruitment of endogenous GRASP65 to mitochondria by T20-GFP-GM130^{Cterm} (Fig 2-7N). Thus, the GM130 C-terminus recruited endogenous GRASP65 to mitochondria and this induced their clustering. Because GM130 is required for GRASP65 localization to Golgi membranes (Kodani and Sutterlin, 2008; Puthenveedu et al., 2006) and because the GRASP65 binding site in GM130 is required for

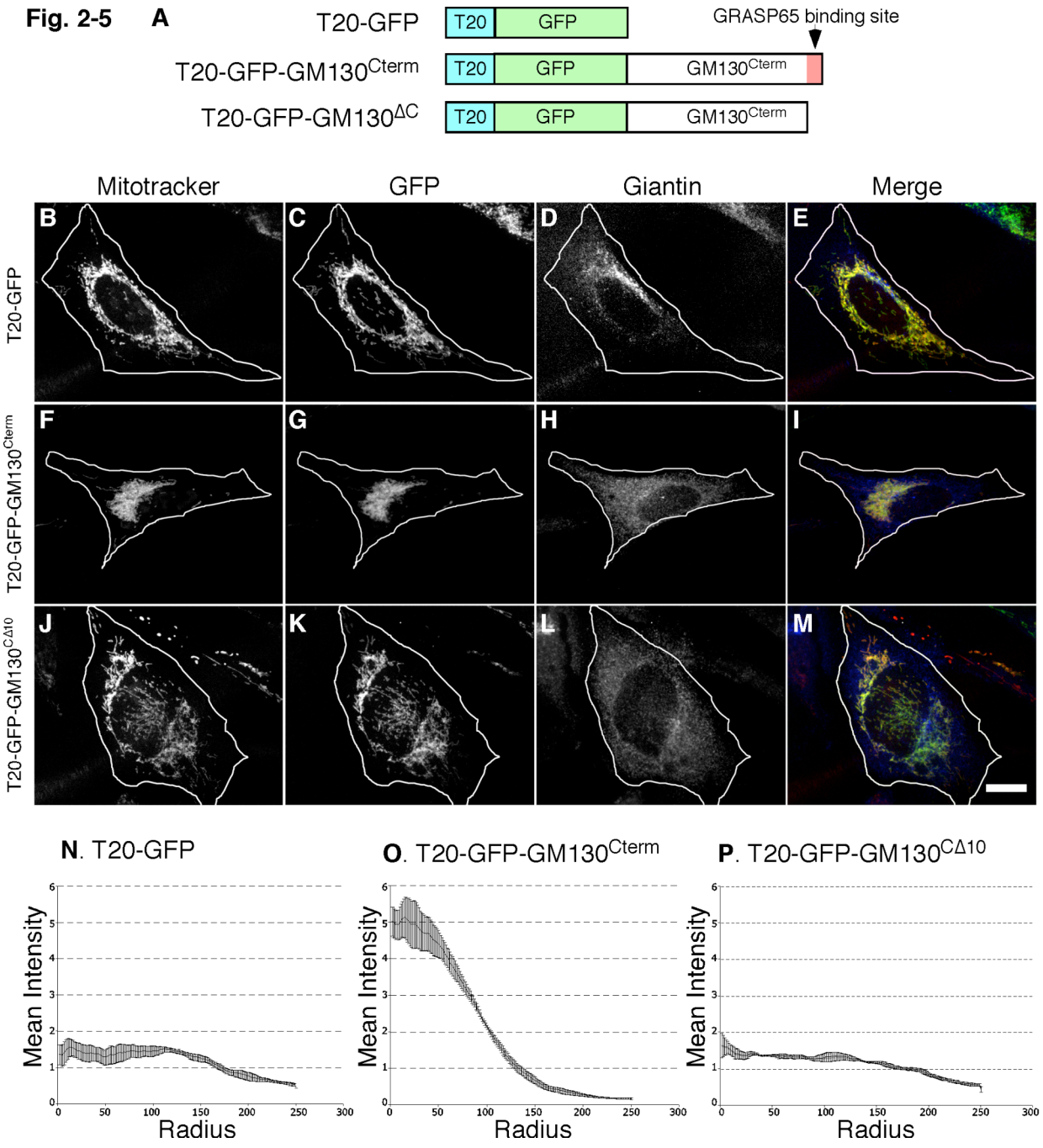

Figure 2-5 Clustering by the GRASP65 binding domain of GM130. Schematic diagram of the constructs (A). At 24 h post-transfection HeLa cells expressing T20-GFP (B-E), T20-GFP-GM130^{Cterm} (F-I), or T20-GFP-GM130$^{C\Delta10}$ (J-M) were BFA-treated for 30 min and analyzed using Mitotracker (red) , GFP fluorescence (green), and giantin staining (blue). Bar=10 μm. Radial profile plots (n=3, ±SEM, >15 cells/experiment) of T20-GFP (N), T20-GFP-GM130^{Cterm} (O), or T20-GFP-GM130$^{C\Delta10}$ (P).

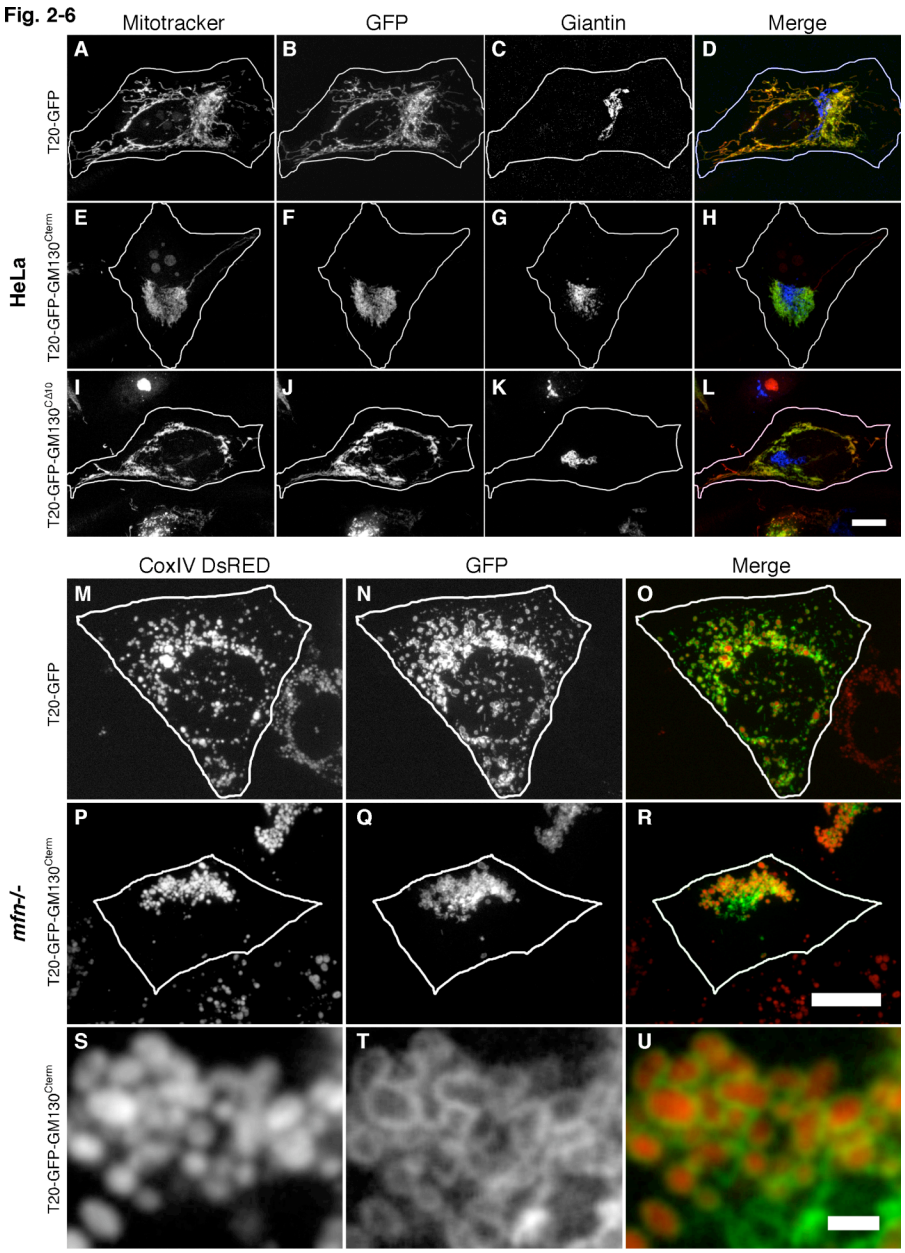

Figure 2-6 Clustering by the GRASP65 binding domain of GM130. A-L. HeLa cells expressing T20-GFP (A-D), T20-GFP-GM130^{Cterm} (E-H) or T20-GFP-GM130$^{C\Delta10}$ (I-L) without BFA treatment were analyzed using Mitotracker to stain mitochondria, GFP fluorescence to localize the transfected proteins, and giantin staining to image the Golgi apparatus. A merged image is also shown (Mitotracker=red, GFP=green, giantin=blue). Bar=10 μm. M-U**.** Mouse embryonic fibroblasts lacking the mitofusin-1 and mitofusin-2 genes and expressing the matrix marker COX-IV-DsRed were transfected with T20-GFP (M-O) or T20-GFP-GM130^{Cterm} (P-R), BFA-treated, and processed to reveal mitochondrial distribution (COX-IV-DsRed), the localization of the expressed proteins (GFP fluorescence), or a merged image (COX-IV-DsRed=red, GFP=green). Bar=10 μm. An enlarged view of a single optical section of the T20-GFP-GM130^{Cterm} expressing cells is also shown to illustrate the appearance of intact outer membranes surrounding intact matrix compartments (S-U). Bar=1 μm.

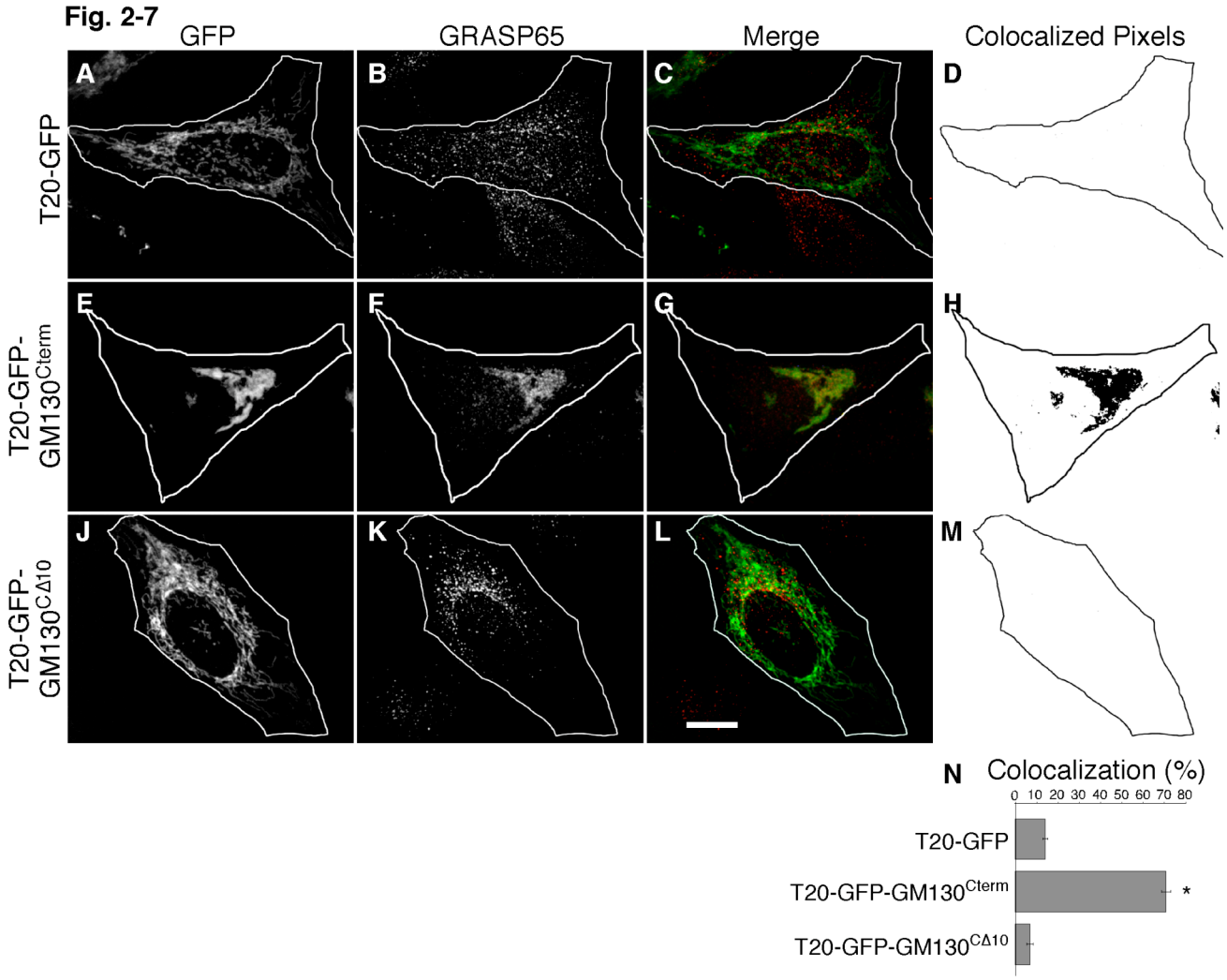

Figure 2-7 Endogenous GRASP65 is recruited to mitochondria by GM130. HeLa cells expressing T20-GFP (A-D), T20-GFP-GM130^{Cterm} (E-H) or T20-GFP-GM130$^{C\Delta10}$ (J-M) were BFA-treated and processed to reveal GFP fluorescence, GRASP65 staining, merged images and, from single optical sections, representations of the colocalized pixels. Bar=10 μm. GRASP65 recruitment (N) was assayed by determining the fraction of total GFP-positive pixels in single optical sections (chosen to maximize mitochondrial representation) that colocalized with GRASP65 staining (n=3, ±SEM, >15 cells/experiment,*p<0.0001).

GM130-dependent Golgi linking (Puthenveedu et al., 2006), these results strongly suggest that GM130 links Golgi ribbons by recruiting GRASP65, which in turn is sufficient to link membranes. Additionally, the results show that endogenous levels of GRASP65 are sufficient to induce mitochondrial clustering ruling out concerns regarding overexpression of exogenous constructs.

Although unlikely, we wished to rule out the possibility that GRASP65 might link membranes by recruiting GM130. Cells were treated with control siRNA or a previously described siRNA targeting GM130 (Puthenveedu et al., 2006) and then transfected with G65-GFP-ActA. In control knockdown cells, G65-GFP-ActA induced mitochondrial clustering and the clusters appeared co-labeled with GM130 presumably reflecting binding of GM130 to G65-GFP-ActA (Fig 2-8A-D). Significantly, GM130 recruitment did not appear functionally important. GM130 knockdown cells lacked detectable specific GM130 staining and yet the mitochondria remained clustered (Fig 2-8E-H). These results were also confirmed by radial profile analysis (Fig 2-8I,J). Thus, GRASP65, independent of its binding partner GM130, induces membrane crosslinking and the role of GM130 in membrane linking appears to be membrane recruitment of GRASP65.

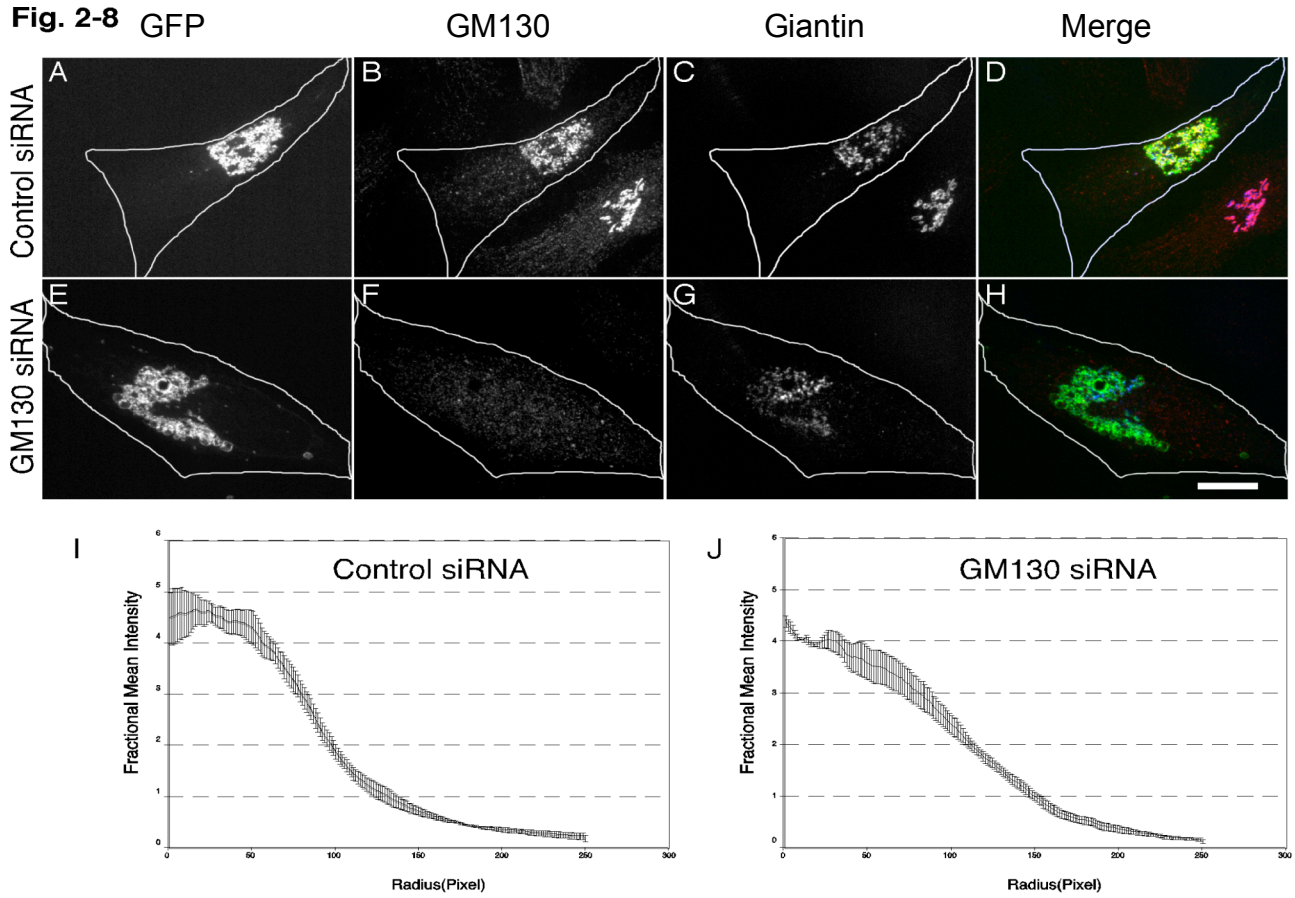

Figure 2-8 GRASP65 mediates clustering in cells lacking GM130. A-H**.** HeLa cells were mock transfected (A-D) or transfected with siRNA targeting GM130 (E-H). After 48 h the cells were transfected with the G65-GFP-ActA construct and after a further 24 h the cells (not BFA-treated) were processed to reveal GFP fluorescence, GM130 staining, giantin staining, and a merged image (GFP=green, GM130=red, giantin=blue). Bar=10 μm. I-J**.** The radial profile analysis is also shown (n=3, ±SEM, >15 cells/experiment).

GRASP65 PDZ1 is required for homotypic oligomerization and organelle tethering.

The GRASP65 N-terminus contains a tandem array of PDZ-like domains that might mediate organelle tethering. The PDZ domain is a wide spread protein module involved in protein-protein interactions (Fan and Zhang, 2002; Harris and Lim, 2001; Hung and Sheng, 2002). The canonical structure consists of five to six β-strands (β1-6) and 2 α-helices (α1, α2) forming a groove such that a ligand inserts between β2 and α2 completing a sheet with β2 and β3 (Doyle et al., 1996; Hung and Sheng, 2002; Im et al., 2003a; Kang et al., 2003). When purified after expression in bacteria, GRASP65 molecules self-interact to form oligomeric complexes and this activity is mediated by the N-terminus (Wang et al., 2005). To test whether one or both PDZ-like domains mediate GRASP65 homotypic interactions a series of GRASP65 constructs (Fig 2-9A) were purified and attached to beads and incubated in a pull down assay with HeLa cell extracts containing transfected wild type GRASP65. GRASP65 specifically bound full length, bead-attached GRASP65, but it did not bind a version of bead-attached GRASP65 lacking both PDZ1 and PDZ2 (Fig 2-9B). Further, deletion of PDZ1 blocked binding whereas deletion of PDZ2 did not. Interestingly, in the pull down assay, the GRASP65 N-terminus and even PDZ1 itself was sufficient for the interaction (Fig 2-9B). To confirm that the PDZ1 interaction was direct, GRASP65 with a C-terminal hexahistidine tag was purified from bacteria co-expressing N-myristoyltransferase. The purified protein bound the bead-attached PDZ1 domain in a specific and concentration-dependent manner (Fig. 2-10).

Based on these results, we tested the role of the GRASP65 PDZ-like domains in mitochondrial clustering induced by G65-GFP-ActA. HeLa cells were first transfected $G65^{\Delta PDZ1/2}$-GFP-ActA in which both PDZ-like domains were excised. The construct appeared stably targeted to mitochondria but the mitochondria remained filamentous and distributed throughout the cytoplasm indicating that the PDZ-like domains were indeed required for clustering (Fig 2-9C). This finding was confirmed by expressing $G65^{\Delta PDZ1/2}$-GFP-ActA in *mfn*-/- cells (Fig 2-9D) and by radial profile analysis (Fig 2-9E). Next, we tested $G65^{\Delta PDZ1}$-GFP-ActA and $G65^{\Delta PDZ2}$-GFP-ActA in which the PDZ-like domains were individually deleted. Interestingly, $G65^{\Delta PDZ1}$-GFP-ActA failed to induce mitochondrial clustering in either HeLa or *mfn*-/- cells (Fig 2-9F-H), but clustering was clearly evident in cells expressing $G65^{\Delta PDZ2}$-GFP-ActA (Fig 2-9I-K). Thus,

Fig. 2-9

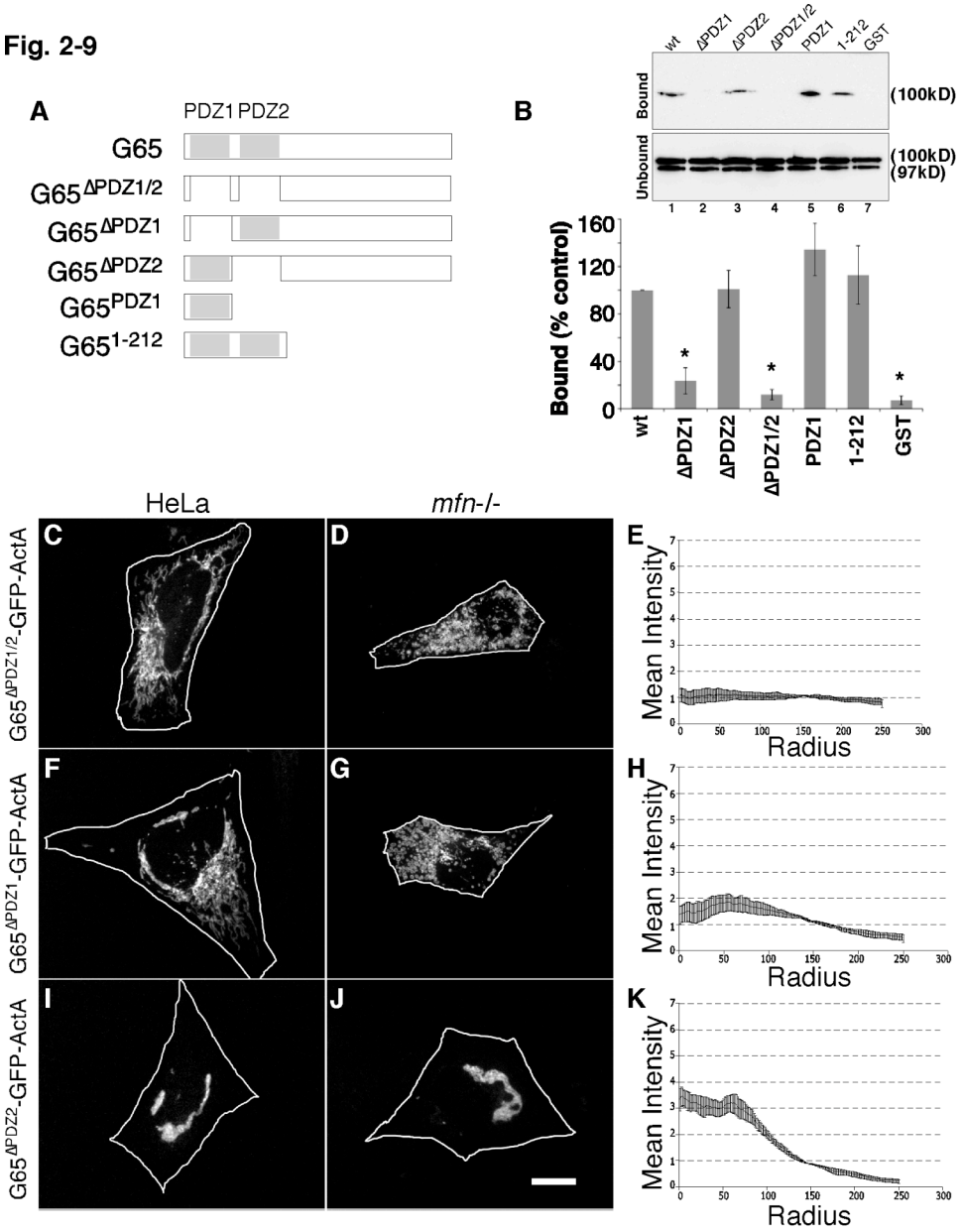

Figure 2-9 PDZ1 mediates homotypic GRASP65 oligomerization and clustering. Schematic diagram of the constructs (A). **(B)** Immunoblot analysis to detect recovery of G65-myc out of HeLa cell extracts by the indicated purified GST-GRASP65 constructs after incubation with glutathione agarose beads. Ten percent of the unbound fraction was loaded for comparison and for each construct the percent bound relative to that bound by the wild-type (wt) control is plotted (n=3,±SEM, >15 cells/experiment, *p<0.003). Transfected GRASP65-myc yielded a doublet, which was quantified, although only the upper band bound. Approximately 0.5% of total was bound by the wt control. HeLa or *mfn*-/- cells expressing G65$^{\Delta PDZ1/2}$-GFP-ActA (C-E), G65$^{\Delta PDZ1}$-GFP-ActA (F-H), and G65$^{\Delta PDZ2}$-GFP-ActA (I-K) were analyzed using GFP fluorescence after BFA treatment (bar=10 μm) and radial profile plots (n=3, ±SEM, >15 cells/experiment).

Fig. 2-10

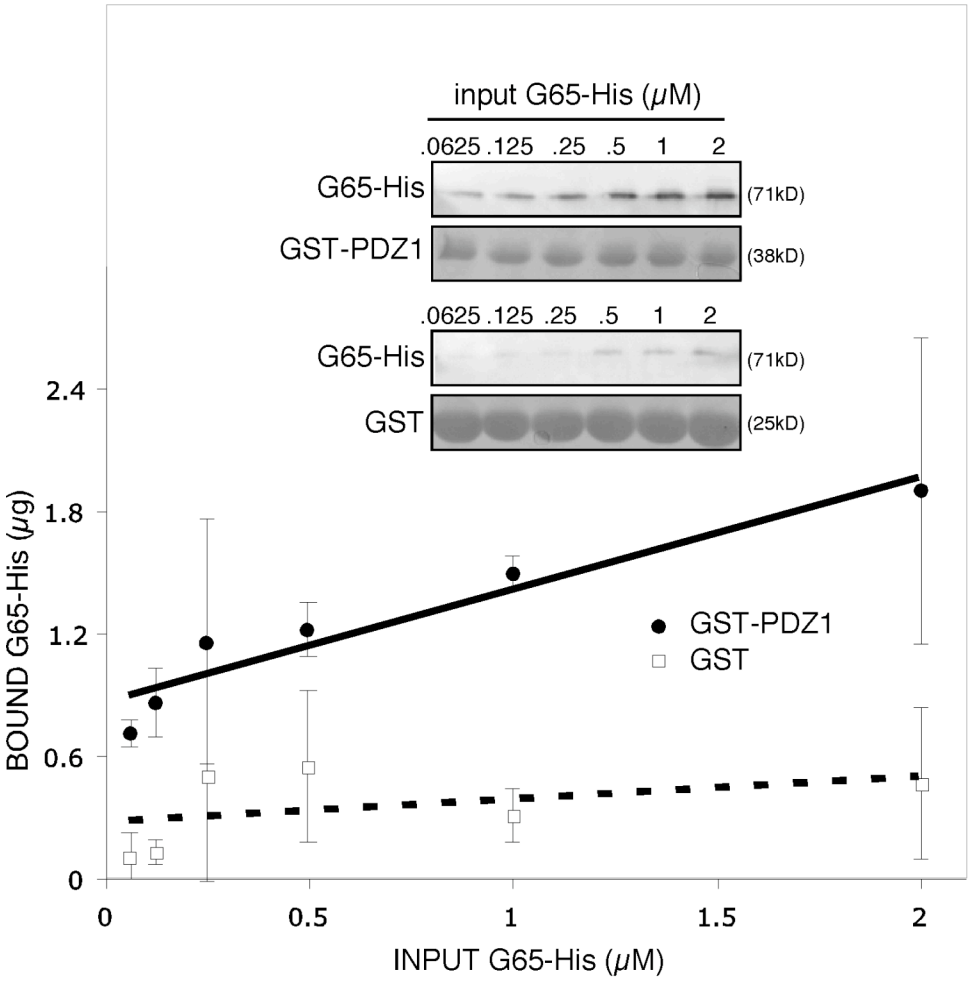

Figure 2-10 PDZ1 binds GRASP65 directly. Recovery of purified G65-His after incubation at various amounts with bead-attached GST (squares) and GST-PDZ1 (circles). The amount bound for each input amount is indicated (n=2, ±SD). Inset shows immunoblot assay detecting bound G65-His and corresponding Ponceau S staining of the GST and GST-PDZ1 present in each incubation.

GRASP65 clustering activity required PDZ1 whereas PDZ2 was dispensable. For an unknown reason constructs containing either PDZ domain in isolation from the rest of the molecule failed to express. In sum, the strong correlation between clustering activity and homotypic binding activity of these constructs argues that organelle clustering by GRASP65 is mediated by homotypic interactions occurring in trans between adjacent mitochondria and that it involves PDZ1.

The PDZ-like domains of GRASP65 show low homology with known PDZ domains. However, alignment analysis and computed structural modeling yielded a strong prediction of the sequence comprising the specificity conferring α2 element of the binding groove of PDZ1 (Fig 2-11A). To test whether the binding groove is involved in tethering, we introduced serine substitutions of two leucines in α2 that, in the model, face the binding pocket (Fig 2-11B). The construct was expressed in HeLa or *mfn*-/- cells. Strikingly, $G65^{LL58,59SS}$-GFP-ActA failed to cluster mitochondria in both cell types (Fig 2-111C-D). As evidence arguing that this effect was specific, another double amino acid change was made inside α2 ($G65^{LK55,56RR}$) and several were made outside of α2 ($G65^{LG3,4SS}$, $G65^{GF16,17RR}$, and $G65^{EE81,83RR}$). All constructs exhibited clear localization to mitochondria and the change inside α2 blocked clustering whereas the changes outside of α2 had no effect on clustering (not shown).

Having mapped residues in GRASP65 that are critical for its tethering activity we sought to test the role of GRASP65 mediated tethering in Golgi ribbon formation using gene replacement after siRNA-mediated knockdown (Puthenveedu and Linstedt, 2004). GRASP65 expression was inhibited using a siRNA targeting the 3' untranslated region of the GRASP65 mRNA. As previously reported (Puthenveedu et al., 2006), GRASP65 knockdown induced unlinking of the Golgi ribbon in HeLa cells stably expressing the GFP-tagged Golgi enzyme N-acetylgalactosaminyltransferase 2 (GalNAcT2) (Fig 2-11F-H). The fragmented Golgi phenotype was rescued by expression G65-myc, a version of GRASP65 tagged at the C-terminus with the myc epitope and lacking the 3' untranslated region targeted by the siRNA (Fig 2-11I-K). In marked contrast, failure to rescue was observed for a version of the replacement construct, $G65^{LL58,59SS}$-myc, containing the same serine substitutions in the predicted binding groove that prevented tethering (Fig 2-11L-N). The replacement constructs were present on Golgi membranes at comparable levels and also showed some cytoplasmic accumulation, which was

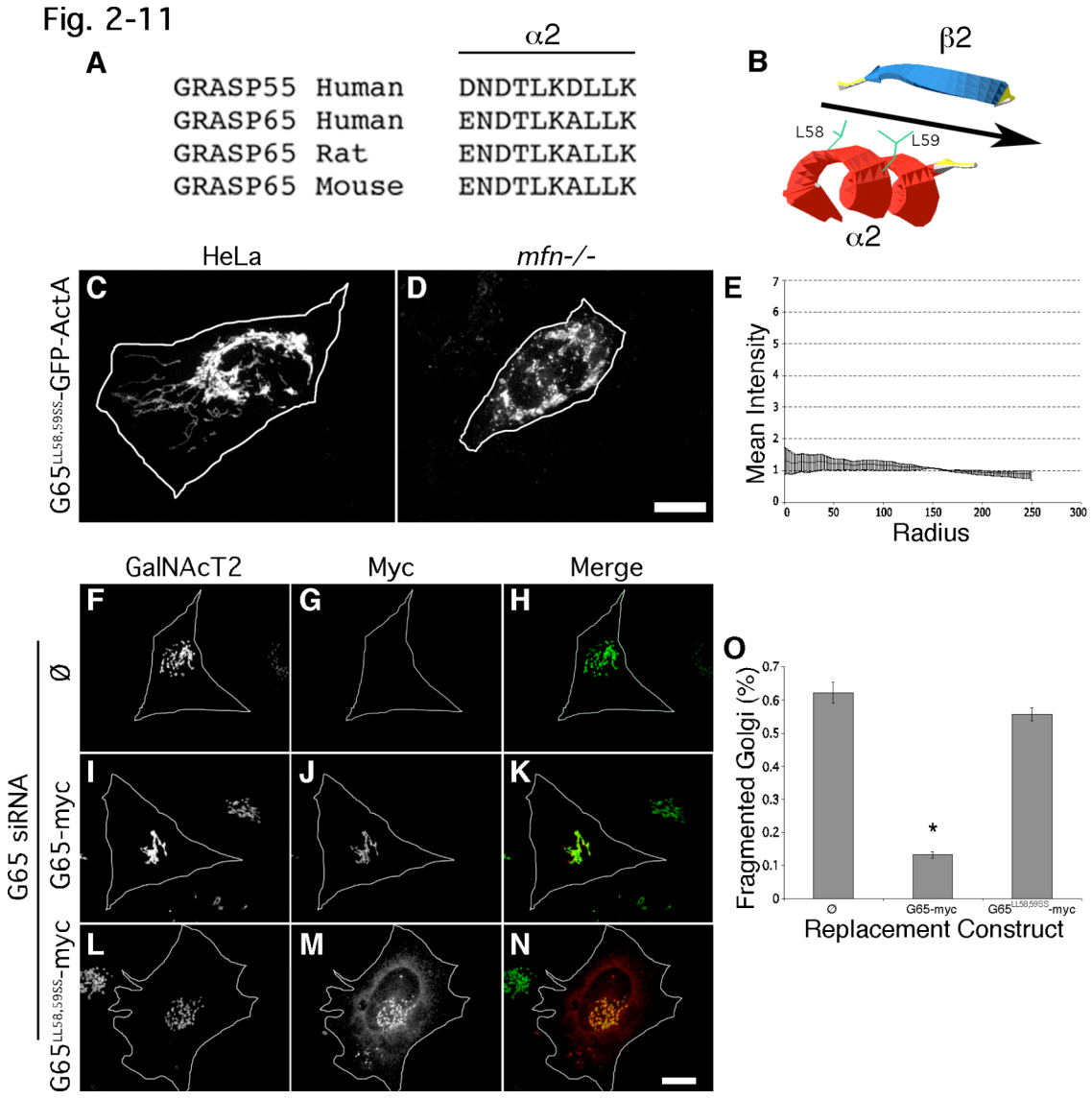

Figure 2-11 Mutation of the predicted PDZ1 ligand-binding groove blocks clustering. GRASP sequences are shown aligned at the position predicted by the TASSERlite modeling program to correspond to the second alpha helix of the first PDZ domain (A). As illustrated in the diagram (B), this helix is oriented in the model such that two leucines (L58, L59) face the binding pocket formed between the alpha helix and a beta strand. HeLa (C) or *mfn*-/- (D) cells expressing G65^{LL58,59SS}-GFP-ActA were analyzed using GFP fluorescence after BFA treatment (bar=10 μm) and the radial profile plot for *mfn*-/- cells (E) is shown (n=3, ±SEM, >15 cells/experiment). HeLa cells expressing GalNAcT2-GFP and transfected with GRASP65 siRNA and either no vector (F-H), G65-myc (I-K) or G65^{LL58,59SS}-myc (L-N) were analyzed to assess Golgi morphology (green) and replacement construct expression (red). Bar=10μm. Percentage of cells transfected with G65-myc or G65^{LL58,59SS}-myc exhibiting a fragmented Golgi after knockdown with GRASP65 siRNAs (±SEM, n=3, >50 cells each, *p<0.0001).

more evident for the mutated version. The results were quantified confirming a loss of GRASP65 activity in Golgi ribbon formation due to point mutation in the predicted PDZ1 binding groove (Fig 2-11O). Thus, the homotypic PDZ1 interaction revealed by targeting GRASP65 to the mitochondrial outer membrane underlies its ability to maintain the Golgi ribbon.

Another outcome of this analysis was the possible separation of function for the two GRASP65 PDZ-like domains in that tethering activity mapped to PDZ1 while previous work had mapped the GM130 binding site to the C-terminal end of PDZ2 (Barr et al., 1998). To test this prediction, we assayed GRASP65-mediated GM130 recruitment to the mitochondria of BFA-treated cells. Consistent with the result for non BFA-treated cells (Fig 2-8), G65-GFP-ActA recruited GM130 to mitochondria that were clustered (Fig 2-12A-C). In contrast, GM130 was not recruited to mitochondria by $G65^{\Delta PDZ2}$-GFP-ActA yet(Fig 2-12D-F), as indicated above, the construct exhibited clustering activity(Fig 2-9I-K). Finally, GM130 was recruited to mitochondria bearing $G65^{LL58,59SS}$-GFP-ActA, which, as expected, failed to cluster mitochondria due to the mutation in PDZ1 (Fig 2-12G-I). These results were confirmed by quantifying colocalization of GM130 with the mitochondrial constructs (Fig 2-12J). Thus, the mitochondrial assay allowed dissection of GRASP65 clustering and GM130 binding activities.

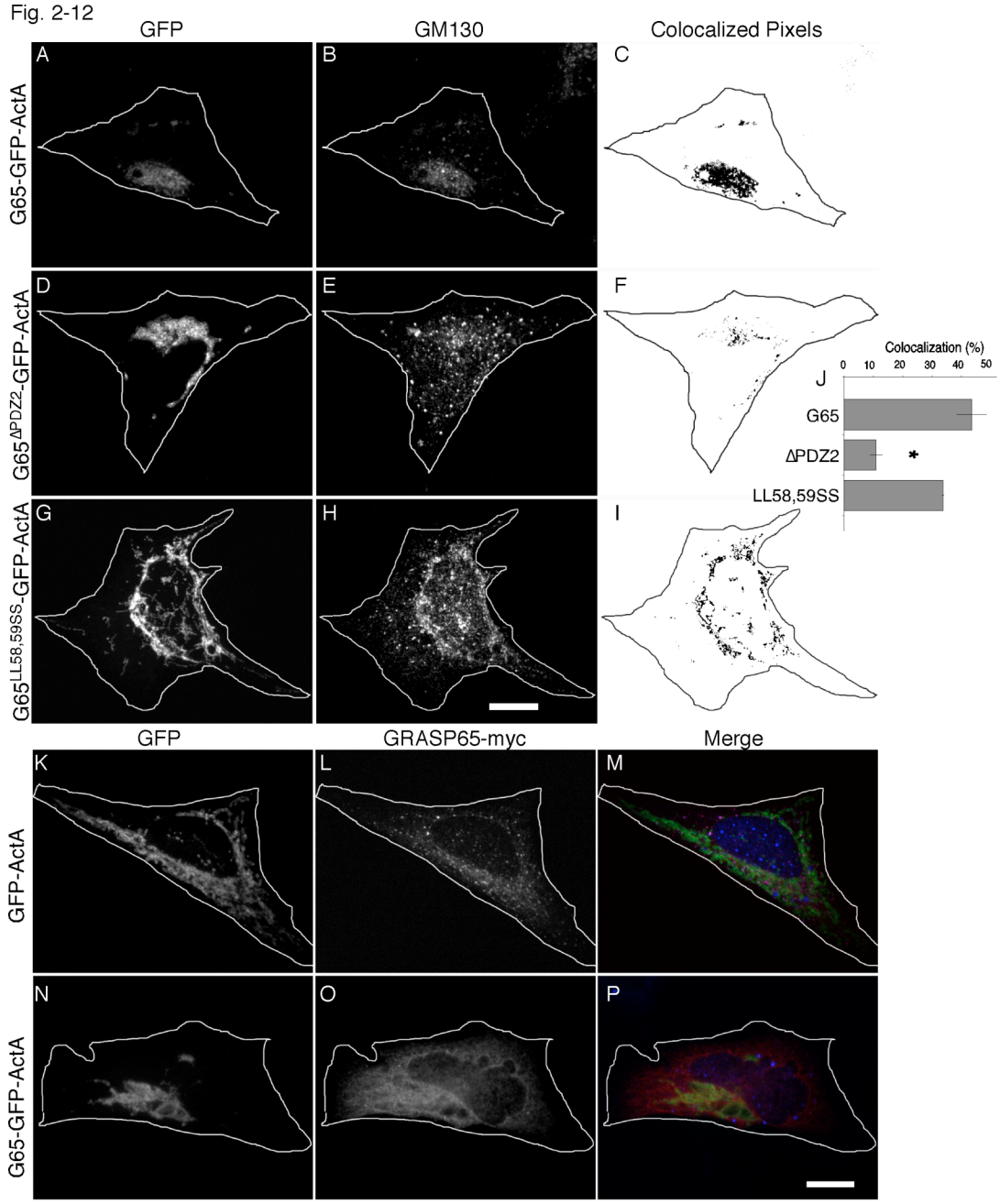

Figure 2-12 Recruitment of GM130 by G65-GFP-ActA depends on PDZ2, whereas soluble GRASP65-myc is not substantially recruited.

A-I. HeLa cells expressing G65-GFP-ActA (A-C), $G65^{\Delta PDZ2}$-GFP-ActA (D-F) or $G65^{LL58,59SS}$-GFP-ActA (G-I) were BFA-treated for 30 min to disassemble the Golgi apparatus and processed to reveal GFP fluorescence, GM130 staining, and representations of the colocalized pixels. Colocalized pixels shown are single optical sections. Bar=10μm.

J. GM130 recruitment was assayed by determining the fraction of total GFP-positive pixels in single optical sections (chosen to maximize mitochondrial representation) that colocalized with GM130 staining (n=3, ±SEM, >15 cells/experiment, *p<0.005).

K-P. HeLa cells expressing GFP-ActA (K-M), or G65-GFP-ActA (N-P) were BFA-treated for 30 min to disassemble the Golgi apparatus and processed to reveal GFP fluorescence, myc staining, and a merged image. Bar=10 μm.

A role for membrane association of GRASP65 N-terminus

GRASP65 is myristoylated at its N-terminus and this modification, together with GM130 binding, mediates GRASP65 localization to the Golgi membrane (Barr et al., 1998; Puthenveedu et al., 2006). Although the G65-GFP-ActA construct is expected to be N-myristoylated, the construct also has a C-terminal transmembrane anchor that would presumably make its membrane integration independent of myristoylation. Indeed, when the construct was modified by alanine substitution of the glycine acceptor site to prevent its myristoylation, the resulting construct, $G65^{G2A}$-GFP-ActA, was targeted to mitochondria as indicated by colocalization with Mitotracker™ staining (Fig 2-13A-D). Unexpectedly, however, $G65^{G2A}$-GFP-ActA failed to cause mitochondrial clustering as verified using radial profile analysis (Fig 2-13K) and also expression in mfn-/- cells (not shown). In light of the fact that previous studies of GRASP65 oligomerization-induced crossbridging were carried out in vitro using non-myristoylated protein (Wang et al., 2005; Wang et al., 2003), this result underscores the importance of demonstrating organelle tethering by GRASP65 in vivo.

Interestingly, the N-terminal myristoylation site in the GRASP family of proteins is mostly conserved and even in cases where it is missing, there seems to be an alternative mode of N-terminal membrane association. For example, the *S. cerevisiae* homologue contains an acetylated N-terminal amphipathic helix and *P. falcifarun* and *P. vivax* express splice variants with transmembrane signal anchors in place of the myristoylated N-terminus (Behnia et al., 2007; Struck et al., 2008). These observations suggest a critical role for membrane association of the N-terminus whether it is mediated by myristic acid or by other means. If so, the crossbridging activity of the non-myristoylated $G65^{G2A}$-GFP-ActA might be rescued by anchoring its N-terminus to the mitochondrial outer membrane. As a test, we generated T20-G65-GFP-Acta, which was expected to be N-terminally anchored but not myristoylated because the non-myristoylated TOM20 signal sequence was introduced at the N-terminus of the GRASP65 sequence. As a negative control, T20-GFP-ActA was generated, which contained both N- and C-terminal membrane anchors but lacked the GRASP65 sequence. Remarkably, expression of T20-G65-GFP-ActA induced mitochondrial clustering (Fig 2-13E-G, L), whereas the control construct T20-GFP-ActA did not (Fig 2-13H-J, M). These results demonstrate an additional role for the interaction of the GRASP65 N-terminus with membranes. Not only does

it contribute to stable membrane targeting (Barr et al., 1998), it is also critical for organelle tethering activity. The finding that the T0M20 signal sequence can substitute for the myristic acid contradicts a possibility in which the myristic acid at the GRASP65 N-terminus extends out and inserts in *trans* into adjacent membranes. Instead, the importance of N-terminal membrane association, taken together with the role of the N-terminal PDZ1 domain, argues that membrane insertion of the N-terminus activates and/or orients the PDZ1 binding groove so that it can carryout homotypic interactions in *trans*. This could obviate two potential problems for the homotypic tethering mechanism: interference by cis interactions in the membrane and interference by interactions with the soluble pool, if any. Indeed, over-expressed G65-myc yielded a clear cytosolic pattern yet this protein did not appear appreciably targeted to mitochondrial clusters bearing G65-GFP-ActA (Fig 2-12K-P). Thus, membrane association appears to regulate GRASP65 self-association.

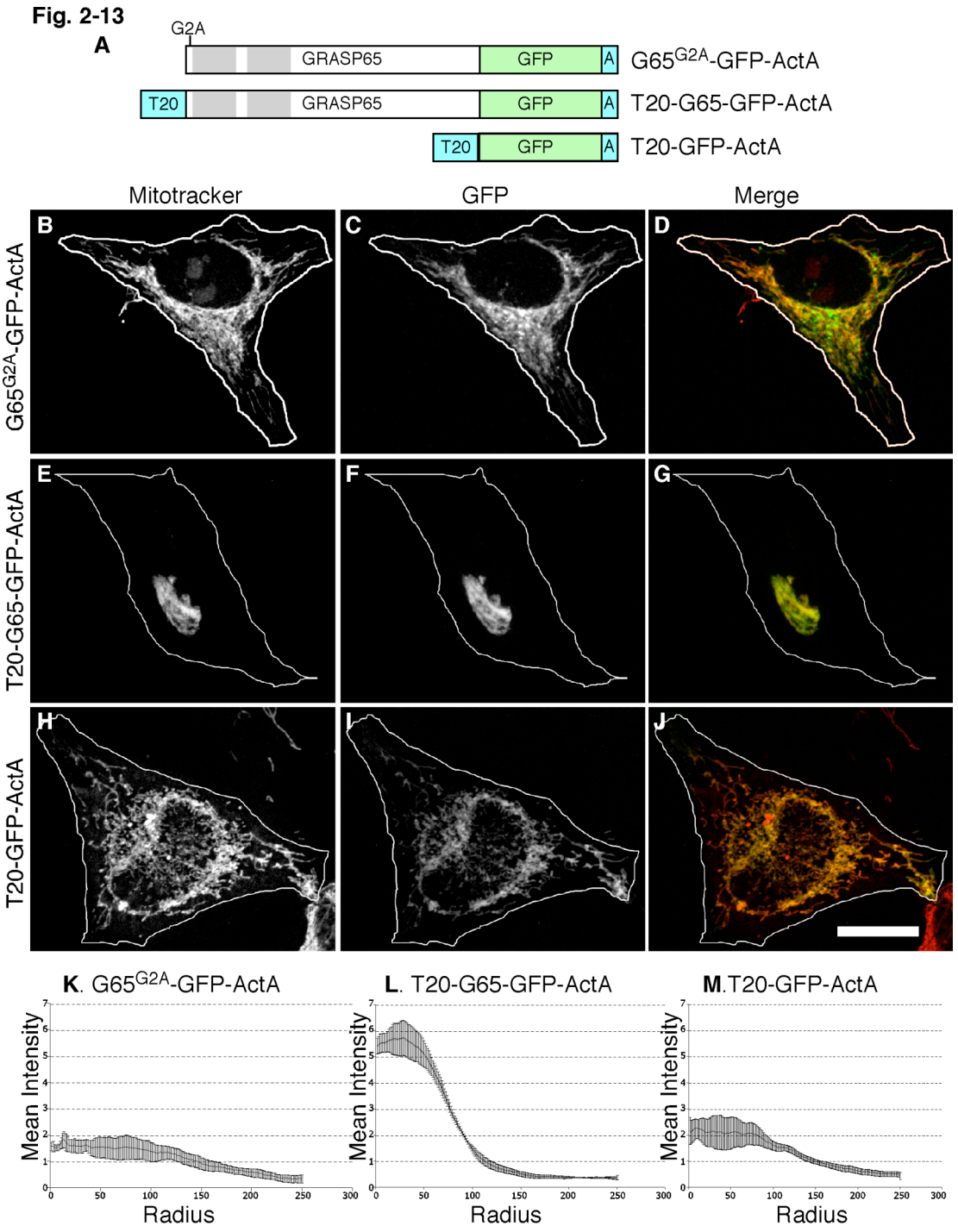

Figure 2-13 Membrane insertion of the GRASP65 N-terminus is required. Schematic diagram of the constructs (A). HeLa cells expressing G65^{G2A}-GFP-ActA (B-D,K), T20-G65-GFP-ActA (E-G,L), or T20-GFP-ActA (H-J,M) were BFA-treated and analyzed using Mitotracker (red), GFP fluorescence (green). and radial profile plots. Bar=10 μm

Discussion

The ability of GRASP65 to participate directly in organelle tethering was tested using two methods of targeting the protein to the cytoplasmic face of the mitochondrial outer membrane. Each yielded clustering of mitochondria in the absence of the microtubule cytoskeleton or an intact Golgi apparatus arguing that cluster formation was due to crossbridging connections formed by GRASP65. Indeed, the N-terminal domain of GRASP65, which mediates its homo-oligomerization (Wang et al., 2005), was required for mitochondrial clustering. Of the two PDZ-like domains present in the GRASP65 N-terminus, the first was found to be required for both GRASP65 self-interaction and for mitochondrial clustering. Some PDZ domains form oligomers involving a PDZ ligand in one partner binding the groove in the other or, alternatively, a back-to-back association that is independent of the binding groove and therefore not a bone fide PDZ interaction (Im et al., 2003a; Im et al., 2003b; Marfatia et al., 2000; Xu et al., 1998). To test the involvement of a bona fide PDZ interaction in GRASP65-mediated organelle tethering, the structure of the PDZ1 domain was computationally modeled allowing us to identify and mutate the putative PDZ1 binding groove. Mutation at this site blocked mitochondrial clustering confirming the specificity of the assay and strongly suggesting the novel involvement of a homotypic PDZ interaction in homotypic membrane tethering. Further, the same mutation blocked GRASP65-mediated Golgi ribbon formation arguing that the structure/function analysis carried out on the mitochondrial membrane recapitulates key aspects of Golgi membrane network formation and that GRASP65 acts as a homotypic organelle tether.

Homotypic interactions underlie homotypic tethering

Golgi membranes form a network that is subcompartmentalized such that there is extensive continuity within a subcompartment and little continuity between subcompartments. The model that GRASP65 is the tether for fusion of cis Golgi membranes is appealing because a homotypic interaction mediates crossbridging of like membranes. This is conceptually analogous to homotypic mitofusin interactions in homotypic fusion of mitochondria (Koshiba et al., 2004). Because the GRASP65 interaction is a PDZ-ligand type interaction it raises the possibility that crossbridging is stabilized by reciprocal interactions in which each PDZ domain contributes a ligand that associates with the binding groove of the partner. Alternatively, a higher order set of interactions may take place in which a PDZ domain contributes a ligand to one partner and a

binding groove to another. In either case, because it is homotypic, the interaction is likely to involve two-fold symmetry. Our data also suggest that the interaction involves an internal PDZ ligand rather than a more typical C-terminally positioned ligand. Whereas the terminal carboxylic acid in a C-terminally positioned ligand is coordinated by a conserved GLGF motif in the PDZ domain (Harris and Lim, 2001; Hung and Sheng, 2002), the C–terminus is replaced by a sharp β turn or loop structure in an internal ligand (Brenman et al., 1996; Christopherson et al., 1999; Gee et al., 1998; Harris et al., 2001). This key structural feature can be highly degenerate in sequence making identification difficult. The mechanism of homotypic membrane fusion at sites of contact formed by GRASP65 crossbridging remains to be determined but it is noteworthy that GM130, which stabilizes GRASP65 on the Golgi membrane, interacts with the SNARE protein syntaxin-5 (Diao et al., 2008) suggesting that this interaction may coordinate tethering with fusion.

Membrane contact may regulate GRASP65 interactions

Membrane recruitment and tethering activity of GRASP65 requires two contact points with the organellar membrane. The first contact is binding to the GM130 C-terminus. GM130 is required for GRASP65 Golgi localization (Kodani and Sutterlin, 2008; Puthenveedu et al., 2006). Recruitment of endogenous GRASP65 by a mitochondrial GM130 C-terminus was sufficient for mitochondrial clustering and the same deletion of ten amino acids that disrupts GM130 function in Golgi ribbon formation (Puthenveedu et al., 2006) blocked clustering activity. These amino acids are required for GM130 to bind GRASP65 (Barr et al., 1998) and, as expected, in their absence GM130 failed to recruit GRASP65 to the mitochondrial outer membrane. Thus, the results support a model in which GM130 recruits GRASP65 to the Golgi membrane and the recruited GRASP65 is the active factor in tethering.

The second point of membrane contact is the myristoylated GRASP65 N-terminus. Under normal circumstances, membrane targeting of GRASP65 requires myristoylation in conjunction with GM130 binding (Barr et al., 1998). The N-terminal myristic acid is immediately adjacent to the PDZ1 module. Mutation of the glycine residue that becomes myristoylated blocked G65-GFP-ActA-mediated mitochondrial clustering, but this construct has its own membrane anchor and the myristoylation site was not needed for its stable membrane association. Thus, the

requirement for myristoylation suggests that the N-terminus must be imbedded in the membrane and, indeed, substituting a transmembrane domain restored tethering. It can be further argued that the myristic acid is not needed for proper folding or even for the homotypic interaction, per se, because non-myristoylated GRASP65, purified after expression in bacteria, retains oligomerization activity (Wang et al., 2005). In the cellular context, however, membrane association may facilitate the interaction. One idea is that N-terminal anchoring positions the binding groove such that it faces the cytosol favoring *trans*-pairing over *cis*-pairing. Another possibility, not mutually exclusive, is that membrane association triggers a conformational change that activates GRASP65 for binding, thereby preventing soluble GRASP65 from inadvertently inhibiting the trans pairing interactions. In sum, these findings uncover a direct functional role, beyond membrane targeting, for anchoring the GRASP65 N-terminus.

Functional divergence of GRASP isoforms may maintain subcompartment identity

Mammals and other vertebrates that form Golgi ribbon networks express two GRASP proteins. GRASP65 is principally localized to the cis Golgi whereas GRASP55 is localized to medial and trans cisternae (Shorter et al., 1999). In common with GRASP65, GRASP55 has a tandem arrangement of PDZ-like domains at its N-terminus (Shorter et al., 1999) and GRASP55 is required for Golgi ribbon formation (Feinstein and Linstedt, 2008). Each protein interacts with itself but does not interact with the other GRASP (data not shown) suggesting specificity-conferring differences in the PDZ1 domain of each molecule. Thus, it is likely that GRASP65 and GRASP55 act in parallel reactions with GRASP65 supporting membrane fusion to laterally link and elongate cis cisternae and GRASP55 doing the same for medial cisternae. From an evolutionary perspective, functional divergence of the GRASP PDZ domains after gene duplication may have been a necessary step to maintain Golgi subcompartments once microtubule-based motility brought Golgi ministacks into close proximity in the region of the microtubule organizing center. PDZ modules are well suited as divergence in the PDZ1 binding groove and ligand, and also in the interactions determining compartmental localization, would confer specificity such that lateral fusion within the membrane network is specific between cis and medial subcompartments.

GRASP65 and GRASP55 were initially characterized as requirements for stacking Golgi cisternae in an in vitro assay (Barr et al., 1997; Shorter et al., 1999). Subsequently it was observed that Golgi stacks persist after effective GRASP knockdown (Feinstein and Linstedt, 2008; Puthenveedu et al., 2006; Sutterlin et al., 2005). While the mechanism elucidated here could also underlie cisternal stacking, this would place a homotypic interaction in a heterotypic membrane linkage. Further, we noted that the ultrastructure of the juxtaposed mitochondrial membranes linked by G65-GFP-ActA was distinct from the parallel less than 15 nm (Mollenhauer and Morre, 1991) spacing present in Golgi stacks. Even so, given its ability to bridge membranes by self association and the inherent slop in protein targeting, it is arguable that to some extent GRASP65 participates in linking cisternae, not just laterally, but also in a stacked configuration. A possible explanation for the predominate role of the GRASP proteins in lateral homotypic Golgi connections is that membrane insertion and orientation of PDZ1 might render its binding curvature sensitive such that ligand binding by PDZ1 is favored at the highly curved rim regions and disfavored at the relatively flat intra-cisternal contacts within a ministack. The enrichment of the GRASP65 binding partner GM130 at the rim regions of cis cisternae is consistent with this (Marra et al., 2001). Intriguingly, the clustered mitochondria that we observed using electron microscopy exhibited regions of high and low curvature and the closest points of contact were frequently present at zones of highest curvature.

In lower eukaryotes a single GRASP gene is present and Golgi membranes, even when present as stacked cisternae, are neither confined to a central position nor fused laterally to form a ribbon-like membrane network. Nevertheless, the yeast GRASP homologue possesses an acetylated N-terminal amphipathic helix adjacent to a PDZ-like domain indicating conservation, via an alternative mechanism, of membrane anchoring and suggesting a commonality in mechanism (Behnia et al., 2007). Possibly, ribbon formation in vertebrates is a more extreme form of cisternal elongation carried out by lower eukaryotes. If so, homotypic membrane tethering mediated by membrane anchored PDZ1 could represent the fundamental mechanism of GRASP65 action. The physical distance separating cisternae or ministacks may contribute to prevention of lateral fusion which, given the presence of only a single GRASP, might otherwise impair maintenance of subcompartment identity. Recent observations indicate that the GRASP present in *Dictyostelium* and *Drosophila* is required in developmentally specific steps involving

non-conventional secretion (Kinseth et al., 2007; Schotman et al., 2008). It is not yet clear whether this activity involves PDZ1-mediated membrane tethering.

In summary, our results indicate a direct role for GRASP65 in Golgi membrane network formation and, for the first time, identify a PDZ interaction as a membrane tethering mechanism. Homotypic PDZ-mediated membrane crossbridging provides a compelling view of how subcompartments are maintained in the Golgi network and suggests modes of regulation that uncouple Golgi ministacks to promote mitotic entry and subsequent Golgi partitioning.

Material and Methods

Constructs

For GFP-ActA, residues 599-624 of the ActA protein from *Listeria Monocytogens* were cloned into the *HindIII* and *BamHI* sites of pEGFP-C1 (Clontech). GRASP65 was then inserted upstream of EGFP using an *NheI* site to yield G65-GFP-ActA. mCherry was substituted for GFP using *Age1* and *Sac1* sites to yield mCherry-ActA and G65-mCherry-ActA, respectively. PDZ1 (residues 6-74) and/or PDZ2 (residues 85-167) were deleted using a PCR-based loop-out modification of the Quickchange protocol (Stratagene). Point mutations were introduced using Quickchange. For TOM20-GFP, four rounds of loop-in PCR yielded TOM20 (residues 1-47) upstream of EGFP in pEGFP-C1. GM130 (residues 788-888) was inserted into *BamHI* and *HindIII* sites to yield TOM20-GFP-GM130^{Cterm}. A stop codon (position 878) by Quickchange yielded TOM20-GFP-GM130$^{C\Delta 10}$. For GST-G65, GRASP65 was inserted into the EcoRI site of pGEX-4T-1 (GE Lifesciences). Quickchange introduced a stop codon for GST-G65$^{1-212}$. Deletion of the PDZ domains was as above. For GST-G65^{PDZ1}, GRASP65 (residues 6-74) was inserted into pGEX-2T using the BamHI and EcoRI sites. For G65-myc, GRASP65 was inserted into pCS2-MT (Turner and Weintraub, 1994). For G65-His, GRASP65 was inserted into the EcoR1 site of pRSET-B (Invitrogen) followed by removal and reinsertion of the N-terminal hexahistidine tag to achieve a C-terminal position.

Cell culture and immunofluorescence

HeLa cells were grown in Minimal Essential Medium and mitofusin null cells were grown in Dulbecco's Modified Eagle's Medium containing 5μg/ml of uridine (Sigma). The media also contained 10% fetal bovine serum (Atlanta Biological) and 100 IU/ml of penicillin and streptomycin (Sigma) and the cells were maintained at 37^{o}C in a 5% CO_2 incubator. Transient transfection of HeLa was carried out with Transfectol (Genechoice) according to manufacturers specifications and after 24 h the cells were labeled by adding Mitotraker (Invitrogen) to 15 nM for 30 min and fixed. Transient transfection of mitofusin null cells was with LIPO2000 (Invitrogen) according to manufacturers specifications and fixation was after 24 h. Paraformaldehyde fixation and immunofluorescence staining were as described (Jesch and Linstedt, 1998). Antibodies were: rabbit anti-GM130 (Puthenveedu and Linstedt, 2001), mouse

anti-giantin (Linstedt and Hauri, 1993), and Alexa-568 or Cy5-conjugated anti- secondary antibodies (Invitrogen). Knockdown of GM130 by RNA interference was as described (Puthenveedu et al., 2006). The GRASP65 sequence targeted by siRNA was AAAAGAGATCACTGTTTAAGT. For gene replacement, transfection was carried out with 60 nM chemically synthesized siRNA (Ambion) using Oligofectamine (Invitrogen). After 24 h, the cells were transfected with plasmids using Transfectol (GeneChoice). After another 24 h the cells were re-transfected siRNA and, after another 24 h, Golgi fragmentation was analyzed. For cell fusion, HeLa cells were transfected using JetPIE (Polyplus-transfection), and after 24 h, trypsinized and seeded in 1:1 ratios. After 16-24 h, the cells were treated for 30 min with 20μg/ml cyclohexamide (Sigma-Aldrich) and then 30 sec with 45% polyethylene glycol (Roche) in DMEM. After 5 washes with DMEM the cells were cultured for 3 h in the continued presence of cyclohexamide and then fixed and analyzed.

Image capture and analysis

Microscopy was performed using a spinning disk confocal scan head equipped with three-line laser and independent excitation and emission filter wheels (PerkinElmer) and a 12-bit Orca ER digital camera (Hamamatsu) mounted on an Axiovert 200 microscope with a 100x, 1.4 NA oil-immersion objective (Carl Zeiss MicroImaging, Inc.). Sections at 0.3 μm spacing were acquired using Imaging Suite software (PerkinElmer). The "Radial profile analysis" plugin of ImageJ (rsbweb.nih.gov/ij) was used after background subtraction and selecting the region of interest using the wand function. The "Co-localization" plugin of ImageJ used single optical sections chosen to maximize mitochondrial representation (Guo et al., 2008). Fluorescence recovery after photobleaching was carried out using a Carl Zeiss LSM 510 Meta/ UV DuoScan Inverted Spectral Confocal Microscope system. Fluorescence was bleached to 20% of its initial value and recovery was monitored for 120 sec at intervals of 10 sec.

Protein purification & binding assays

Proteins were purified and eluted from glutathione agarose as described (Guo et al., 2008). For the binding assays, HeLa cells were transiently transfected with G65-myc and harvested 24-48 hours post-transfection in lysis buffer (10mM HEPES pH 7.2, 100mM KCl, 1% Triton X-100, 1mM DTT) in the presence of protease inhibitors. Lysates were pre-cleared with glutathione-

agarose beads and then rotated 2 hr at 4°C with 50 μg of purified protein. Complexes were collected by addition of 10μl glutathione-agarose beads, rotation for 1 hr at 4°C, and centrifugation in a microfuge. The isolated beads were washed 4 times with 1 ml PBS containing 1mM DTT and 0.1% Tween-20 and analyzed by immunoblot and enhanced chemiluminescence using a LAS-3000 digital camera and ImageGauge software (Fujifilm). G65-His was purified using Ni-NTA beads (Invitrogen) and the manufacturer's protocol from BL21(DE3)-pLysS cells cotransformed with pBB131 encoding N-myristoyltransferase (Duronio et al., 1990) that were IPTG-induced in the presence of 200 μM myrstic acid. After elution and dialysis against binding buffer (20mM HEPES, 200mM KCl, 1mM EDTA, 0.01% Triton-100, 1.4mM β-mercaptoethanol), the purified G65-His was incubated for 4 h at 4°C in a 200μl volume with GST or GST-PDZ1 immobilized on 5μl of glutathioune beads in the presence of 10 μg bovine serum albumin and protease inhibitors. Recovery of G65-His on the beads after washing was analyzed by immunoblot using an anti-His antibody (Bethyl Laboratories).

CHAPTER 3: Mitotic inhibition of GRASP65 organelle tethering involves PLK1 phosphorylation proximate to an internal PDZ ligand

Abstract

GRASP65 links cis Golgi cisternae via a homotypic, N-terminal PDZ interaction. Its mitotic phosphorylation by cyclin-dependent kinase 1/cyclin B (CDK1) disrupts this activity. Neither the identity of the PDZ ligand involved in GRASP65 self-interaction nor the mechanism by which phosphorylation inhibits its interaction is known. Phospho-mimetic mutation of the known CDK1 sites, all of which are in the C-terminal "regulatory domain" of the molecule, failed to block organelle tethering. However, we identified a site phosphorylated by Polo-like kinase 1 (PLK1) in the GRASP65 N-terminal domain for which mutation to aspartic acid blocked tethering and alanine substitution prevented mitotic Golgi unlinking. Further, using interaction assays, we discovered an internal PDZ ligand adjacent to the PLK phosphorylation site that was required for tethering. As PLK1 is known to bind mitotic GRASP65, these results support at two-step model of phospho-inhibition in which CDK1 or other kinases first create a binding site for PLK1 and then PLK1 directly inhibits the PDZ ligand underlying the GRASP65 self-interaction.

Introduction

The Golgi apparatus, which exists as a single copy organelle in higher eukaryotes, fragments in a stepwise fashion into vesicles and vesicle clusters that are partitioned into daughter cells during mitosis (Lucocq *et al.*, 1987; Misteli and Warren, 1995; Jesch and Linstedt, 1998; Kano *et al.*, 2000; Hidalgo Carcedo *et al.*, 2004; Feinstein and Linstedt, 2007). The organelle is present during interphase as interconnected ministacks forming a ribbon-like membrane network. In late G2 phase of the cell cycle, the ribbon becomes unlinked resulting in multiple ministacks clustered around the microtubule organizing center (Puthenveedu *et al.*, 2006; Colanzi *et al.*, 2007; Feinstein and Linstedt, 2007, 2008). From prophase to metaphase the unlinked ministacks vesiculate and the vesicles largely disperse with some vesicles aggregating to form vesicle clusters (Lucocq *et al.*, 1989; Jesch *et al.*, 2001b). Interestingly, in addition to being a consequence of mitotic regulation, Golgi fragmentation also appears to play a causal role. Failure of Golgi unlinking in G2 phase delays mitotic entry possibly serving as a checkpoint (Sutterlin *et al.*, 2002; Hidalgo Carcedo *et al.*, 2004; Feinstein and Linstedt, 2007).

Aspects of the mechanism underlying Golgi unlinking are beginning to emerge in part due to a better understanding of Golgi ribbon formation (Puthenveedu *et al.*, 2006; Rabouille and Kondylis, 2007; Feinstein and Linstedt, 2008). Ribbon formation requires GRASP65 and GRASP55, which are localized to cis and medial Golgi cisternae, respectively (Puthenveedu *et al.*, 2006; Feinstein and Linstedt, 2008). GRASP65 is associated with the membrane via both binding to GM130 and insertion of its myristoylated N-terminus (Barr et al., 1998; Puthenveedu et al., 2006). GRASP55 binds golgin-45 and other proteins on the Golgi and is myristoylated and palmitoylated (Kuo *et al.*, 2000; Short *et al.*, 2001). Each GRASP self-associates and this underlies homotypic tethering of adjacent ministacks (Feinstein and Linstedt, 2008; Puthenveedu et al., 2006; Sengupta et al., 2009; Wang et al., 2005; Xiang and Wang, 2010). Oligomer formation depends on the conserved tandem PDZ-like domains at the N-terminus referred to as the GRASP domain and point mutations in the predicted binding groove of GRASP65's first PDZ domain, PDZ1, block tethering activity and Golgi ribbon formation (Wang *et al.*, 2005; Sengupta *et al.*, 2009). Experiments suggest that GRASP65 is oriented on the membrane in such a way that it favors self-interaction in *trans* (Bachert and Linstedt, 2010), but the identity of the PDZ ligand is unknown.

Cyclin-dependent kinase 1/cyclin B (CDK1), a MEK/ERK cascade, and Polo-like kinase 1 (PLK1) contribute to mitotic Golgi breakdown and each phosphorylates one or both GRASP proteins (Acharya *et al.*, 1995; Acharya *et al.*, 1998; Kano *et al.*, 2000; Jesch *et al.*, 2001a; Sutterlin *et al.*, 2002; Feinstein and Linstedt, 2007). ERK directly phosphorylates GRASP55 and inhibition of its upstream activator MEK1 blocks both GRASP55 phosphorylation and G2 phase Golgi unlinking (Jesch *et al.*, 2001a; Feinstein and Linstedt, 2007, 2008). Further, mutation of ERK phosphorylation sites in GRASP55 to mimic the phosphorylated state blocks GRASP55 activity in both Golgi ribbon formation and self-association (Bisel et al., 2008; Feinstein and Linstedt, 2008). Thus, GRASP55 phosphorylation drives Golgi unlinking by blocking *trans* complexes involved in membrane tethering. This model also applies to GRASP65. It is directly phosphorylated by CDK1, ERK and PLK1 and phosphorylation blocks its homo-oligomerization (Lin *et al.*, 2000; Sutterlin *et al.*, 2001; Wang *et al.*, 2003; Yoshimura *et al.*, 2005). However, the direct involvement of these kinases and their phosphorylation sites has not been established. Further, phospho-regulation of the GRASP proteins occurs outside the GRASP domain in a long non-conserved segment referred to as the serine-proline-rich regulatory domain (Jesch *et al.*, 2001a; Wang *et al.*, 2003; Wang *et al.*, 2005; Yoshimura *et al.*, 2005). It is unclear how phosphorylation of the C-terminal domain regulates this tethering activity of the N-terminal self-interacting domain.

In considering GRASP65 phosphorylation by multiple kinases we were intrigued that the PLK family of kinases initially bind substrate and become activated through their Polo box domains. The Polo box domain binds to a phospho-serine/threonine motif that includes proline, S-[pS/pT]-P, and then the kinase can phosphorylate distant sites (Elia *et al.*, 2003; Barr *et al.*, 2004; Lowery *et al.*, 2005). Because CDK1 and ERK phosphorylate serine or threonine residues adjacent to proline it could be that GRASP phosphorylation by these kinases creates a binding site in the C-terminal domain for PLK1. Indeed, PLK1 binds the GRASP65 C-terminal domain under mitotic conditions (Preisinger *et al.*, 2005). Thus, recruitment of PLK1 to the GRASP C-terminal domain could activate PLK1 for phosphorylation of additional sites, perhaps including in the GRASP domain to directly block tethering.

To test whether either CDK1or PLK1 directly inhibits GRASP65-mediated organelle tethering, we mutated the known CDK1 sites and mapped and mutated a novel PLK1 site and assayed the

tethering activity of GRASP65 using a recently described assay on the outer membrane of mitochondria (Sengupta *et al.*, 2009). Only a phospho-mimic mutation of the PLK1 site blocked tethering and the same mutation blocked Golgi ribbon formation in a gene replacement assay. We also mapped the PDZ ligand underlying GRASP65 self-interaction and found that it was next to the PLK1 site. Altogether, the results support a model in which phosphorylation by PLK1 alters the activity of an adjacent internal PDZ ligand so that it can no longer bind the PDZ1 groove of a GRASP65 molecule on an apposing membrane.

Results

Phospho-mimic mutations of GRASP65 CDK1 sites do not block tethering

To test whether CDK1-mediated phosphorylation directly blocks tethering by GRASP65, we converted all potential CDK1 sites in the C-terminal domain to aspartic acid to mimic the phosphorylated state. The resulting construct, $G65^{7XD}$-GFP-ActA, also contained GFP and the mitochondrial targeting sequence ActA appended to its C-terminus (Fig 3-1A). As previously described (Sengupta *et al.*, 2009), a control GFP-ActA sequence localized to the mitochondrial outer membrane yielding a "hyphal" pattern colocalized with mitochondrial markers such as Mitotracker™ (Fig 3-1B-D). In contrast, G65-GFP-ActA induced mitochondrial clustering (Fig 3-1E-G), which was previously shown to involve its self-interaction in *trans* (Sengupta *et al.*, 2009). Mitochondrial clustering was also evident for $G65^{7XD}$-GFP-ActA (Fig 3-1H-J). These results were quantified for multiple cells by determining the fluorescence distribution in concentric circles emanating from the centroid of mitochondrial fluorescence. Whereas the radial profile of fluorescence in control cells was uniform, there was strong clustering of the fluorescence in cells expressing G65-GFP-ActA and $G65^{7XD}$-GFP-ActA (Fig 3-1K-M). Thus, phospho-mimic mutations of the GRASP65 CDK1 sites did not block tethering prompting us to search for sites elsewhere in the molecule that directly inhibit its organelle tethering activity.

PLK1 phosphorylation of GRASP65 S189 blocks tethering and Golgi ribbon formation

To test whether PLK1 might directly inhibit GRASP65 tethering we identified and mutated three phosphorylation sites matching the PLK1 substrate consensus sequence E-X-S/T-Φ, where X is any residue and Φ is hydrophobic (Nakajima *et al.*, 2003). One of these, S189 yielded no effect when mutated to alanine to prevent phosphorylation (Fig 3-2A-C) but potently blocked clustering when mutated to aspartic acid to mimic phosphorylation (Fig 3-2D-F). The result was confirmed for cell populations using the radial profile algorithm (Fig 3-2G-H). The fact that alanine substitution at the same position did not interfere argues that loss of tethering for S189D was due to mimicking the phosphorylated state rather than perturbed protein folding. Interestingly, multiple sequence alignment indicates that S189 is conserved in organisms with mitotically disassembled Golgi ribbons but not others (Fig 3-2I).

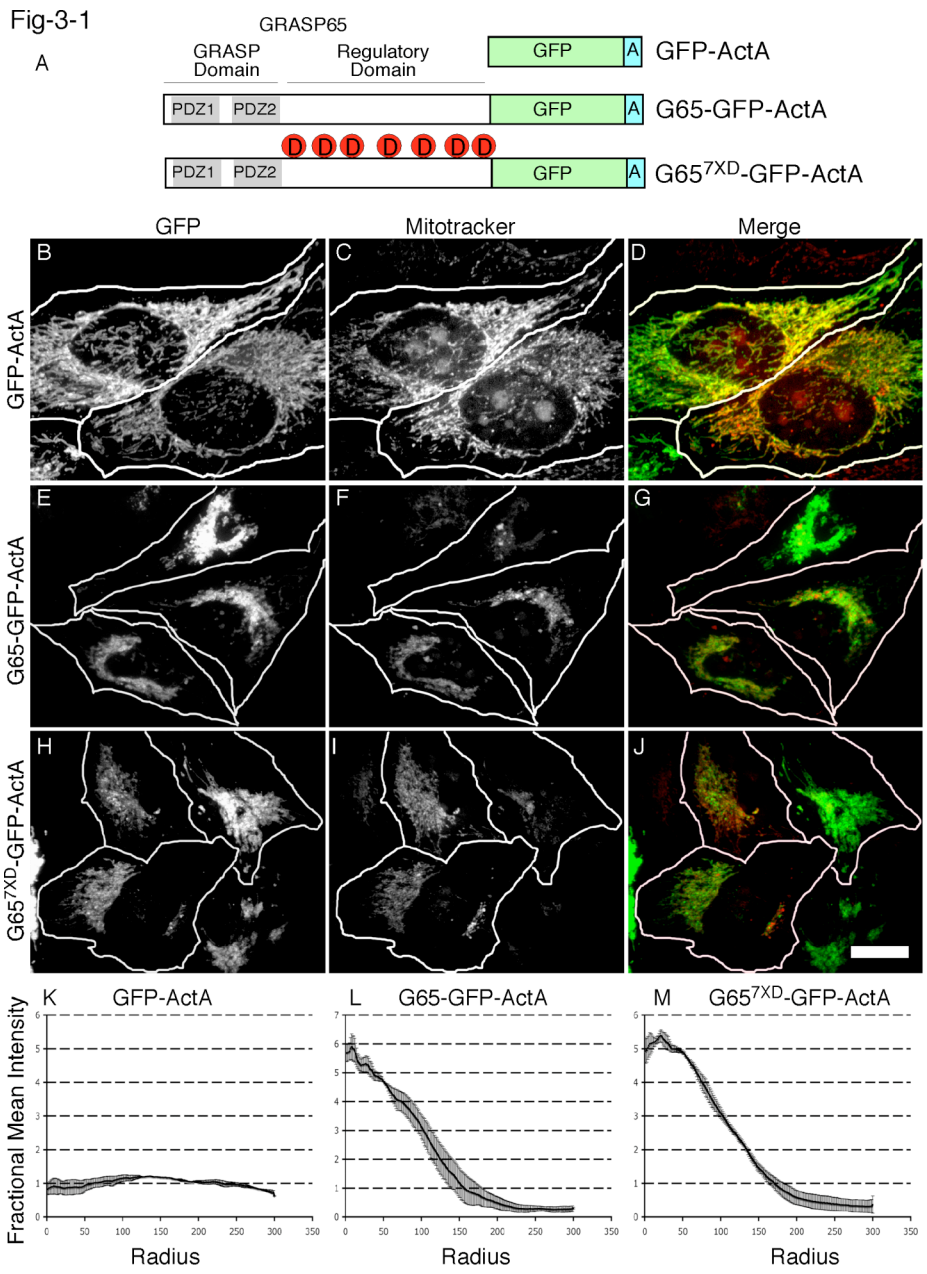

Figure 3-1 Phospho-mimic mutations of mapped CDK1 sites of GRASP65 fail to block tethering. Schematic diagram of the constructs used (A). HeLa cells expressing GFP-ActA (B-D), G65-GFP-ActA (E-G) and G65^{7XD}-GFP-ActA (H-J) were analyzed 24 h post-transfection using Mitotracker to stain mitochondria (C,F,I) and GFP fluorescence to localize the transfected proteins (A,D,G). A false-colored, merged image is also shown (Mitotracker and GFP are red and green, respectively).. Radial profile plots show the spread of mitochondrial fluorescence starting from the centroid and extending to the cell periphery for cells expressing GFP-ActA (K), G65-GFP-ActA (L), or G65^{7XD}-GFP-ActA (M). Analysis was carried out after a 30 min BFA treatment Values are averages corresponding to the fraction of total fluorescence present in each concentric circle drawn from the centroid (n=3, SEM, >15 cells/experiment). Bar=10 μm.

Because phosphorylation of S189 had not been previously described, we tested for phosphorylation of this site by PLK1. Purified proteins were used rather than a cell-based assay so that we could test for direct phosphorylation. Further, in cells, GRASP65 is phosphorylated on many sites by multiple kinases making it difficult to test a single site. GRASP65 was His-tagged at its C-terminus and purified out of bacteria using nickel-agarose beads. The purified preparation was incubated with ATP in the presence and absence of purified PLK1. Phosphorylation was detected when PLK1 was present using an anti-phospho-serine antibody and this was inhibited by the S189A mutation (Fig 3-3). Thus, S189 of GRASP65 is directly phosphorylated by PLK1.

Having mapped a PLK1 phosphorylation site on GRASP65 that inhibits its tethering activity, we sought to test its role in Golgi ribbon formation using gene replacement after siRNA-mediated knockdown of GRASP65. GRASP65 knockdown and rescue were carried out as previously described (Sengupta *et al.*, 2009). Cells depleted of GRASP65 exhibited fragmented Golgi ribbons and this phenotype was rescued by expressing an siRNA resistant version of GRASP65 tagged at its C-terminus with the myc epitope (Fig 3-4A-C). In contrast, a rescue construct containing the S189D substitution, $G65^{S189D}$-myc failed to rescue (Fig 3-4D-F). This construct appeared stably targeted to the fragmented Golgi membranes suggesting proper folding. Further, alanine substitution at the same site yielded a construct, $G65^{S189A}$-myc, which promoted rescue to the same extent as wildtype (Fig 3-4 G-I). Thus, GRASP65 tethering activity is dependent on the phosphorylation state of S189.

Phosphorylation of GRASP65 S189 is required for cell cycle-dependent Golgi unlinking and fragmentation.

PLK1 is activated late in the G2 phase of the cell cycle (Golsteyn *et al.*, 1994; Macurek *et al.*, 2008) the time of Golgi unlinking (Hidalgo Carcedo *et al.*, 2004; Feinstein and Linstedt, 2007). To test whether GRASP65 phosphoinhibition at S189 is required for Golgi unlinking we assayed Golgi unlinking in cells expressing GRASP65-myc, $G65^{S189A}$-myc and $G65^{S189D}$-myc. Synchronized cells were arrested in late G2 using olomoucine II, which is an inhibitor of CDK1. Consistent with previous work (Feinstein and Linstedt, 2007), fragmented Golgi ribbons were observed in 60% of control cells and also cells expressing wildtype G65 (Fig 3-5A,B,G). Cells

Fig 3-2

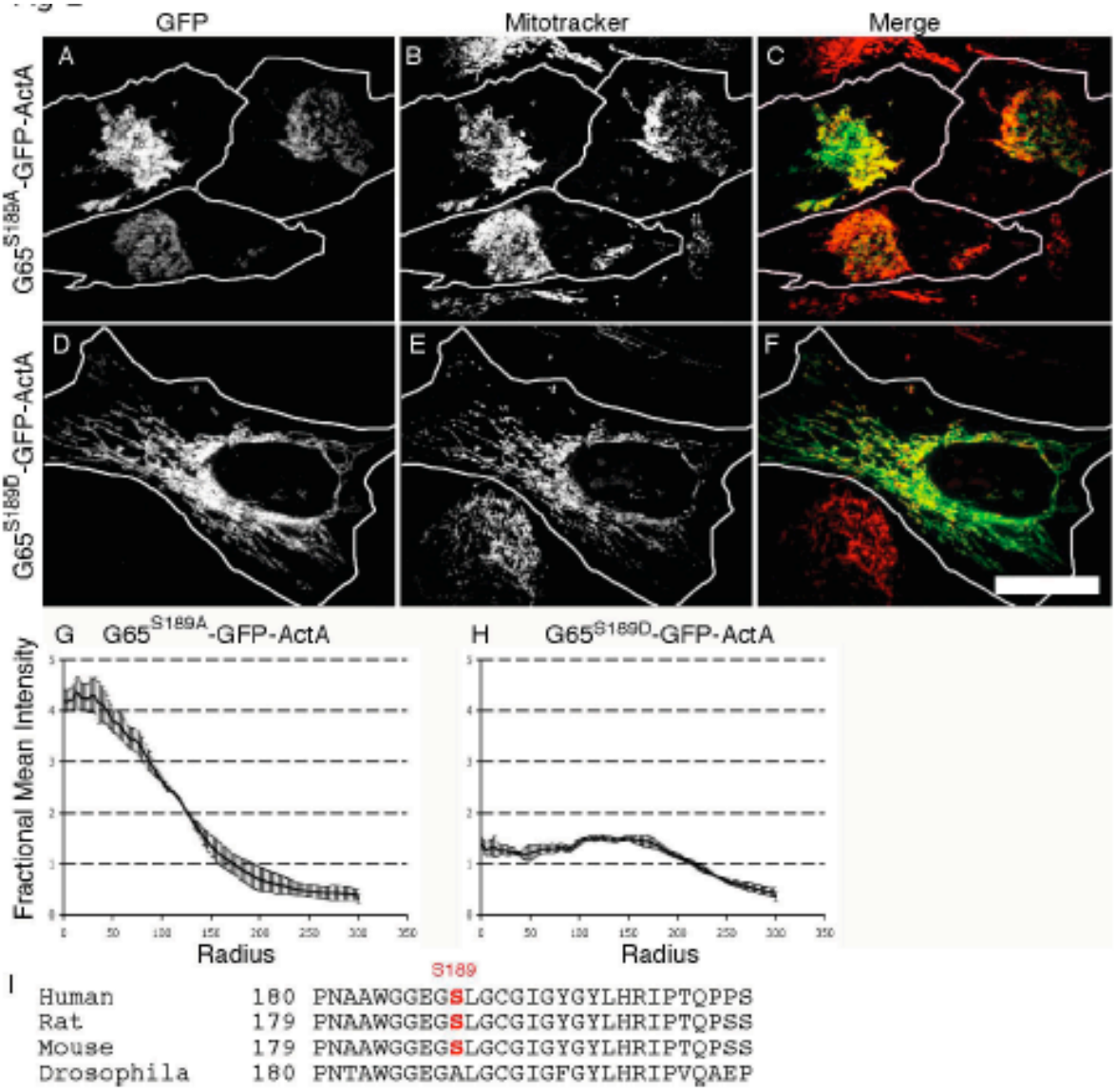

Figure 3-2 Phospho-mimic mutation S189 inhibits GRASP65 tethering activity. HeLa cells expressing G65^{S189A}-GFP-ActA (A-C) and G65^{S189D}-GFP-ActA (D-F) were analyzed 24 h post-transfection using Mitotracker to stain mitochondria (B,E) and GFP fluorescence (A,D) to localize the transfected proteins. A false-colored, merged image is also shown (Mitotracker and GFP are red and green, respectively). Analysis was also carried out after a 30 min BFA treatment (G,H). Bar=10 μm. Radial profile plots show the spread of mitochondrial fluorescence starting from the centroid and extending to the cell periphery for cells expressing G65^{S189A}-GFP-ActA (G) or G65^{S189D}-GFP-ActA (H). Also shown is a sequence alignment indicating conservation of S189 in higher eukaryotes (I).

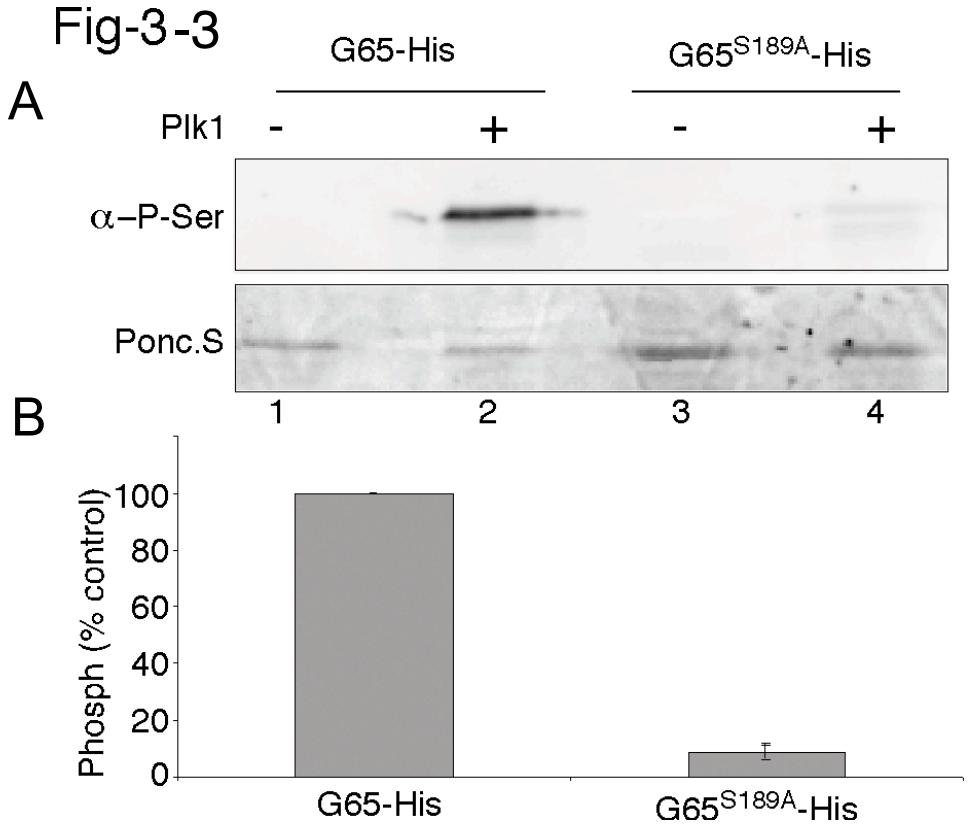

Figure 3-3 PLK1 phosphorylates GRASP65 S189. The reactivity to phospho-serine specific antibody was determined for equivalent amounts (1μg) of purified G65-His and G65^{S189A}-His after incubation in the presence or absence of active PLK1 kinase (A). Ponceau S staining shows amount of protein present. Phosphorylation was quantified (B) by determining the signal intensity normalized to G65-His (n=3, ±SD, $p<0.01$).

Fig-3-4

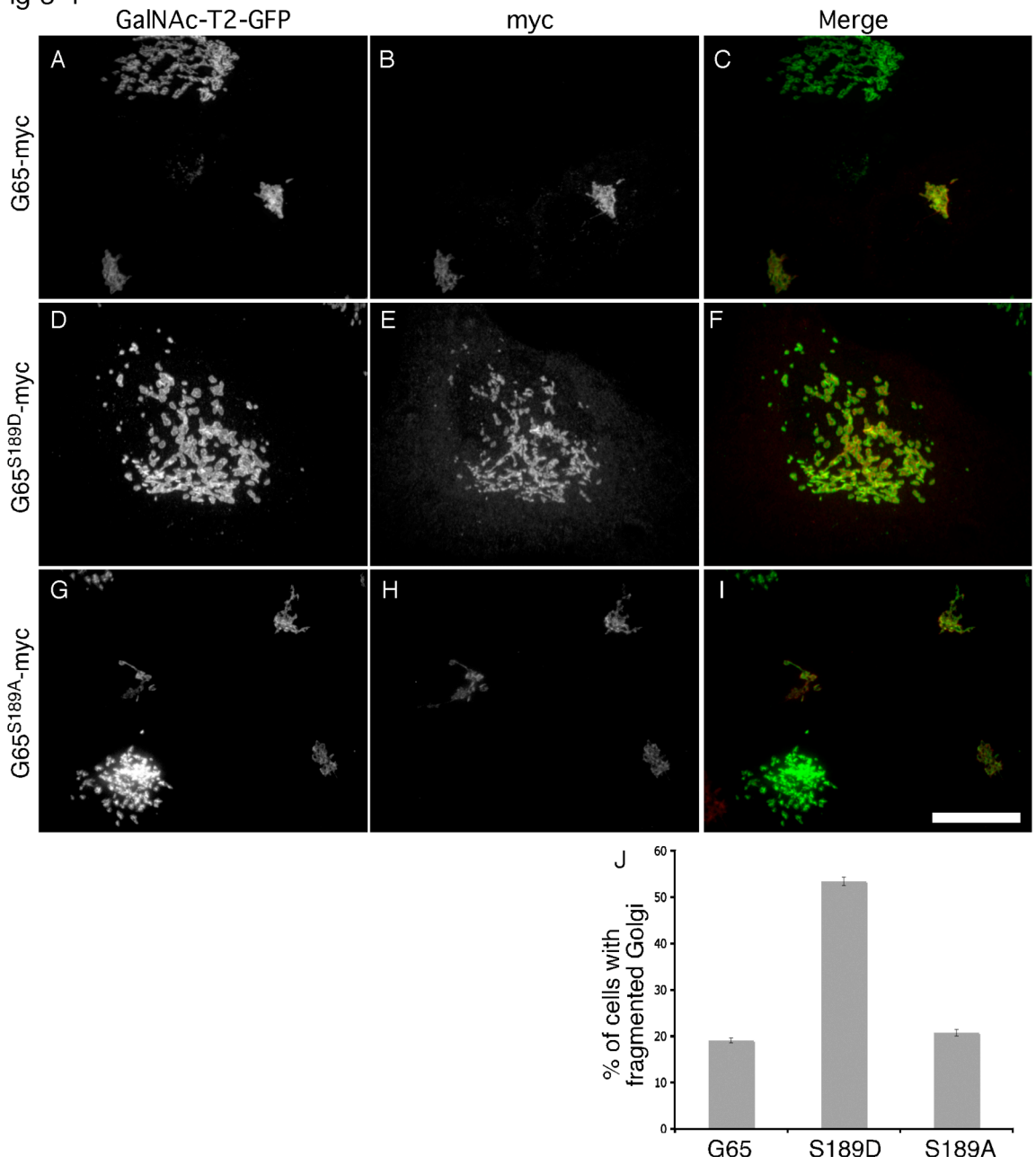

Figure 3-4 Phospho-mimic GRASP65^{S189D} fails to rescue Golgi ribbon formation. HeLa cells expressing GalNAcT2-GFP and transfected with GRASP65 siRNA and siRNA resistant forms of G65-myc (A-C), G65^{S189D}-myc (D-F), or G65^{S189A}-myc (G-I) were analyzed to assess Golgi morphology (green) and replacement construct expression (red). Bar=10μm. Percentage of cells (J) expressing G65-myc, G65^{S189D}-myc or G65^{S189A}-myc exhibiting a fragmented Golgi after knockdown with GRASP65 siRNAs (±SEM, n=4, >100 cells in each, $p< 0.01$).

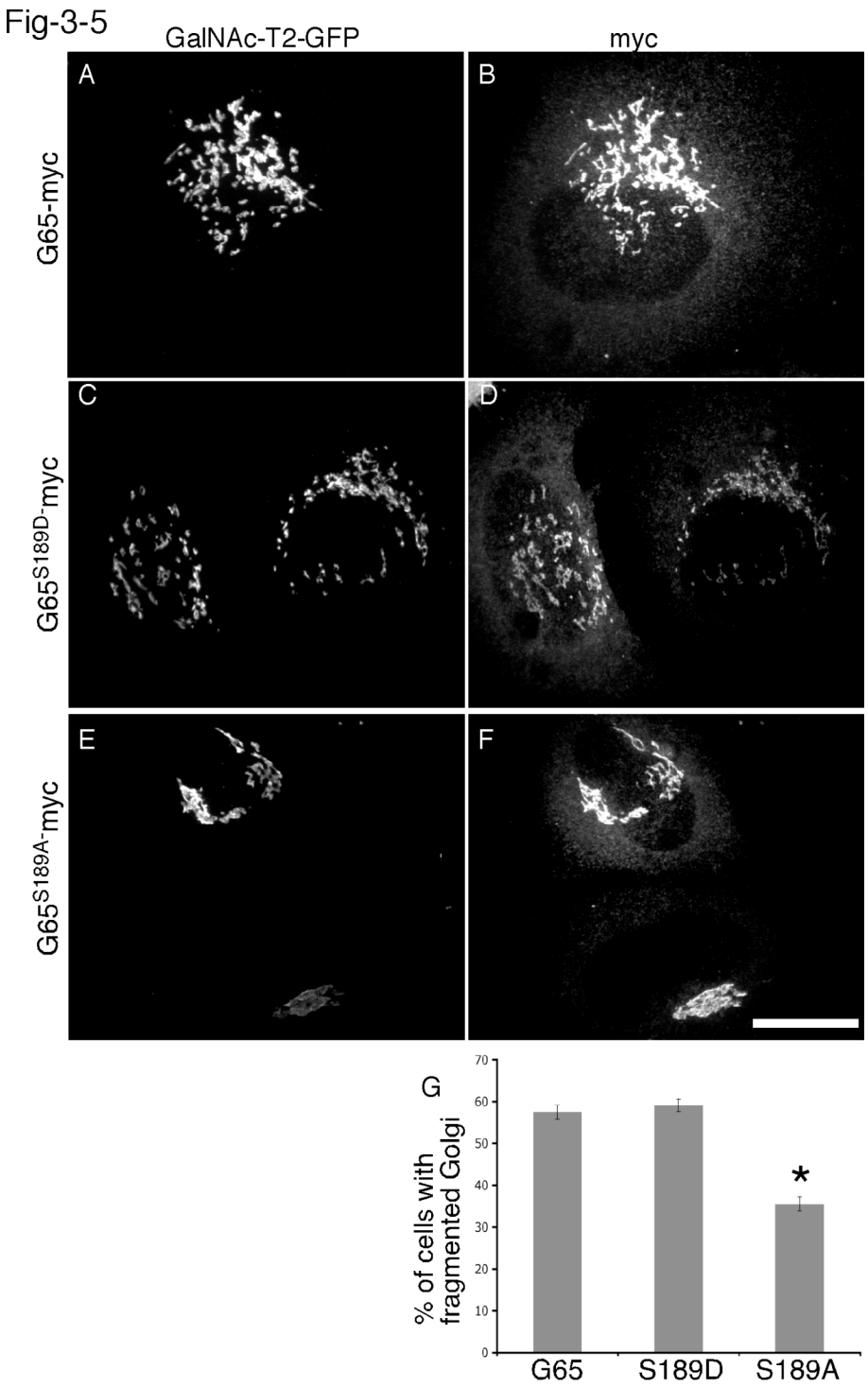

Figure 3-5 Evidence that PLK1 phosphorylation of GRASP65 is required for late G2 unlinking. G65-myc (A, B), G65^{S189D}-myc (C,D), and G65^{S189A}-myc (E,F) were transiently transfected and the cells were synchronized in late G2 phase by a 5 h release from thymidine and then a 6 h treatment with olomoucine II. Expressing cells were identified by myc staining (B,D,F) and the Golgi was analyzed based on GalNAc-T2-GFP (A,C,E). Bar=10 μm. The percentage of cells (G) expressing G65-myc, G65^{S189D}-myc and G65^{S189A}-myc and exhibiting an unlinked Golgi was quantified (±SEM, n=4, >100 cells in each, $p< 0.01$).

expressing G65^{S189D}-myc also exhibited unlinked Golgi ribbons (Fig 3-5 C,D,G) as was expected given that this construct lacked tethering activity as shown above. In contrast, only 35% of cells expressing G65^{S189A}-myc had fragmented ribbons (Fig 3-5 E-G). This finding implies that phosphorylation of the GRASP65 PLK1 site, S189, is required for late G2 unlinking of the Golgi ribbon.

Because CDK1-mediated phosphorylation of GRASP65 perturbs mitotic Golgi fragmentation causing accumulation of larger mitotic Golgi clusters (Wang *et al.*, 2003; Tang *et al.*, 2010) we tested whether mutation of the PLK1 site S189 might have a similar effect. Average cluster volume was determined in mitotic cells expressing G65-myc or G65^{S189A}-myc. Indeed, mitotic cells expressing G65^{S189A}-myc, identified using anti-myc and anti-phospho-histone H3 antibodies, had mitotic Golgi clusters that were 1.7 fold larger on average than those in the control cells (Fig 3-6).

Fig 3-6

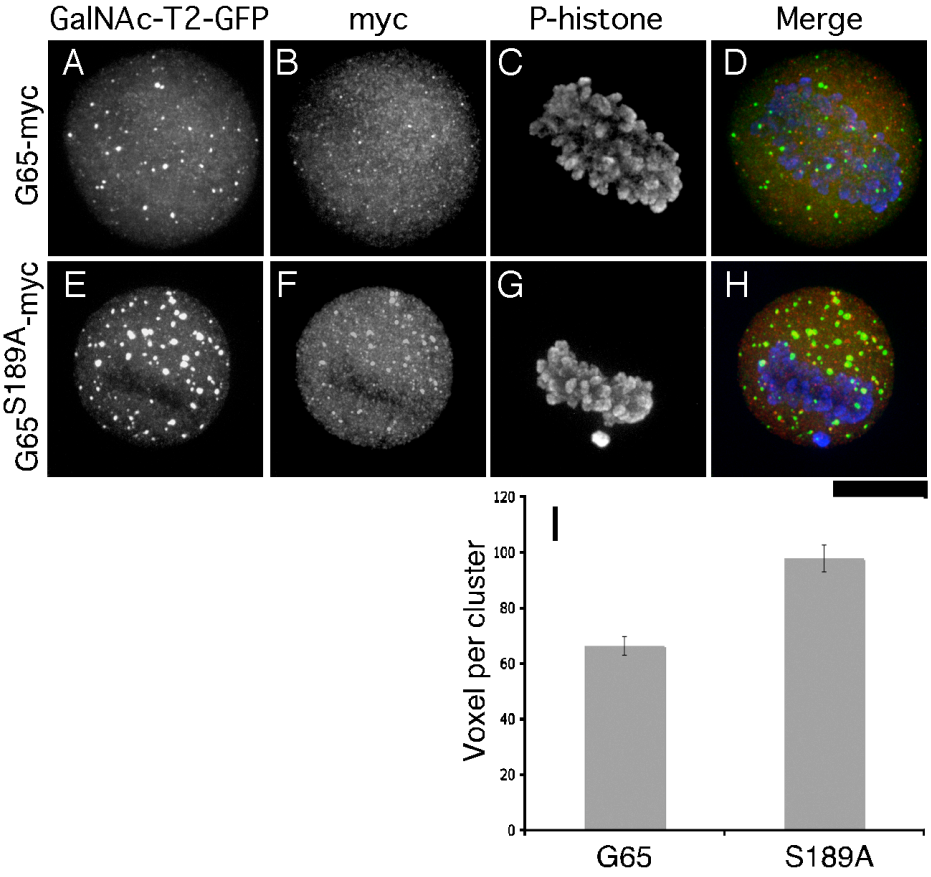

Figure 3-6 Evidence that GRASP65 phosphorylation by PLK1 is required for mitotic Golgi disassembly Cells transiently transfected with G65-myc (A-D) or $G65^{S189A}$-myc (E-H) were synchronized in M-Phase by thymidine release into olomoucine II for 6 h followed by 45 min release from olomoucine II. Mitotic cells were identified by phospho-histone staining (C,G), expressing cells were identified by myc staining (B,F), and Golgi morphology was observed by GalNAc-T2 GFP florescence (A,E). Bar=10 μm. Mitotic Golgi cluster size (I) was determined using the ImageJ "Voxel counter" plug-in based on GalNAcT2-GFP florescence (±SEM, n=3, >15 cells in each, $p<0.01$).

The S189D phospho-mimic mutation does not affect GM130 binding

GRASP65 is targeted to the Golgi by using its second PDZ-like domain (PDZ2) to bind the C-terminal PDZ ligand of GM130 (Barr *et al.*, 1998; Bachert and Linstedt, 2010). Although S189 is near the GM130 binding site, $G65^{S189D}$-myc was Golgi-localized upon expression (Fig 3-4D-F; Fig 3-5C-D), suggesting that the phosphorylation of S189 does not interfere with GM130 binding. To confirm this finding, we used recruitment to mitochondria as an interaction test. As expected, the G65-GFP-ActA construct localized to mitochondria, induced mitochondrial clustering, and, because it binds GM130, recruited GM130 to the mitochondria (Fig 3-7A-C). Brefeldin A was used in these experiments to disassemble the Golgi complex. Although $G65^{S189D}$-GFP-ActA failed to induce clustering, GM130 recruitment was evident on the dispersed mitochondria (Fig 3-7D-F). Thus, the S189D phospho-mimic construct binds GM130 and its loss of tethering activity is not due to impaired interaction with GM130.

An internal PDZ ligand binding GRASP65 PDZ1 is adjacent to S189

GRASP65 self-association during tethering involves its first PDZ-like domain, PDZ1, binding to an unidentified ligand located within GRASP65 but outside of residues 85-167 (Sengupta *et al.*, 2009). Because S189D blocked tethering, we asked whether residues surrounding S189 contain the ligand that binds PDZ1. An *in vitro* binding assay was established in which purified monomeric His-tagged GRASP65, G65-His, was incubated with a series of purified, GST-tagged peptides from this region of GRASP65 (Fig 3-8A). Significantly, the sequence stretch 173-212 bound GRASP65 at levels above background. Bisection of this stretch yielded strong binding by the C-terminal half, residues 192-212 (Fig 3-8B). This was confirmed by quantification of multiple experiments (Fig 3-8C). Further deletions reduced binding to near background levels, but the weak binding of 192-204 compared to the lack of binding for 200-212 suggested that the activity resides in residues 192-199. As a test, we performed alanine-scanning mutagenesis of the 191-212 construct. Significantly, alanine substitution at residues I194, Y196, Y198 or L199 specifically reduced or abolished binding to GRASP65 (Fig 3-9), indicating that this stretch was responsible for the interaction.

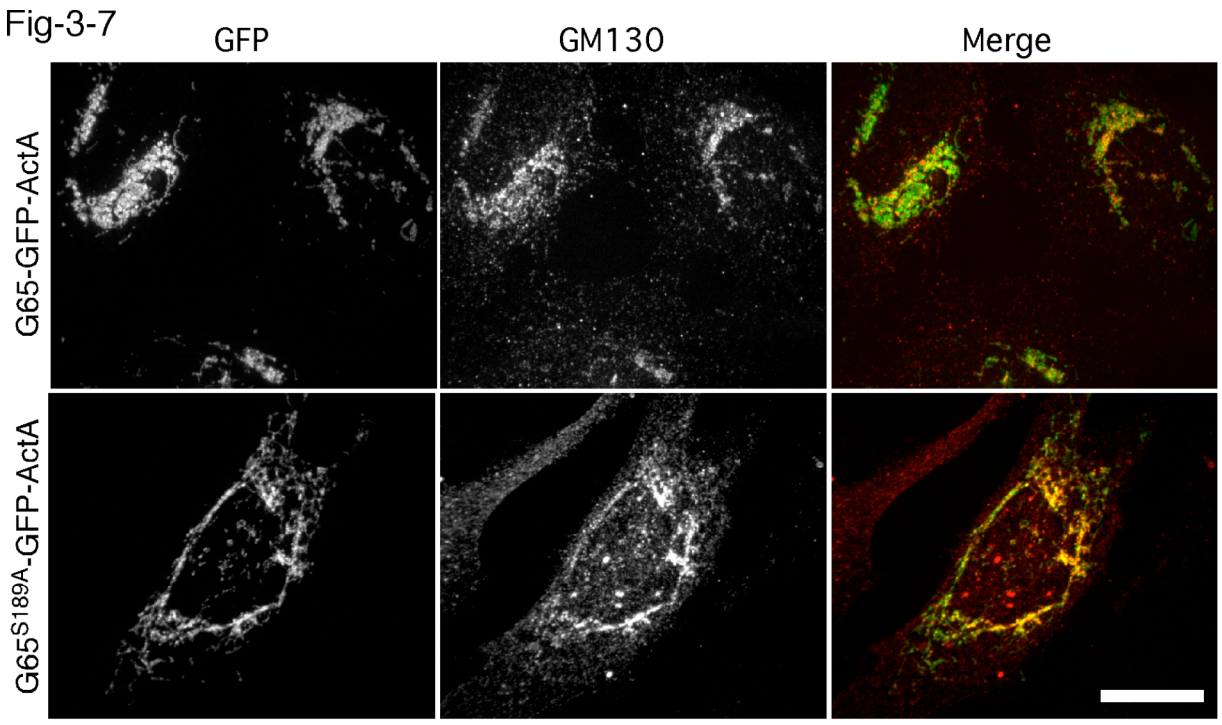

Figure 3-7 Phospho-mimic GRASP65^{S189D} retains GM130 binding. HeLa cells expressing G65-GFP-ActA (A-C) or G65^{S189D}-GFP-ActA (D-F) were BFA-treated for 30 min to disassemble the Golgi apparatus and processed to reveal GFP fluorescence (A,D) and GM130 staining (B,E). A false-colored, merged image is also shown (GFP and GM130 are red and green, respectively). Bar=10 μm.

Consistent with our results, internal PDZ ligands typically have a length requirement of greater than 10 residues and, within this stretch, a central cluster of about five residues whose side chains are
essential (Hillier *et al.*, 1999; Runyon *et al.*, 2007; Zhang *et al.*, 2009). To test whether the stretch we identified was binding the GRASP65 PDZ1 groove, we mutated the predicted groove to block binding. Purified G65-His, with or without a LK55,56NI substitution that blocks tethering (unpublished), was incubated with the purified GST-fusion containing GRASP65 residues 192-212. Mutation of the predicted PDZ1 groove significantly reduced binding relative to wildtype (Fig 3-10A-B). As a further test, we asked whether the ligand sequence would specifically bind an isolated version of PDZ1. Indeed, the purified GST-tagged residues 192-212 bound purified His-tagged PDZ1 but not PDZ2 (Fig 3-10C). This interaction was specific because binding to PDZ1 was blocked by alanine substitution of either Y196 or Y198 in the ligand sequence (Fig 3-10D). Altogether these experiments indicate that the sequence stretch IGYGYL functions as an internal PDZ ligand binding to PDZ1.

Next, we sought to determine whether the mapped ligand is required for GRASP65 tethering and Golgi ribbon formation. To test tethering, we expressed a mitochondrially-targeted version of GRASP65 containing a single point mutation that blocked the in vitro interaction, Y196A. The resulting construct, $G65^{Y196A}$-GFP-ActA was targeted to mitochondria but failed to induce clustering (Fig 3-11A). Inhibition by Y196A was confirmed using the radial profile analysis on a population of cells (Fig 3-11B). To test Golgi ribbon formation, we expressed the same mutated form of GRASP65 in cells lacking endogenous GRASP65 due to knockdown. Significantly, GRASP65 knockdown caused Golgi unlinking and this phenotype was rescued by G65-myc but not $G65^{Y196A}$-myc (Fig 3-11C). The lack of activity in Golgi ribbon formation for this point mutation in the internal ligand sequence was confirmed by quantification (Fig 3-11D).

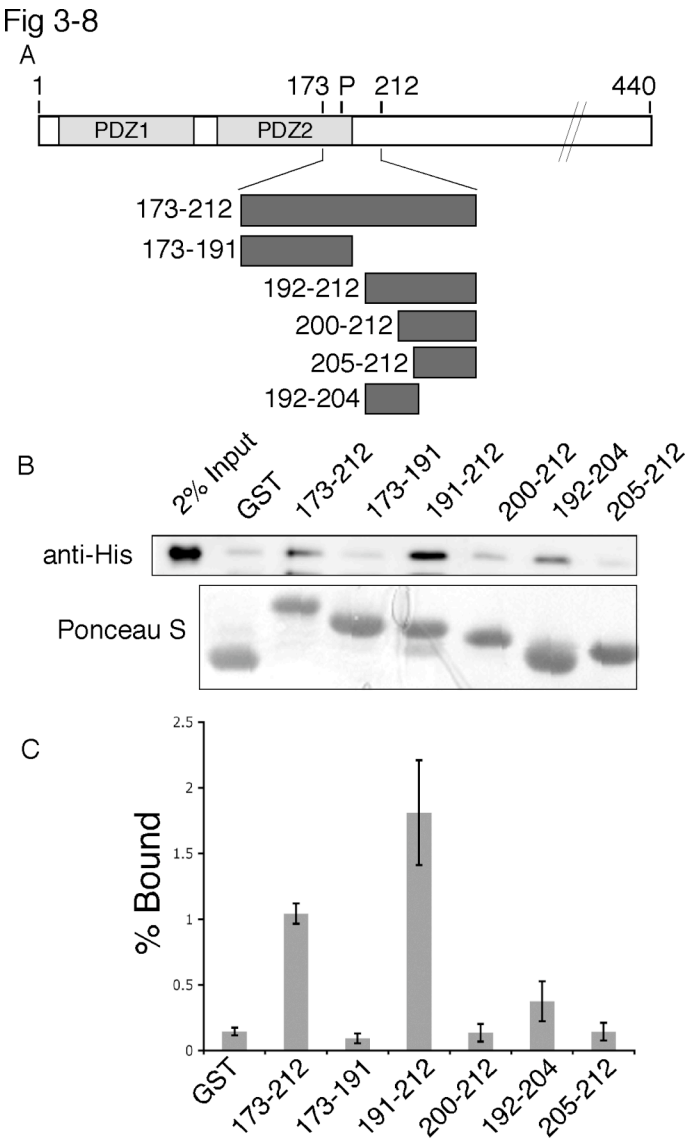

Figure 3-8 Residues 192-212 bind full length GRASP65. Schematic depicting GRASP65 GST fusion proteins tested for binding (A). Equivalent amounts (5 μg) of each fusion protein were incubated with 5 μg of purified G65-His for 3 h and complexes were recovered on glutathione agarose beads. G65-His binding was determined by immunoblotting with anti-His-tag antibody (B) and quantified (C) relative to a 2% loading control (n=3, ±SEM, *p< 0.05).

Fig 3-9

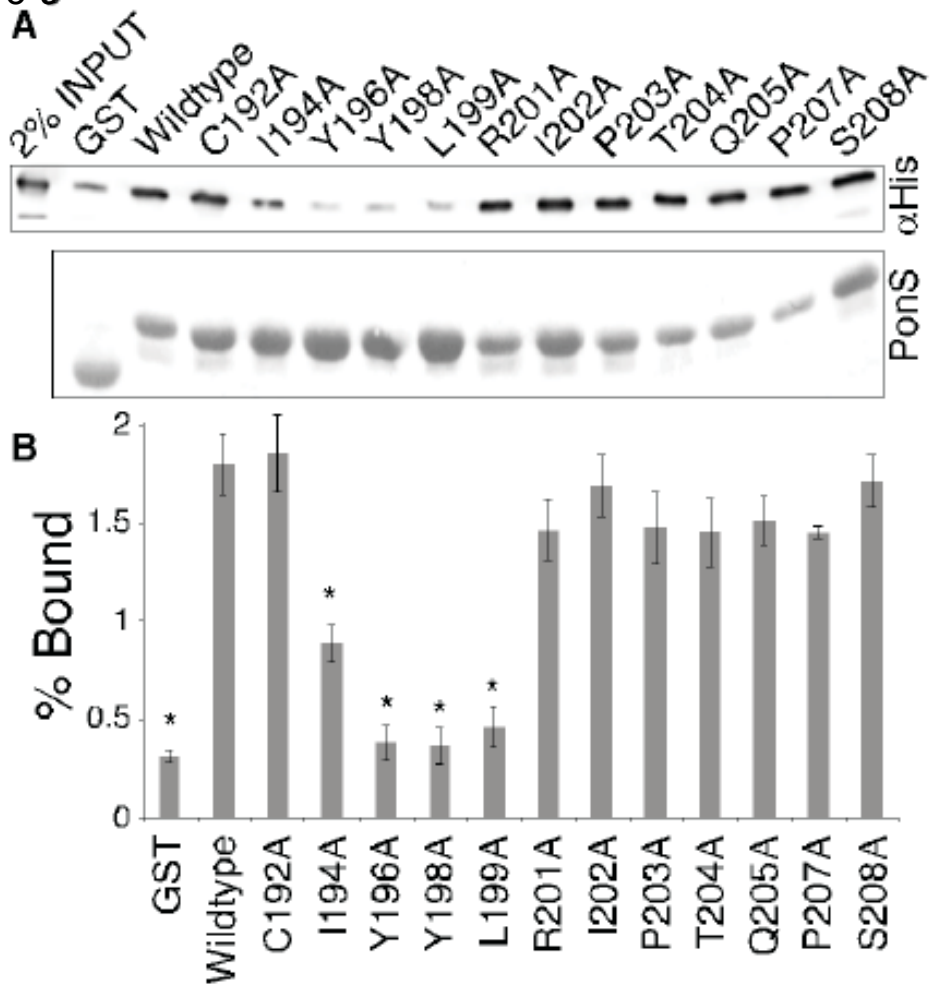

Figure 3-9 Alanine scanning maps binding domain to residues 194-199. GST alone or GST fused to GRASP65 residues 192-212 containing the indicated individual alanine substitutions was incubated with 5 μg G65-His and complexes were recovered on glutathione agarose beads. G65-His binding was determined by immunoblotting with anti-His-tag antibody (A) and quantified (B) relative to a 2% loading control (n=3, ±SEM, *p< 0.01).

Fig 3-10

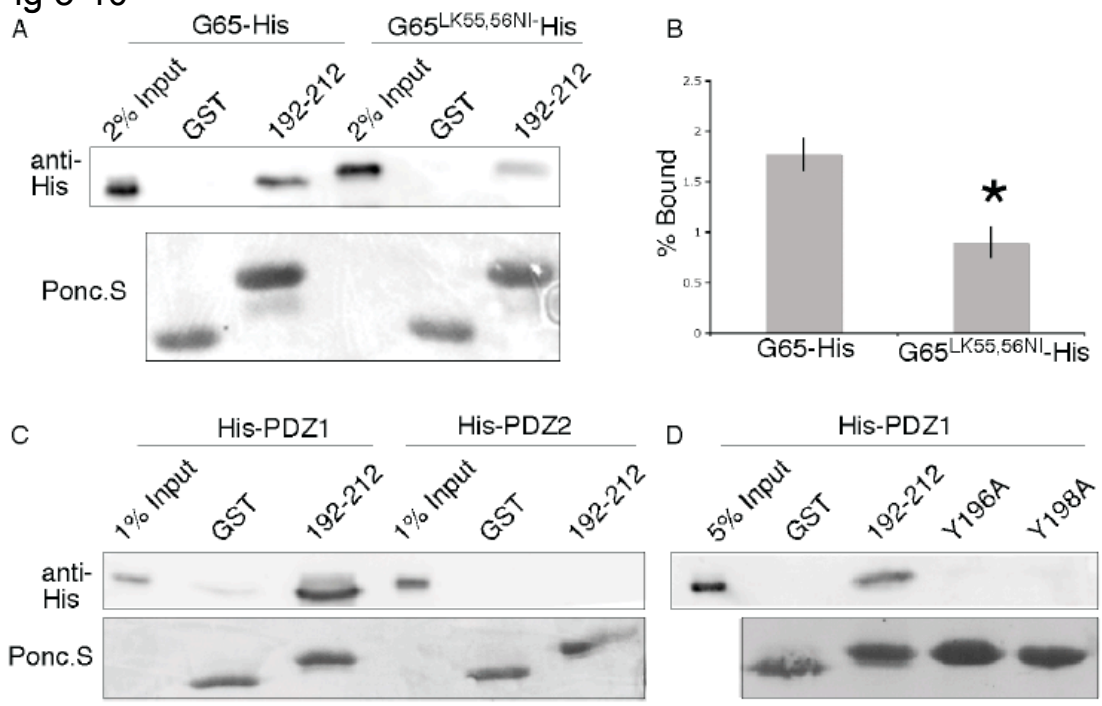

Figure 3-10 Residues 192-212 bind the PDZ1 groove of GRASP65. Equivalent amounts (5µg) of GST alone or GST fused to GRASP65 residues 192-212 were incubated with 2.5 µg of either G65-His or GRASP65^{LK55,56NI}-His, which had mutations in its predicted PDZ1 binding groove. Complexes were recovered on glutathione agarose beads and binding of the His-tagged GRASP65 proteins was determined by immunoblotting with anti-His-tag antibody (A). The results were quantified (B) relative to a 2% loading control (n=4, ±SEM, *p< 0.01). GST alone or GST-192-212 (5µg) were also incubated with 5 µg of the isolated GRASP PDZ domains, His-PDZ1 and His-PDZ2, and binding was compared to 1% loading controls (C). Finally, GST alone or GST-192-212 (5µg) with or without the indicated alanine substitutions were incubated with 5 µg of His-PDZ1 and compared to a 5% loading control (D).

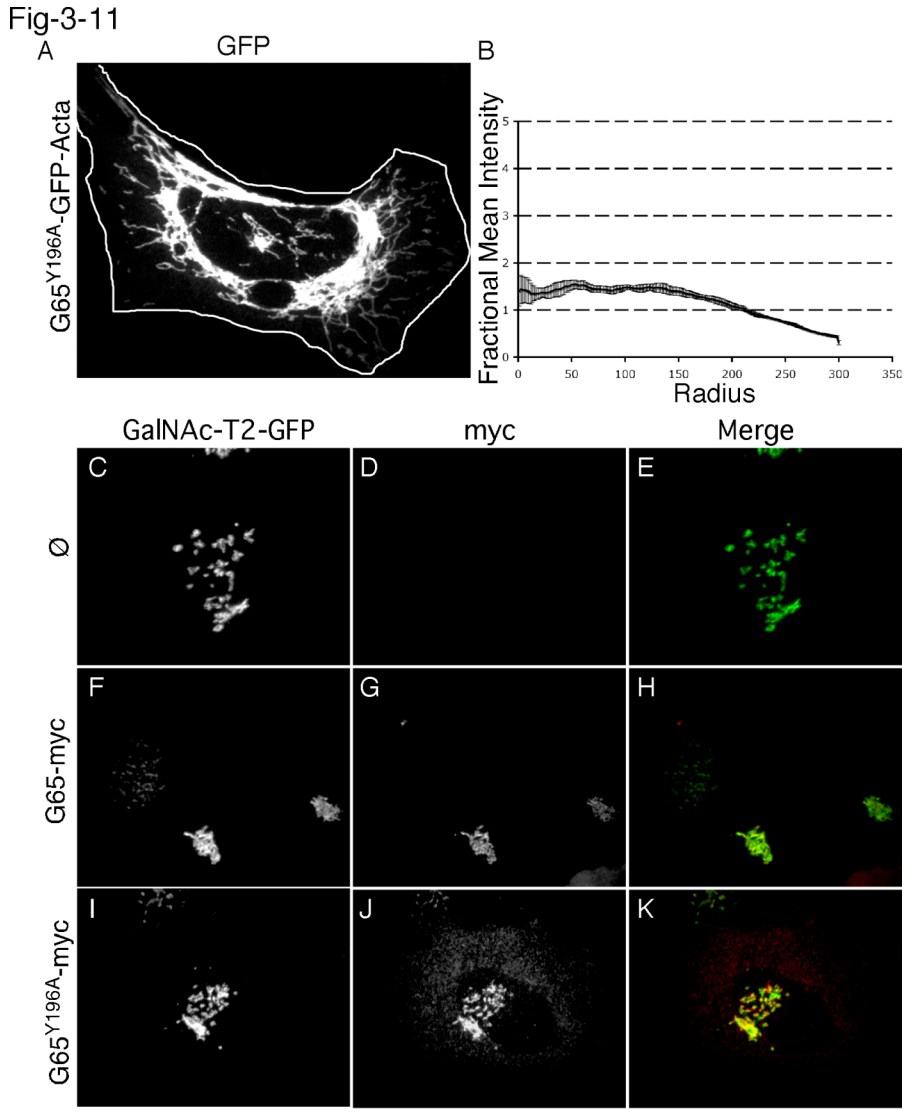

Figure 3-11 Residues 192-212 bind the PDZ1 groove of GRASP65. Equivalent amounts (5µg) of GST alone or GST fused to GRASP65 residues 192-212 were incubated with 2.5 µg of either G65-His or GRASP65^{LK55,56NI}-His, which had mutations in its predicted PDZ1 binding groove. Complexes were recovered on glutathione agarose beads and binding of the His-tagged GRASP65 proteins was determined by immunoblotting with anti-His-tag antibody (A). The results were quantified (B) relative to a 2% loading control (n=4, ±SEM, *p< 0.01). GST alone or GST-192-212 (5µg) were also incubated with 5 µg of the isolated GRASP PDZ domains, His-PDZ1 and His-PDZ2, and binding was compared to 1% loading controls (C). Finally, GST alone or GST-192-212 (5µg) with or without the indicated alanine substitutions were incubated with 5 µg of His-PDZ1 and compared to a 5% loading control (D).

Discussion

The GRASP65 binding groove is known to be required for Golgi ribbon formation but the corresponding ligand had not been identified (Sengupta *et al.*, 2009). Similarly, PLK1 was shown to be important for mitotic Golgi disassembly and to bind and phosphorylate GRASP65, but the site of phosphorylation had not been mapped and the significance of PLK1 phosphorylation of GRASP65 was not determined (Lin *et al.*, 2000; Sutterlin *et al.*, 2001; Wang *et al.*, 2003; Preisinger *et al.*, 2005). Our identification of the PDZ ligand mediating GRASP65 self-association and a nearby PLK1 site that functionally regulates the interaction significantly extend our understanding of Golgi ribbon formation and its unlinking at M-phase. These findings support a model in which the binding groove of the first PDZ domain of GRASP65 on one membrane interacts with an internal ligand within the second PDZ domain of GRASP65 on an adjacent membrane to mediate organelle tethering; and, at the onset of mitosis, PLK1 blocks this interaction by phosphorylating a site next to the ligand (Fig 3-12).

A twenty residue peptide at the end of the GRASP domain, C192-K212, bound the PDZ1 binding groove and mutations within the stretch IGYGYL(194-199) blocked binding (Fig 3-10), tethering (Fig 3-11A,B), and Golgi ribbon formation (Fig 3-11C,D). PDZ ligands are typically located at the carboxy-terminus and have been classified into several types defined largely by the four terminal residues of the protein. Although the GRASP65 ligand sequence most closely matches the type II PDZ ligand consensus sequence Φ–X–Φ, the GRASP65 sequence is internal. Internal ligands are less common but several examples are well characterized and different modes of interaction have been identified (Hillier *et al.*, 1999; Penkert *et al.*, 2004). Some internal ligands contain an acidic residue that mimics the free carboxy-terminus of typical ligands, but these are not obligatory (Penkert *et al.*, 2004; Runyon *et al.*, 2007; Zhang *et al.*, 2009) and the GRASP65 ligand lacks this feature. Other internal ligands form a β-hairpin "finger-like" fold in which a β strand mimics the canonical ligand interaction and the sharp turn overcomes the steric constraints at the terminus of the ligand binding groove (Hillier *et al.*, 1999). This is also an unlikely mode of interaction for the GRASP65 internal ligand as secondary structure prediction suggests that it is unlikely to form a β-hairpin fold. A final mode of interaction involves conformational flexibility and seems most relevant. In this mode, glycines in internal ligands confer flexibility that neutralize the effect of steric barriers in the ligand

Fig 3-12

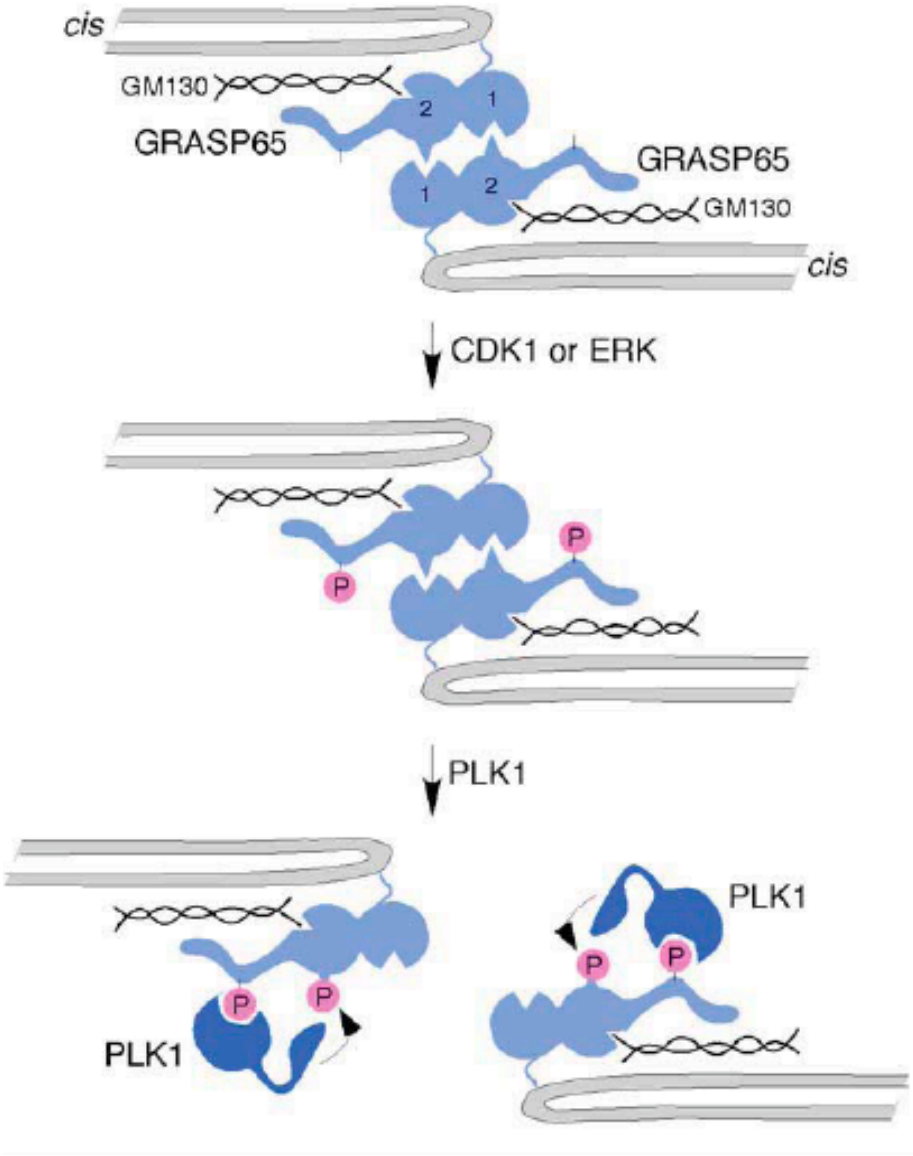

Figure 3-12 Model depicts two-step phosphoinhibition. GRASP65 is first shown tethering *cis* cisternae membranes. It is membrane anchored by GM130 binding and myristic acid insertion and self-interacts via a reciprocal insertion of its ligand, present in PDZ2, into the groove of PDZ1. The unstructured C-terminal domain is then phosphorylated by CDK1 or ERK creating a docking site for PLK1. Then the Polo box domain of PLK1 docks and the PLK1 catalytic domain phosphorylates S189 inactivating the PDZ ligand thereby inhibiting the tethering complex.

binding groove (Runyon *et al.*, 2007; Zhang *et al.*, 2009). The presence of two glycines in the GRASP65 internal ligand suggests that it uses a similar mechanism. The core and surrounding residues in the GRASP65 ligand sequence are conserved among GRASP proteins of higher eukaryotes suggesting conservation of function. However, it is puzzling that GRASP55 has this sequence because it does not bind GRASP65. Determing the basis of specificity in GRASP homo-oligomer formation is an important future direction.

Interestingly, the binding of internal ligand sequence at the end of the GRASP domain to the PDZ1 groove suggests that the interaction involves a type of head-to-tail arrangement. Head-to-tail binding could involve reciprocal contacts if both groove and ligand align symetrically on the same interaction surface (Fig 3-12). Such an arrangement would yield cooperative binding and would be compatible with a groove and ligand orientation projecting away from the membrane such that it favors *trans* pairing over *cis* pairing (Bachert and Linstedt, 2010). Alternatively, the groove and ligand may be on opposite surfaces because in this arrangement head-to-tail binding would allow formation of multimeric complexes of variable size. This has been observed for GRASP65 in *in vitro* preparations of the protein (Wang *et al.*, 2005; Tang *et al.*, 2010).

The presence of a PLK1 phosphorylation site, S189, next to the PDZ ligand sequence suggests several possible inhibitory mechanisms. Binding of known internal ligands depends on both interactions within the ligand sequence as well as interactions involving adjoining residues (Hillier *et al.*, 1999). The latter increase the strength and specificity of binding and thus phosphorylation of adjoining residues could regulate binding. The carboxy-terminal ligand in ErbB2 provides an example as its affinity for the Erbin PDZ domain is reduced by phoshorylation of a tyrosine residue outside the ligand sequence that, in its unphosphorylated state, contributes to binding (Birrane *et al.*, 2003). Alternatively, phosphorylation of S189 might alter presentation of the ligand on the surface of the molecule. In other words, adjoining residues including S189 may adopt a conformation in the folded PDZ2 domain that exposes the IGYGYL sequence and phosphorylation of S189 may induce a conformational change in the ligand that blocks its access to the binding groove. This mode of regulation has been suggested for the NMDA receptor subunit NR2C which is phosphorylated on a serine adjacent to its PDZ ligand sequence that binds PSD-95 (Chen *et al.*, 2006). A final possibility is that S189 phosphorylation

alters orientation of GRASP65 on the membrane. Dual anchoring of the GRASP domain to the membrane by myristic acid insertion and GM130 binding facilitates *trans* pairing possibly by conferring a favorable orientation of the binding groove and/or ligand (Bachert and Linstedt, 2010). As S189 is in the domain that binds GM130, its phosphorylation could conceivably influence the way in which GM130 orients GRASP65 and thereby block binding. Interestingly, a sequence stretch in GRASP65 that is required for GM130 binding roughly corresponds to the sequence stretch identified here as the internal ligand (Barr *et al.*, 1998). Although the role of specific residues such as Y198 and L199 differs in these two interactions, this coincidence could relate to regulation of the internal ligand by GM130.

Based on our findings, the available evidence supports a two-step model for phosphoinhibition of GRASP65 (Fig 3-12). First, CDK1 phosphorylates the C-terminal regulatory domain creating a docking site for PLK1. Second, PLK1 binds the docking site, becomes activated and phosphorylates S189, which blocks tethering. While this likely takes place in M-phase, a variation of the model is needed to explain Golgi unlinking in G2 phase because CDK1 is not yet active. One possibility is that a MEK/ERK cascade creates the PLK1 docking site. MEK/ERK signaling is active in late G2 and phosphorylates a site in the regulatory domain of GRASP65 (Yoshimura *et al.*, 2005). The phosphorylation may be mediated by a splice variant of ERK1, ERK1c, which is recruited to the Golgi (Shaul and Seger, 2006). Interestingly, GRASP55 is also a substrate of ERK and S189 is conserved, but PLK1 does not bind mitotic GRASP55 (Preisinger *et al.*, 2005). Thus, while the mechanism of GRASP55 phospho-regulation may or may not be distinct, GRASP65 is likely phosphorylated on it regulatory domain to create a PLK1 docking site to promote PLK1 phosphorylation of S189, which blocks the internal PDZ ligand from binding the PDZ1 groove in another molecule.

Golgi ribbons are primarily evident in higher eukaryotic cells and this organization converts the compartment from multiple distinct units into a “single-copy” organelle. To ensure equal partitioning at mitosis the Golgi ribbon is fragmented. GRASP proteins are multifunctional and a version of GRASP is expressed in simpler eukaryotes that lack Golgi ribbons (Kondylis *et al.*, 2005; Behnia *et al.*, 2007). In these cells GRASP is likely involved in cargo secretion by conventional and unconventional pathways (Kinseth *et al.*, 2007; Duran *et al.*; Schotman *et al.*,

2008; D'Angelo *et al.*, 2009; Manjithaya *et al.*, 2010) and may also perform membrane tethering in a simpler reaction such as cisternal elongation. Interestingly, the GRASP phosphorylation site hit by PLK1, S189, is apparently only present in cells with Golgi ribbons and it is only these cell types that express both GRASP isoforms. Thus, the mechanism inducing fragmentation of the Golgi ribbon may have co-evolved with the mechanism of Golgi ribbon formation.

Materials and Methods

Reagents

Primary antibodies were as follows: anti-myc 9e10(Jesch *et al.*, 2001a), anti-phospho-Serine (Zymed), anti-His-tag (Bethyl Laboratories, Inc.), anti-phospho-histone-H3 (Upstate Cell signaling solutions) and anti-GM130 (Puthenveedu *et al.*, 2006). Mitotracker (Invitrogen) was used to stain mitochondria as described (Sengupta *et al.*, 2009). Olomoucine II and thymidine were from Sigma.

Constructs

$G65^{7XD}$-GFP-ActA was generated by sequential introduction of aspartic acid codons corresponding to residues T216, T237, S241, S274, S291, S373, S397 into the human G65-myc construct (Sengupta *et al.*, 2009) following the QuikChange protocol (Stratagene) and then by cloning the resulting GRASP65 sequence in frame into the *NheI* site of GFP-ActA (Sengupta *et al.*, 2009). $G65^{S189A}$-GFP-ActA, $G65^{S189D}$-GFP-ActA, $G65^{Y196A}$-GFP-ActA, $G65^{S189A}$-myc, $G65^{S189D}$-myc, $G65^{Y196A}$-myc, and $G65^{LK55,56NI}$-His were generated using QuikChange to change the indicated codons in the parent vectors. GST-$G65^{173-212}$ was generated from GST-G65 (Sengupta *et al.*, 2009) by deleting codons for residues 7-172 and adding a stop codon at residue 213. GST-$G65^{192-212}$, GST-$G65^{200-212}$ and GST-$G65^{205-212}$ were made from GST-$G65^{173-212}$ using a loop out protocol. GST-$G65^{173-191}$ and GST-$G65^{192-204}$ were made by adding stop codons at the indicated positions of GST-$G65^{173-212}$ and GST-$G65^{192-212}$, respectively. Alanine scan mutations of GST-$G65^{192-212}$ were made by using QuikChange to substitute alanine codons at the indicated positions. For His-PDZ1 (residues 7-108) and His-PDZ2 (residues 106-197) the indicated GRASP65 sequence was cloned between BamH1 and EcoR1 sites of pRSET-B.

Cell culture and transfection

HeLa cells were grown in Minimal Essential Medium (Sigma) containing 10% fetal bovine serum (Atlanta Biological) and 100 IU/ml of penicillin and streptomycin (Sigma) and maintained at 37°C in a 5% CO_2 incubator. Transient transfection was carried out with jetPEI™ (Polyplus) according to manufacturer's specifications. After 24 h, the cells were labeled with 15 nM Mitotracker (Invitrogen) for 30 min and fixed. Knockdown of GRASP65 by RNA interference

and gene replacement was performed as described (Sengupta *et al.*, 2009). To score G2- and M-phase Golgi morphology, cells expressing GFP-GalNAc-T2 were plated at 50% confluence and subjected to double thymidine arrest as described (Feinstein and Linstedt, 2007). At 5 h after release from the second thymidine block, the media was adjusted to 10 μM olomoucine II for another 6 h to arrest cells in late G2. For M-phase, the olomoucine II was washed out and the cells were recultured for another 45 min.

Image capture and analysis

Imaging was performed using a spinning disk confocal scan head equipped with three-line laser and independent excitation and emission filter wheels (PerkinElmer) and a 12-bit Orca ER digital camera (Hamamatsu) mounted on an Axiovert 200 microscope with a 100x, 1.4 NA oil-immersion objective (Carl Zeiss MicroImaging, Inc.). Sections at 0.3 μm spacing were acquired using Imaging Suite software (PerkinElmer). Radial profile analysis was as previously described (Sengupta *et al.*, 2009). Mitotic cluster volume was determined using the "Voxel counter" plug-in of ImageJ (rsbweb.nih.gov/ij) after background subtraction to remove vesicular haze. Total volume was divided by the number of clusters from the "Particle count" function of ImageJ to yield volume per cluster.

Protein purification and binding assays

Full-length GRASP65 proteins (G65-His, $G65^{LK55,56NI}$-His, and $G65^{S189A}$-His) were purified after expression in BL21(DE3)-pLysS cells cotransformed with pBB131 encoding N-myristoyltransferase (Duronio *et al.*, 1990). Expression was induced by 1mM isopropyl β–D-thiogalactopyranoside (IPTG) at 30°C for 4h in the presence of 200 μM myrstic acid. Purification on Ni-NTA beads (Invitrogen) was according to manufacturer's protocol. The preparations were then dialyzed against HK buffer (10mM HEPES, 100mM KCl, 1.4mM β-mercaptoethanol) and further purified on a Superdex-200 gel filtration column attached to an FPLC (Pharmacia). Monomeric fractions were collected and dialyzed against HKT binding buffer (HK adjusted to 0.5%-TritonX-100 and 5% glycerol). GST-tagged GRASP65 peptides were purified as previously described (Linstedt *et al.*, 2000) after expression in DH5α and induction using 1mM IPTG for 3-5 hr at 30°C. Binding was carried out in 100μl of HKT binding buffer containing 5μg

of each purified protein, unless indicated otherwise. After 3 h at 4°C, glutathione agarose beads (5 μl), which had been blocked with 10μg of BSA, were added to the reaction for 1hr. Proteins recovered on the beads after 3 washes with HKT were analyzed by immunoblot using the anti-His antibody.

PLK1 phosphorylation assay

Purified G65-His and$G65^{S189A}$-His were incubated with 200 ng of active PLK1 (Cell signaling Technology) and 50 μM ATP in kinase buffer (5 mM MOPS pH 7.2, 2.5 mM β-glycerophosphate, 1 mM EGTA, 4 mM $MgCl_2$, 0.05 mM DTT) at room temperature for 25 min. The samples were immunoblotted using the anti-phospho-Serine antibody.

CHAPTER 4: Discussion and Future Directions

The molecular mechanism driving cisternal linking to generate a ribbon-like Golgi structure is not very well understood. We propose a novel model for homotypic membrane tethering mediated by homo-oligomerization of GRASP65, which is involved in cisternal linking. The results presented in this thesis suggest that GRASP65 homo-oligomerization is mediated by an interaction between the first PDZ domain and an internal ligand motif, within the GRASP65 molecule. This interaction in *trans* allows GRASP65 to tether organellar membranes. We also present evidence that a PLK1 phosphorylation site, S189, proximal to the internal ligand sequence regulates this tethering.

The central feature of the new homotypic tethering model is the interaction of the ligand-binding groove of the first PDZ domain with an internal ligand sequence. When this study was initiated we did not have any structural information that would have allowed us to unequivocally identify the ligand-binding groove of GRASP65 PDZ domains. Therefore, most of the analyses were based on computational structure predictions. Moreover, our attempts to crystallize GRASP65 have been unsuccessful. Significantly, we recently determined the structure of the GRASP55 N-terminal GRASP domain (7-208) (Truschel et al., unpublished data, Fig 4-1). A DALI structural similarity search (Holm & Sander 1995) identified two tandem PDZ-like folds in the GRASP domain. Interestingly, neither of the PDZ domains resembles a typical eukaryotic PDZ domain. Rather, they are circularly permutated, and resemble prokaryotic PDZ domains, in which the β-strand lining the ligand-binding groove is contributed by a C-terminal sequence element. The functional relevance of the atypical PDZ domain is not clear. Significantly, the mutations described in the thesis, and generated to disrupt the PDZ1 ligand-binding groove, do contribute to the ligand-binding pocket of PDZ1, as observed in the structure (Fig 4-1A, B; the residues L55, K56, L58, L59 are highlighted in grey). This validates our interpretation that the PDZ1 ligand-binding groove is required for tethering.

The proximity of the internal ligand and the PDZ2 ligand-binding groove may serve to orient the molecule for trans interactions. The residues contributing to the internal ligand sequence form a prominent surface feature of the GRASP domain, proximate to the PDZ2 ligand-binding groove (Fig 4-1 C, D in Red). In an independent study from our group it is shown that the C-terminus

Fig 4-1

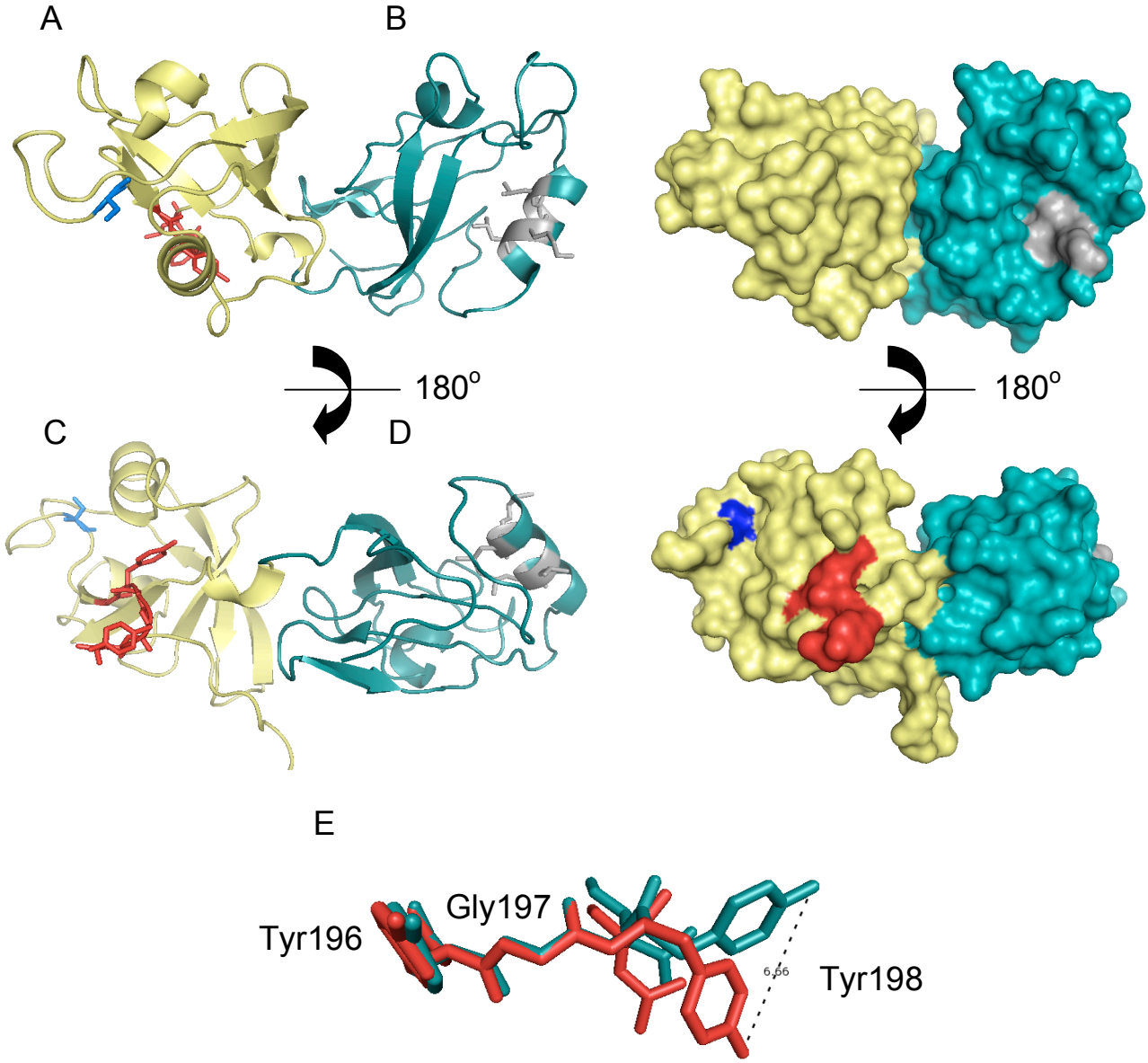

Figure 4-1- Crystal Structure of GRASP domain of GRASP55 Cartoon view(A) and surface view(B) of the GRASP domain facing the ligand binding groove of PDZ1(Cyan) and the residues within the PDZ1 ligand binding groove mutated in the previous chapters(L55, K56, L58, L59) are color coded in Grey. Cartoon view(C) and surface view(D) facing the internal ligand(Red). PLK1 Phosphorylation site S189 color coded in Blue. PDZ2 is color coded in Yellow. (E) Structural alignment of the internal ligand sequence of wild type GRASP domain(Red) and GRASP^{S189D}. The dotted lines represent a 6 A shift in the T198 side chain.

residues of GM130 interact with ligand-binding groove of the second PDZ domain (Bachert & Linstedt 2010). This interaction is required for membrane recruitment of GRASP65 as well as promoting trans pairing (Bachart, 2010). It is likely that the PDZ2-GM130 interaction orients the ligand and the PDZ1 binding groove on the opposing membrane promoting the formation of the tethering complex. This model can be further tested in an *in vitro* liposomal system. Based on the model presented in this thesis, GRASP65 will tether liposomes, and mutations identified in this thesis will inhibit tethering. This assay will further test the sufficiency of GRASP65 to tether membranes and validate our model of its self-interaction.

Specificity in cisternae linking is critical for maintenance of the subcompartmentalized Golgi. It is believed that GRASP65 interacts with itself but not with GRASP55. Although the mapped internal ligand residues are conserved in GRASP55, we observe very weak binding between GRASP65 and GRASP55 (data not shown), suggesting that specificity can be ascribed to residues adjoining the ligand sequence that are not conserved. The difference in the binding may also be attributed to minor differences in the ligand-binding groove of the first PDZ domain of GRASP65 and GRASP55. The residues, V98 and I100 contribute to the ligand-binding groove of PDZ1 of GRASP55. The corresponding residues of GRASP65, A98 and V100, are not conserved. In order to test the role of these and other non-conserved residues, a chimera of GRASP65 and GRASP55 could be generated and analyzed using the assays described in this document. For example, the PDZ1 domain of GRASP65 can be swapped with GRASP55 PDZ1 domain and tested for the tethering. Tethering would indicate that the specificity is achieved at the level of localization of the GRASP proteins. If the chimera fails to tether it would suggest that the PDZ-ligand interaction contributes to the specificity of tethering. To identify the key residues, mutagenesis of chimera could then be performed to rescue tethering.

How phosphorylation of S189 inhibits GRASP-mediated tethering is not well understood. In order to test the possible contribution of a conformational change induced by phosphorylation of S189, Mingrui Zhang in collaboration with Steven T. Truschel, determined the structure of the GRASP domain phospho-mimic, GRASP55^{S189D}. The structure of GRASP^{S189D} did not reveal a gross change as compared to wild type. However, GRASP55^{S189D} did show a torsional twist in the ligand sequence that results in a 6.6A shift of Y198 side chain atoms (Fig 4-1 E). This is

exciting because this conformational difference could easily interfere with oligomerization of GRASP65.

We propose a two-step model for PLK1 mediated regulation of GRASP65. The first step involves phosphorylation of GRASP65 to generate the PLK1 docking site. The second step involves PLK1 mediated phosphorylation that inhibits tethering. It has been shown previously that mitotic kinases can generate a PLK1 docking site on GRASP65 (Preisinger et al 2005). However, we present data showing that phosphorylation of GRASP65 is required for late G2 unlinking. It is not known whether PLK1 binds and phosphorylates GRASP65 at G2. Interaction analyses of PLK1 and GRASP65 in G2 arrested cells could provide an answer. Another approach would be to develop an anti-phospho GRASP65 antibody recognizing phospho-S189 and determine exactly when in the cell cycle the site becomes phosphorylated.

In summary, in this thesis we have presented a novel mechanism for organelle tethering mediated by PDZ domain dependent homo-oligomerization and regulated by mitotic phosphorylation. These results assign a new function to PDZ-ligand interactions. Thus, our work not only increases understanding of cisternal linking and Golgi ribbon formation, it also suggests that other membrane tethering reactions might be mediated by yet to be identified PDZ domain containing proteins.

REFERENCES

Acharya, U., Jacobs, R., Peters, J.M., Watson, N., Farquhar, M.G., and Malhotra, V. 1995. The formation of Golgi stacks from vesiculated Golgi membranes requires two distinct fusion events. Cell *82*, 895-904

Acharya, U., A. Mallabiabarrena, J.K. Acharya, and V. Malhotra. 1998. Signaling via mitogen-activated protein kinase kinase (MEK1) is required for Golgi fragmentation during mitosis. *Cell*. 92:183-92

Aridor M, Bannykh SI, Rowe T, Balch WE. 1999. Cargo can modulate COPII vesicle formation from the endoplasmic reticulum. *J Biol Chem* 274: 4389-99

Aridor M, Guzik AK, Bielli A, Fish KN. 2004. Endoplasmic reticulum export site formation and function in dendrites. *J Neurosci* 24: 3770-6

Audhya A, Foti M, Emr SD. 2000. Distinct roles for the yeast phosphatidylinositol 4-kinases, Stt4p and Pik1p, in secretion, cell growth, and organelle membrane dynamics. *Mol Biol Cell* 11: 2673-89

Bachert C, Linstedt AD. 2010. Dual anchoring of the GRASP membrane tether promotes trans pairing. *J Biol Chem* 285:16294-301

Bard F, Malhotra V. 2006. The formation of TGN-to-plasma-membrane transport carriers. *Annu Rev Cell Dev Biol* 22: 439-55

Bard F, Mazelin L, Pechoux-Longin C, Malhotra V, Jurdic P. 2003. Src regulates Golgi structure and KDEL receptor-dependent retrograde transport to the endoplasmic reticulum. *J Biol Chem* 278: 46601-6

Baron CL, Malhotra V. 2002. Role of diacylglycerol in PKD recruitment to the TGN and protein transport to the plasma membrane. *Science* 295: 325-8

Barr FA, Puype M, Vandekerckhove J, Warren G. 1997. GRASP65, a protein involved in the stacking of Golgi cisternae. *Cell* 91: 253-62

Barr, F.A., N. Nakamura, and G. Warren. 1998. Mapping the interaction between GRASP65 and GM130, components of a protein complex involved in the stacking of Golgi cisternae. *Embo J*. 17:3258-68

Barr, F.A., Sillje, H.H., and Nigg, E.A. 2004. Polo-like kinases and the orchestration of cell division. *Nat Rev Mol Cell Biol 5*, 429-440

Barresi R, Campbell KP. 2006. Dystroglycan: from biosynthesis to pathogenesis of human disease. *J Cell Sci* 119: 199-207

Beck R, Adolf F, Weimer C, Bruegger B, Wieland FT. 2009. ArfGAP1 activity and COPI vesicle biogenesis. *Traffic* 10: 307-15

Becker B, Melkonian M. 1996. The secretory pathway of protists: spatial and functional organization and evolution. *Microbiol Rev* 60: 697-721

Behnia R, Barr FA, Flanagan JJ, Barlowe C, Munro S. 2007. The yeast orthologue of GRASP65 forms a complex with a coiled-coil protein that contributes to ER to Golgi traffic. *J Cell Biol* 176: 255-61

Bevis BJ, Hammond AT, Reinke CA, Glick BS. 2002. De novo formation of transitional ER sites and Golgi structures in Pichia pastoris. *Nat Cell Biol* 4: 750-6

Birrane, G., Chung, J., and Ladias, J.A. 2003. Novel mode of ligand recognition by the Erbin PDZ domain. *J Biol Chem 278*, 1399-1402

Bisel B, Wang Y, Wei JH, Xiang Y, Tang D, et al. 2008. ERK regulates Golgi and centrosome orientation towards the leading edge through GRASP65. *J Cell Biol* 182: 837-43

Bonifacino JS, Rojas R. 2006. Retrograde transport from endosomes to the trans-Golgi network. *Nat Rev Mol Cell Biol* 7: 568-79

Brenman, J.E., K.S. Christopherson, S.E. Craven, A.W. McGee, and D.S. Bredt. 1996. Cloning and characterization of postsynaptic density 93, a nitric oxide synthase interacting protein. *J Neurosci*. 16:7407-15.

Buckhaults P, Chen L, Fregien N, Pierce M. 1997. Transcriptional regulation of N-acetylglucosaminyltransferase V by the src oncogene. *J Biol Chem* 272: 19575-81

Burman JL, Hamlin JN, McPherson PS. 2010. Scyl1 regulates Golgi morphology. *PLoS One* 5: e9537

Chen, B.S., Braud, S., Badger, J.D., 2nd, Isaac, J.T., and Roche, K.W. 2006. Regulation of NR1/NR2C N-methyl-D-aspartate (NMDA) receptors by phosphorylation. *J Biol Chem 281*, 16583-16590

Chen CY, Ingram MF, Rosal PH, Graham TR. 1999. Role for Drs2p, a P-type ATPase and potential aminophospholipid translocase, in yeast late Golgi function. *J Cell Biol* 147: 1223-36

Chen, H., and D.C. Chan. 2005. Emerging functions of mammalian mitochondrial fusion and fission. *Hum Mol Genet*. 14 Spec No. 2:R283-9.

Chen, H., S.A. Detmer, A.J. Ewald, E.E. Griffin, S.E. Fraser, and D.C. Chan. 2003. Mitofusins Mfn1 and Mfn2 coordinately regulate mitochondrial fusion and are essential for embryonic development. *J Cell Biol*. 160:189-200.

Chisari M, Saini DK, Kalyanaraman V, Gautam N. 2007. Shuttling of G protein subunits between the plasma membrane and intracellular membranes. *J Biol Chem* 282: 24092-8

Christopherson, K.S., B.J. Hillier, W.A. Lim, and D.S. Bredt. 1999. PSD-95 assembles a ternary complex with the N-methyl-D-aspartic acid receptor and a bivalent neuronal NO synthase PDZ domain. *J Biol Chem*. 274:27467-73.

Clermont Y, Rambourg A, Hermo L. 1995. Trans-Golgi network (TGN) of different cell types: three-dimensional structural characteristics and variability. *Anat Rec* 242: 289-301

Clermont Y, Xia L, Rambourg A, Turner JD, Hermo L. 1993. Structure of the Golgi apparatus in stimulated and nonstimulated acinar cells of mammary glands of the rat. *Anat Rec* 237: 308-17

Cluett EB, Brown WJ. 1992. Adhesion of Golgi cisternae by proteinaceous interactions: intercisternal bridges as putative adhesive structures. *J Cell Sci* 103 (Pt 3): 773-84

Colanzi A, Hidalgo Carcedo C, Persico A, Cericola C, Turacchio G, et al. 2007. The Golgi mitotic checkpoint is controlled by BARS-dependent fission of the Golgi ribbon into separate stacks in G2. *Embo J* 26: 2465-76

Colanzi, A., and D. Corda. 2007. Mitosis controls the Golgi and the Golgi controls mitosis. *Curr Opin Cell Biol*. 19:386-93.

Comelli EM, Head SR, Gilmartin T, Whisenant T, Haslam SM, et al. 2006. A focused microarray approach to functional glycomics: transcriptional regulation of the glycome. *Glycobiology* 16: 117-31

Connerly PL, Esaki M, Montegna EA, Strongin DE, Levi S, et al. 2005. Sec16 is a determinant of transitional ER organization. *Curr Biol* 15: 1439-47

Corda D, Colanzi A, Luini A. 2006. The multiple activities of CtBP/BARS proteins: the Golgi view. *Trends Cell Biol* 16: 167-73

Corthesy-Theulaz I, Pauloin A, Pfeffer SR. 1992. Cytoplasmic dynein participates in the centrosomal localization of the Golgi complex. *J Cell Biol* 118: 1333-45

D'Angelo G, Prencipe L, Iodice L, Beznoussenko G, Savarese M, et al. 2009. GRASP65 and GRASP55 sequentially promote the transport of C-terminal valine-bearing cargos to and through the Golgi complex. *J Biol Chem* 284: 34849-60

de Figueiredo P, Drecktrah D, Katzenellenbogen JA, Strang M, Brown WJ. 1998. Evidence that phospholipase A2 activity is required for Golgi complex and trans Golgi network membrane tubulation. *Proc Natl Acad Sci U S A* 95: 8642-7

de Graffenried CL, Bertozzi CR. 2004. The roles of enzyme localisation and complex formation in glycan assembly within the Golgi apparatus. *Curr Opin Cell Biol* 16: 356-63

De Matteis MA, Luini A. 2008. Exiting the Golgi complex. *Nat Rev Mol Cell Biol* 9: 273-84

Derganc J, Mironov AA, Svetina S. 2006. Physical factors that affect the number and size of Golgi cisternae. *Traffic* 7: 85-96

Diaz Anel AM, Malhotra V. 2005. PKCeta is required for beta1gamma2/beta3gamma2- and PKD-mediated transport to the cell surface and the organization of the Golgi apparatus. *J Cell Biol* 169: 83-91

Diao, A., L. Frost, Y. Morohashi, and M. Lowe. 2008. Coordination of golgin tethering and SNARE assembly: GM130 binds syntaxin 5 in a p115-regulated manner. *J Biol Chem*. 283:6957-67.

Dippold HC, Ng MM, Farber-Katz SE, Lee SK, Kerr ML, et al. 2009. GOLPH3 bridges phosphatidylinositol-4- phosphate and actomyosin to stretch and shape the Golgi to promote budding. *Cell* 139: 337-51

Drenan RM, Liu X, Bertram PG, Zheng XF. 2004. FKBP12-rapamycin-associated protein or mammalian target of rapamycin (FRAP/mTOR) localization in the endoplasmic reticulum and the Golgi apparatus. *J Biol Chem* 279: 772-8

Doyle, D.A., A. Lee, J. Lewis, E. Kim, M. Sheng, and R. MacKinnon. 1996. Crystal structures of a complexed and peptide-free membrane protein-binding domain: molecular basis of peptide recognition by PDZ. *Cell*. 85:1067-76

Duran, J.M., Kinseth, M., Bossard, C., Rose, D.W., Polishchuk, R., Wu, C.C., Yates, J., Zimmerman, T., and Malhotra, V. 2008. The role of GRASP55 in Golgi fragmentation and entry of cells into mitosis. *Mol Biol Cell 19*, 2579-2587

Duronio, R.J., E. Jackson-Machelski, R.O. Heuckeroth, P.O. Olins, C.S. Devine, W. Yonemoto, L.W. Slice, S.S. Taylor, and J.I. Gordon. 1990. Protein N-myristoylation in Escherichia

coli: reconstitution of a eukaryotic protein modification in bacteria. *Proc Natl Acad Sci U S A*. 87:1506-10.

Egea G, Lazaro-Dieguez F, Vilella M. 2006. Actin dynamics at the Golgi complex in mammalian cells. *Curr Opin Cell Biol* 18: 168-78

Elia, A.E., Cantley, L.C., and Yaffe, M.B. 2003. Proteomic screen finds pSer/pThr-binding domain localizing Plk1 to mitotic substrates. *Science 299*, 1228-1231

Fan, J.S., and M. Zhang. 2002. Signaling complex organization by PDZ domain proteins. *Neurosignals*. 11:315-21.

Farhan H, Weiss M, Tani K, Kaufman RJ, Hauri HP. 2008. Adaptation of endoplasmic reticulum exit sites to acute and chronic increases in cargo load. *Embo J* 27: 2043-54

Farhan H, Wendeler MW, Mitrovic S, Fava E, Silberberg Y, et al. MAPK signaling to the early secretory pathway revealed by kinase/phosphatase functional screening. *J Cell Biol* 189: 997-1011

Feinstein TN, Linstedt AD. 2007. Mitogen-activated protein kinase kinase 1-dependent Golgi unlinking occurs in G2 phase and promotes the G2/M cell cycle transition. *Mol Biol Cell* 18: 594-604

Feinstein TN, Linstedt AD. 2008. GRASP55 regulates Golgi ribbon formation. *Mol Biol Cell* 19: 2696-707

Folsch H, Mattila PE, Weisz OA. 2009. Taking the scenic route: biosynthetic traffic to the plasma membrane in polarized epithelial cells. *Traffic* 10: 972-81

Forstner G. 1995. Signal transduction, packaging and secretion of mucins. *Annu Rev Physiol* 57: 585-605

Gardiol A, Racca C, Triller A. 1999. Dendritic and postsynaptic protein synthetic machinery. *J Neurosci* 19: 168-79

Gauthier NC, Rossier OM, Mathur A, Hone JC, Sheetz MP. 2009. Plasma membrane area increases with spread area by exocytosis of a GPI-anchored protein compartment. *Mol Biol Cell* 20: 3261-72

Gee, S.H., S.A. Sekely, C. Lombardo, A. Kurakin, S.C. Froehner, and B.K. Kay. 1998. Cyclic peptides as non-carboxyl-terminal ligands of syntrophin PDZ domains. *J Biol Chem* 273:21980-7

Gill DJ, Chia J, Senewiratne J, Bard F. Regulation of O-glycosylation through Golgi-to-ER relocation of initiation enzymes. *J Cell Biol* 189: 843-58

Giraudo CG, Maccioni HJ. 2003. Endoplasmic reticulum export of glycosyltransferases depends on interaction of a cytoplasmic dibasic motif with Sar1. *Mol Biol Cell* 14: 3753-66

Godi A, Di Campli A, Konstantakopoulos A, Di Tullio G, Alessi DR, et al. 2004. FAPPs control Golgi-to-cell-surface membrane traffic by binding to ARF and PtdIns(4)P. *Nat Cell Biol* 6: 393-404

Golsteyn, R.M., Schultz, S.J., Bartek, J., Ziemiecki, A., Ried, T., and Nigg, E.A. (1994). Cell cycle analysis and chromosomal localization of human Plk1, a putative homologue of the mitotic kinases Drosophila polo and Saccharomyces cerevisiae Cdc5. *J Cell Sci 107 (Pt 6)*, 1509-17

Goodwin JS, Drake KR, Rogers C, Wright L, Lippincott-Schwartz J, et al. 2005. Depalmitoylated Ras traffics to and from the Golgi complex via a nonvesicular pathway. *J Cell Biol* 170: 261-72

Gough LL, Fan J, Chu S, Winnick S, Beck KA. 2003. Golgi localization of Syne-1. *Mol Biol Cell* 14: 2410-24

Graham TR, Kozlov MM. Interplay of proteins and lipids in generating membrane curvature. *Curr Opin Cell Biol* 22: 430-6

Griffiths G, Fuller SD, Back R, Hollinshead M, Pfeiffer S, Simons K. 1989. The dynamic nature of the Golgi complex. *J Cell Biol* 108: 277-97

Griffiths G, Pfeiffer S, Simons K, Matlin K. 1985. Exit of newly synthesized membrane proteins from the trans cisterna of the Golgi complex to the plasma membrane. *J Cell Biol* 101: 949-64

Guo HB, Jiang AL, Ju TZ, Chen HL. 2000. Opposing changes in N-acetylglucosaminyltransferase-V and -III during the cell cycle and all-trans retinoic acid treatment of hepatocarcinoma cell line. *Biochim Biophys Acta* 1495: 297-307

Guo Y, Linstedt AD. 2006. COPII-Golgi protein interactions regulate COPII coat assembly and Golgi size. *J Cell Biol* 174: 53-63

Hama H, Schnieders EA, Thorner J, Takemoto JY, DeWald DB. 1999. Direct involvement of phosphatidylinositol 4-phosphate in secretion in the yeast Saccharomyces cerevisiae. *J Biol Chem* 274: 34294-300

Hammond AT, Glick BS. 2000. Dynamics of transitional endoplasmic reticulum sites in vertebrate cells. *Mol Biol Cell* 11: 3013-30

Harris, B.Z., B.J. Hillier, and W.A. Lim. 2001. Energetic determinants of internal motif recognition by PDZ domains. *Biochemistry*. 40:5921-30.

Harris, B.Z., and W.A. Lim. 2001. Mechanism and role of PDZ domains in signaling complex assembly. *J Cell Sci*. 114:3219-31.

Hassinen A, Rivinoja A, Kauppila A, Kellokumpu S. Golgi N-glycosyltransferases form both homo- and heterodimeric enzyme complexes in live cells. *J Biol Chem* 285: 17771-7

Hausser A, Link G, Hoene M, Russo C, Selchow O, Pfizenmaier K. 2006. Phospho-specific binding of 14-3-3 proteins to phosphatidylinositol 4-kinase III beta protects from dephosphorylation and stabilizes lipid kinase activity. *J Cell Sci* 119: 3613-21

Hausser A, Storz P, Martens S, Link G, Toker A, Pfizenmaier K. 2005. Protein kinase D regulates vesicular transport by phosphorylating and activating phosphatidylinositol-4 kinase IIIbeta at the Golgi complex. *Nat Cell Biol* 7: 880-6

Hayes GL, Brown FC, Haas AK, Nottingham RM, Barr FA, Pfeffer SR. 2009. Multiple Rab GTPase binding sites in GCC185 suggest a model for vesicle tethering at the trans-Golgi. *Mol Biol Cell* 20: 209-17

Hidalgo Carcedo C, Bonazzi M, Spano S, Turacchio G, Colanzi A, et al. 2004. Mitotic Golgi partitioning is driven by the membrane-fissioning protein CtBP3/BARS. *Science* 305: 93-6

Hillier, B.J., Christopherson, K.S., Prehoda, K.E., Bredt, D.S., and Lim, W.A. (1999). Unexpected modes of PDZ domain scaffolding revealed by structure of nNOS-syntrophin complex. *Science 284*, 812-815

Holm L, Sander C. 1995. Dali: a network tool for protein structure comparison. *Trends Biochem Sci* 20: 478-80

Hoogenraad, C.C., P. Wulf, N. Schiefermeier, T. Stepanova, N. Galjart, J.V. Small, F. Grosveld, C.I. de Zeeuw, and A. Akhmanova. 2003. Bicaudal D induces selective dynein-mediated microtubule minus end-directed transport. *Embo J*. 22:6004-15.

Horton AC, Ehlers MD. 2003. Dual modes of endoplasmic reticulum-to-Golgi transport in dendrites revealed by live-cell imaging. *J Neurosci* 23: 6188-99

Horton AC, Racz B, Monson EE, Lin AL, Weinberg RJ, Ehlers MD. 2005. Polarized secretory trafficking directs cargo for asymmetric dendrite growth and morphogenesis. *Neuron* 48: 757-71

Hua Z, Fatheddin P, Graham TR. 2002. An essential subfamily of Drs2p-related P-type ATPases is required for protein trafficking between Golgi complex and endosomal/vacuolar system. *Mol Biol Cell* 13: 3162-77

Hung, A.Y., and M. Sheng. 2002. PDZ domains: structural modules for protein complex assembly. *J Biol Chem*. 277:5699-702.

Im, Y.J., J.H. Lee, S.H. Park, S.J. Park, S.H. Rho, G.B. Kang, E. Kim, and S.H. Eom. 2003a. Crystal structure of the Shank PDZ-ligand complex reveals a class I PDZ interaction and a novel PDZ-PDZ dimerization. *J Biol Chem*. 278:48099-104.

Im, Y.J., S.H. Park, S.H. Rho, J.H. Lee, G.B. Kang, M. Sheng, E. Kim, and S.H. Eom. 2003b. Crystal structure of GRIP1 PDZ6-peptide complex reveals the structural basis for class II PDZ target recognition and PDZ domain-mediated multimerization. *J Biol Chem*. 278:8501-7.

Ivan V, de Voer G, Xanthakis D, Spoorendonk KM, Kondylis V, Rabouille C. 2008. Drosophila Sec16 mediates the biogenesis of tER sites upstream of Sar1 through an arginine-rich motif. *Mol Biol Cell* 19: 4352-65

Jackowski S. 1994. Coordination of membrane phospholipid synthesis with the cell cycle. *J Biol Chem* 269: 3858-67

Jamieson JD, Palade GE. 1971. Synthesis, intracellular transport, and discharge of secretory proteins in stimulated pancreatic exocrine cells. *J Cell Biol* 50: 135-58

Jesch, S.A., and A.D. Linstedt. 1998. The Golgi and endoplasmic reticulum remain independent during mitosis in HeLa cells. *Mol Biol Cell*. 9:623-35.

Jesch, S.A., Lewis, T.S., Ahn, N.G., and Linstedt, A.D. 2001a. Mitotic phosphorylation of Golgi reassembly stacking protein 55 by mitogen-activated protein kinase ERK2. *Mol Biol Cell 12*, 1811-1817

Jesch SA, Mehta AJ, Velliste M, Murphy RF, Linstedt AD. 2001b. Mitotic Golgi is in a dynamic equilibrium between clustered and free vesicles independent of the ER. *Traffic* 2: 873-84

Jeyifous O, Waites CL, Specht CG, Fujisawa S, Schubert M, et al. 2009. SAP97 and CASK mediate sorting of NMDA receptors through a previously unknown secretory pathway. *Nat Neurosci* 12: 1011-9

Kanaji, S., J. Iwahashi, Y. Kida, M. Sakaguchi, and K. Mihara. 2000. Characterization of the signal that directs Tom20 to the mitochondrial outer membrane. *J Cell Biol*. 151:277-88.

Kang, B.S., D.R. Cooper, Y. Devedjiev, U. Derewenda, and Z.S. Derewenda. 2003. Molecular roots of degenerate specificity in syntenin's PDZ2 domain: reassessment of the PDZ recognition paradigm. *Structure*. 11:845-53.

Kano, F., Takenaka, K., Yamamoto, A., Nagayama, K., Nishida, E., and Murata, M. 2000. MEK and Cdc2 kinase are sequentially required for Golgi disassembly in MDCK cells by the mitotic Xenopus extracts. *J Cell Biol 149*, 357-368

Kasai H, Fukuda M, Watanabe S, Hayashi-Takagi A, Noguchi J. Structural dynamics of dendritic spines in memory and cognition. *Trends Neurosci* 33: 121-9

Keller P, Simons K. 1997. Post-Golgi biosynthetic trafficking. *J Cell Sci* 110 (Pt 24): 3001-9

Kellokumpu S, Sormunen R, Kellokumpu I. 2002. Abnormal glycosylation and altered Golgi structure in colorectal cancer: dependence on intra-Golgi pH. *FEBS Lett* 516: 217-24

Kinseth MA, Anjard C, Fuller D, Guizzunti G, Loomis WF, Malhotra V. 2007. The Golgi-associated protein GRASP is required for unconventional protein secretion during development. *Cell* 130: 524-34

Kirk SJ, Cliff JM, Thomas JA, Ward TH. Biogenesis of secretory organelles during B cell differentiation. *J Leukoc Biol* 87: 245-55

Kobayashi Y, Katanosaka Y, Iwata Y, Matsuoka M, Shigekawa M, Wakabayashi S. 2006. Identification and characterization of GSRP-56, a novel Golgi-localized spectrin repeat-containing protein. *Exp Cell Res* 312: 3152-64

Kodani, A., and C. Sutterlin. 2008. The Golgi Protein GM130 Regulates Centrosome Morphology and Function. *Mol Biol Cell*. 19:745-53.

Kondylis V, Spoorendonk KM, Rabouille C. 2005. dGRASP localization and function in the early exocytic pathway in Drosophila S2 cells. *Mol Biol Cell* 16: 4061-72

Kondylis V, van Nispen tot Pannerden HE, Herpers B, Friggi-Grelin F, Rabouille C. 2007. The golgi comprises a paired stack that is separated at G2 by modulation of the actin cytoskeleton through Abi and Scar/WAVE. *Dev Cell* 12: 901-15

Koshiba, T., S.A. Detmer, J.T. Kaiser, H. Chen, J.M. McCaffery, and D.C. Chan. 2004. Structural basis of mitochondrial tethering by mitofusin complexes. *Science*. 305:858-62

Kronebusch PJ, Singer SJ. 1987. The microtubule-organizing complex and the Golgi apparatus are co-localized around the entire nuclear envelope of interphase cardiac myocytes. *J Cell Sci* 88 (Pt 1): 25-34

Kuo, A., C. Zhong, W.S. Lane, and R. Derynck. 2000. Transmembrane transforming growth factor-alpha tethers to the PDZ domain-containing, Golgi membrane-associated protein p59/GRASP55. *Embo J*. 19:6427-39.

Ladinsky MS, Mastronarde DN, McIntosh JR, Howell KE, Staehelin LA. 1999. Golgi structure in three dimensions: functional insights from the normal rat kidney cell. *J Cell Biol* 144: 1135-49

Lee MC, Miller EA, Goldberg J, Orci L, Schekman R. 2004. Bi-directional protein transport between the ER and Golgi. *Annu Rev Cell Dev Biol* 20: 87-123

Lee SY, Yang JS, Hong W, Premont RT, Hsu VW. 2005. ARFGAP1 plays a central role in coupling COPI cargo sorting with vesicle formation. *J Cell Biol* 168: 281-90

Legros, F., A. Lombes, P. Frachon, and M. Rojo. 2002. Mitochondrial fusion in human cells is efficient, requires the inner membrane potential, and is mediated by mitofusins. *Mol Biol Cell*. 13:4343-54.

Lenoir G, Williamson P, Holthuis JC. 2007. On the origin of lipid asymmetry: the flip side of ion transport. *Curr Opin Chem Biol* 11: 654-61

Levi SK, Bhattacharyya D, Strack RL, Austin Ii JR, Glick BS. The Yeast GRASP Grh1 Colocalizes with COPII and Is Dispensable for Organizing the Secretory Pathway. *Traffic*

Li J, Shworak NW, Simons M. 2002. Increased responsiveness of hypoxic endothelial cells to FGF2 is mediated by HIF-1alpha-dependent regulation of enzymes involved in synthesis of heparan sulfate FGF2-binding sites. *J Cell Sci* 115: 1951-9

Liljedahl M, Maeda Y, Colanzi A, Ayala I, Van Lint J, Malhotra V. 2001. Protein kinase D regulates the fission of cell surface destined transport carriers from the trans-Golgi network. *Cell* 104: 409-20

Lillie JH, Han SS. 1973. Secretory protein synthesis in the stimulated rat parotid gland. Temporal dissociation of the maximal response from secretion. *J Cell Biol* 59: 708-21

Lin, C.Y., Madsen, M.L., Yarm, F.R., Jang, Y.J., Liu, X., and Erikson, R.L. 2000. Peripheral Golgi protein GRASP65 is a target of mitotic polo-like kinase (Plk) and Cdc2. *Proc Natl Acad Sci U S A 97*, 12589-12594

Linstedt, A.D., and H.P. Hauri. 1993. Giantin, a novel conserved Golgi membrane protein containing a cytoplasmic domain of at least 350 kDa. *Mol Biol Cell*. 4:679-93.

Linstedt, A.D., Jesch, S.A., Mehta, A., Lee, T.H., Garcia-Mata, R., Nelson, D.S., and Sztul, E. (2000). Binding relationships of membrane tethering components. The giantin N terminus and the GM130 N terminus compete for binding to the p115 C terminus. J Biol Chem *275*, 10196-10201

Liu X, Zheng XF. 2007. Endoplasmic reticulum and Golgi localization sequences for mammalian target of rapamycin. *Mol Biol Cell* 18: 1073-82

Lowery, D.M., Lim, D., and Yaffe, M.B. 2005. Structure and function of Polo-like kinases. *Oncogene 24*, 248-259

Lu Z, Joseph D, Bugnard E, Zaal KJ, Ralston E. 2001. Golgi complex reorganization during muscle differentiation: visualization in living cells and mechanism. *Mol Biol Cell* 12: 795-808

Lucocq JM, Warren G. 1987. Fragmentation and partitioning of the Golgi apparatus during mitosis in HeLa cells. *Embo J* 6: 3239-46

Lucocq, J.M., Berger, E.G., and Warren, G. 1989. Mitotic Golgi fragments in HeLa cells and their role in the reassembly pathway. *J Cell Biol 109*, 463-74

Lundmark R, Doherty GJ, Vallis Y, Peter BJ, McMahon HT. 2008. Arf family GTP loading is activated by, and generates, positive membrane curvature. *Biochem J* 414: 189-94

Macurek, L., Lindqvist, A., Lim, D., Lampson, M.A., Klompmaker, R., Freire, R., Clouin, C., Taylor, S.S., Yaffe, M.B., and Medema, R.H. 2008. Polo-like kinase-1 is activated by aurora A to promote checkpoint recovery. *Nature 455*, 119-23

Maeda Y, Kinoshita T. 2008. Dolichol-phosphate mannose synthase: structure, function and regulation. *Biochim Biophys Acta* 1780: 861-8

Mancias JD, Goldberg J. 2008. Structural basis of cargo membrane protein discrimination by the human COPII coat machinery. *Embo J* 27: 2918-28

Manjithaya, R., Anjard, C., Loomis, W.F., and Subramani, S. 2010. Unconventional secretion of Pichia pastoris Acb1 is dependent on GRASP protein, peroxisomal functions, and autophagosome formation. *J Cell Biol 188*, 537-46

Marfatia, S.M., O. Byron, G. Campbell, S.C. Liu, and A.H. Chishti. 2000. Human homologue of the Drosophila discs large tumor suppressor protein forms an oligomer in solution. Identification of the self-association site. *J Biol Chem*. 275:13759-70.

Marra P, Salvatore L, Mironov A, Jr., Di Campli A, Di Tullio G, et al. 2007. The biogenesis of the Golgi ribbon: the roles of membrane input from the ER and of GM130. *Mol Biol Cell* 18: 1595-608

Marra, P., T. Maffucci, T. Daniele, G.D. Tullio, Y. Ikehara, E.K. Chan, A. Luini, G. Beznoussenko, A. Mironov, and M.A. De Matteis. 2001. The GM130 and GRASP65 Golgi proteins cycle through and define a subdomain of the intermediate compartment. *Nat Cell Biol*. 3:1101-13.

Marra, P., L. Salvatore, A. Mironov, Jr., A. Di Campli, G. Di Tullio, A. Trucco, G. Beznoussenko, A. Mironov, and M.A. De Matteis. 2007. The biogenesis of the Golgi ribbon: the roles of membrane input from the ER and of GM130. *Mol Biol Cell*. 18:1595-608.

Marsh BJ, Volkmann N, McIntosh JR, Howell KE. 2004. Direct continuities between cisternae at different levels of the Golgi complex in glucose-stimulated mouse islet beta cells. *Proc Natl Acad Sci U S A* 101: 5565-70

Martens GA, Pipeleers D. 2009. Glucose, regulator of survival and phenotype of pancreatic beta cells. *Vitam Horm* 80: 507-39

Mellman I, Simons K. 1992. The Golgi complex: in vitro veritas? *Cell* 68: 829-40

Miller EA, Beilharz TH, Malkus PN, Lee MC, Hamamoto S, et al. 2003. Multiple cargo binding sites on the COPII subunit Sec24p ensure capture of diverse membrane proteins into transport vesicles. *Cell* 114: 497-509

Missiaen L, Dode L, Vanoevelen J, Raeymaekers L, Wuytack F. 2007. Calcium in the Golgi apparatus. *Cell Calcium* 41: 405-16

Misteli, T., and Warren, G. (1995). Mitotic disassembly of the Golgi apparatus in vivo. *J Cell Sci* 108 (Pt 7), 2715-2727

Mollenhauer HH. 1965. An Intercisternal Structure in the Golgi Apparatus. *J Cell Biol* 24: 504-11

Mollenhauer, H.H., and D.J. Morre. 1991. Perspectives on Golgi apparatus form and function. *J Electron Microsc Tech*. 17:2-14

Morikawa RK, Aoki J, Kano F, Murata M, Yamamoto A, et al. 2009. Intracellular phospholipase A1gamma (iPLA1gamma) is a novel factor involved in coat protein complex I- and Rab6-independent retrograde transport between the endoplasmic reticulum and the Golgi complex. *J Biol Chem* 284: 26620-30

Mossessova E, Bickford LC, Goldberg J. 2003. SNARE selectivity of the COPII coat. *Cell* 114: 483-95

Nakajima, H., Toyoshima-Morimoto, F., Taniguchi, E., and Nishida, E. 2003. Identification of a consensus motif for Plk (Polo-like kinase) phosphorylation reveals Myt1 as a Plk1 substrate. *J Biol Chem 278*, 25277-80

Natarajan P, Liu K, Patil DV, Sciorra VA, Jackson CL, Graham TR. 2009. Regulation of a Golgi flippase by phosphoinositides and an ArfGEF. *Nat Cell Biol* 11: 1421-6

Neuspiel, M., A.C. Schauss, E. Braschi, R. Zunino, P. Rippstein, R.A. Rachubinski, M.A. Andrade-Navarro, and H.M. McBride. 2008. Cargo-selected transport from the mitochondria to peroxisomes is mediated by vesicular carriers. *Curr Biol*. 18:102-8

Nickel W, Rabouille C. 2009. Mechanisms of regulated unconventional protein secretion. *Nat Rev Mol Cell Biol* 10: 148-55

Nilsson T, Hoe MH, Slusarewicz P, Rabouille C, Watson R, et al. 1994. Kin recognition between medial Golgi enzymes in HeLa cells. *Embo J* 13: 562-74

Noske AB, Costin AJ, Morgan GP, Marsh BJ. 2008. Expedited approaches to whole cell electron tomography and organelle mark-up in situ in high-pressure frozen pancreatic islets. *J Struct Biol* 161: 298-313

Novick P, Schekman R. 1979. Secretion and cell-surface growth are blocked in a temperature-sensitive mutant of Saccharomyces cerevisiae. *Proc Natl Acad Sci U S A* 76: 1858-62

Ohtsubo K, Marth JD. 2006. Glycosylation in cellular mechanisms of health and disease. *Cell* 126: 855-67

Oliver C, Hand AR. 1983. Enzyme modulation of the Golgi apparatus and GERL: a cytochemical study of parotid acinar cells. *J Histochem Cytochem* 31: 1041-8

Penkert, R.R., DiVittorio, H.M., and Prehoda, K.E. 2004. Internal recognition through PDZ domain plasticity in the Par-6-Pals1 complex. *Nat Struct Mol Biol 11*, 1122-7

Permutt MA, Kipnis DM. 1972. Insulin biosynthesis. I. On the mechanism of glucose stimulation. *J Biol Chem* 247: 1194-9

Pfeffer, S.R. 2007. Unsolved mysteries in membrane traffic. *Annu Rev Biochem*. 76:629-45

Pierce JP, Mayer T, McCarthy JB. 2001. Evidence for a satellite secretory pathway in neuronal dendritic spines. *Curr Biol* 11: 351-5

Pierce M, Buckhaults P, Chen L, Fregien N. 1997. Regulation of N-acetylglucosaminyltransferase V and Asn-linked oligosaccharide beta(1,6) branching by a growth factor signaling pathway and effects on cell adhesion and metastatic potential. *Glycoconj J* 14: 623-30

Pistor, S., T. Chakraborty, K. Niebuhr, E. Domann, and J. Wehland. 1994. The ActA protein of Listeria monocytogenes acts as a nucleator inducing reorganization of the actin cytoskeleton. *Embo J.* 13:758-63

Pouncey L, Easton J, Heath LS, Grenet J, Kidd VJ. 1991. Beta 1-4-galactosyltransferase gene expression is regulated during entry into the cell cycle and during the cell cycle. *Somat Cell Mol Genet* 17: 435-43

Pulvirenti T, Giannotta M, Capestrano M, Capitani M, Pisanu A, et al. 2008. A traffic-activated Golgi-based signalling circuit coordinates the secretory pathway. *Nat Cell Biol* 10: 912-22

Puthenveedu, M.A., and A.D. Linstedt. 2001. Evidence that Golgi structure depends on a p115 activity that is independent of the vesicle tether components giantin and GM130. *J Cell Biol*. 155:227-38.

Puthenveedu, M.A., and A.D. Linstedt. 2004. Gene replacement reveals that p115/SNARE interactions are essential for Golgi biogenesis. *Proc Natl Acad Sci U S A*. 101:1253-6.

Puthenveedu, M.A., and A.D. Linstedt. 2005. Subcompartmentalizing the Golgi apparatus. *Curr Opin Cell Biol*. 17:369-75

Puthenveedu MA, Bachert C, Puri S, Lanni F, Linstedt AD. 2006. GM130 and GRASP65-dependent lateral cisternal fusion allows uniform Golgi-enzyme distribution. *Nat Cell Biol* 8: 238-48

Rabouille, C., and Kondylis, V. 2007. Golgi ribbon unlinking: an organelle-based G2/M checkpoint. *Cell Cycle 6*, 2723-9

Ralston E. 1993. Changes in architecture of the Golgi complex and other subcellular organelles during myogenesis. *J Cell Biol* 120: 399-409

Ralston E, Ploug T, Kalhovde J, Lomo T. 2001. Golgi complex, endoplasmic reticulum exit sites, and microtubules in skeletal muscle fibers are organized by patterned activity. *J Neurosci* 21: 875-83

Rambourg A, Clermont Y. 1990. Three-dimensional electron microscopy: structure of the Golgi apparatus. *Eur J Cell Biol* 51: 189-200

Rambourg A, Clermont Y, Chretien M, Olivier L. 1993. Modulation of the Golgi apparatus in stimulated and nonstimulated prolactin cells of female rats. *Anat Rec* 235: 353-62

Rios, R.M., A. Sanchis, A.M. Tassin, C. Fedriani, and M. Bornens. 2004. GMAP-210 recruits gamma-tubulin complexes to cis-Golgi membranes and is required for Golgi ribbon formation. *Cell*. 118:323-35

Rocks O, Peyker A, Kahms M, Verveer PJ, Koerner C, et al. 2005. An acylation cycle regulates localization and activity of palmitoylated Ras isoforms. *Science* 307: 1746-52

Runyon, S.T., Zhang, Y., Appleton, B.A., Sazinsky, S.L., Wu, P., Pan, B., Wiesmann, C., Skelton, N.J., and Sidhu, S.S. (2007). Structural and functional analysis of the PDZ domains of human HtrA1 and HtrA3. *Protein Sci 16*, 2454-71

Saini DK, Chisari M, Gautam N. 2009. Shuttling and translocation of heterotrimeric G proteins and Ras. *Trends Pharmacol Sci* 30: 278-86

Saini DK, Kalyanaraman V, Chisari M, Gautam N. 2007. A family of G protein betagamma subunits translocate reversibly from the plasma membrane to endomembranes on receptor activation. *J Biol Chem* 282: 24099-108

Sallese M, Pulvirenti T, Luini A. 2006. The physiology of membrane transport and endomembrane-based signalling. *Embo J* 25: 2663-73

Sato I, Obata Y, Kasahara K, Nakayama Y, Fukumoto Y, et al. 2009. Differential trafficking of Src, Lyn, Yes and Fyn is specified by the state of palmitoylation in the SH4 domain. *J Cell Sci* 122: 965-75

Schmidt JA, Brown WJ. 2009. Lysophosphatidic acid acyltransferase 3 regulates Golgi complex structure and function. *J Cell Biol* 186: 211-8

Schotman, H., L. Karhinen, and C. Rabouille. 2008. dGRASP-Mediated Noncanonical Integrin Secretion Is Required for Drosophila Epithelial Remodeling. *Dev Cell*. 14:171-82

Schuck S, Simons K. 2004. Polarized sorting in epithelial cells: raft clustering and the biogenesis of the apical membrane. *J Cell Sci* 117: 5955-64

Seemann, J., E. Jokitalo, M. Pypaert, and G. Warren. 2000. Matrix proteins can generate the higher order architecture of the Golgi apparatus. *Nature*. 407:1022-6

Sengupta D, Linstedt AD. Mitotic inhibition of GRASP65 organelle tethering involves Polo-like kinase 1 (PLK1) phosphorylation proximate to an internal PDZ ligand. *J Biol Chem* 2010 Oct 11 ePub

Sengupta D, Truschel S, Bachert C, Linstedt AD. 2009. Organelle tethering by a homotypic PDZ interaction underlies formation of the Golgi membrane network. *J Cell Biol* 186: 41-55

Shaul, Y.D., and R. Seger. 2006. ERK1c regulates Golgi fragmentation during mitosis. *J Cell Biol*. 172:885-97

Shima DT, Haldar K, Pepperkok R, Watson R, Warren G. 1997. Partitioning of the Golgi apparatus during mitosis in living HeLa cells. *J Cell Biol* 137: 1211-28

Shima DT, Scales SJ, Kreis TE, Pepperkok R. 1999. Segregation of COPI-rich and anterograde-cargo-rich domains in endoplasmic-reticulum-to-Golgi transport complexes. *Curr Biol* 9: 821-4

Short, B., Preisinger, C., Korner, R., Kopajtich, R., Byron, O., and Barr, F.A. (2001). A GRASP55-rab2 effector complex linking Golgi structure to membrane traffic. *J Cell Biol 155*, 877-83

Shorter J, Warren G. 2002. Golgi architecture and inheritance. *Annu Rev Cell Dev Biol* 18: 379-420

Shorter J, Watson R, Giannakou ME, Clarke M, Warren G, Barr FA. 1999. GRASP55, a second mammalian GRASP protein involved in the stacking of Golgi cisternae in a cell-free system. *Embo J* 18: 4949-60

Silvestre DC, Maccioni HJ, Caputto BL. 2009. Content of endoplasmic reticulum and Golgi complex membranes positively correlates with the proliferative status of brain cells. *J Neurosci Res* 87: 857-65

Simons K, van Meer G. 1988. Lipid sorting in epithelial cells. *Biochemistry* 27: 6197-202

Sinka R, Gillingham AK, Kondylis V, Munro S. 2008. Golgi coiled-coil proteins contain multiple binding sites for Rab family G proteins. *J Cell Biol* 183: 607-15

Struck, N.S., S. Herrmann, C. Langer, A. Krueger, B.J. Foth, K. Engelberg, A.L. Cabrera, S. Haase, M. Treeck, M. Marti, A.F. Cowman, T. Spielmann, and T.W. Gilberger. 2008. Plasmodium falciparum possesses two GRASP proteins that are differentially targeted to the Golgi complex via a higher- and lower-eukaryote-like mechanism. *J Cell Sci*. 121:2123-9

Sutterlin, C., Lin, C.Y., Feng, Y., Ferris, D.K., Erikson, R.L., and Malhotra, V. (2001). Polo-like kinase is required for the fragmentation of pericentriolar Golgi stacks during mitosis. *Proc Natl Acad Sci U S A 98*, 9128-32

Sutterlin, C., Hsu, P., Mallabiabarrena, A., and Malhotra, V. 2002. Fragmentation and dispersal of the pericentriolar Golgi complex is required for entry into mitosis in mammalian cells. *Cell 109*, 359-69

Sutterlin, C., R. Polishchuk, M. Pecot, and V. Malhotra. 2005. The Golgi-associated Protein GRASP65 Regulates Spindle Dynamics and Is Essential for Cell Division. *Mol Biol Cell*. 16:3211-22

Tang, D., Yuan, H., and Wang, Y. (2010). The role of GRASP65 in Golgi cisternal stacking and cell cycle progression. *Traffic 11*, 827-42

Tanaka H, Takenaka H, Yamao F, Yagura T. 1998. Aphidicolin induces alterations in Golgi complex and disorganization of microtubules of HeLa cells upon long-term administration. *J Cell Physiol* 176: 602-11

Tassin AM, Paintrand M, Berger EG, Bornens M. 1985. The Golgi apparatus remains associated with microtubule organizing centers during myogenesis. *J Cell Biol* 101: 630-8

Thyberg J, Moskalewski S. 1999. Role of microtubules in the organization of the Golgi complex. *Exp Cell Res* 246: 263-79

Torre ER, Steward O. 1996. Protein synthesis within dendrites: glycosylation of newly synthesized proteins in dendrites of hippocampal neurons in culture. *J Neurosci* 16: 5967-78

Travers KJ, Patil CK, Wodicka L, Lockhart DJ, Weissman JS, Walter P. 2000. Functional and genomic analyses reveal an essential coordination between the unfolded protein response and ER-associated degradation. *Cell* 101: 249-58

Trucco A, Polishchuk RS, Martella O, Di Pentima A, Fusella A, et al. 2004. Secretory traffic triggers the formation of tubular continuities across Golgi sub-compartments. *Nat Cell Biol* 6: 1071-81

Tu L, Banfield DK. Localization of Golgi-resident glycosyltransferases. *Cell Mol Life Sci* 67: 29-41

Turner, D.L., and H. Weintraub. 1994. Expression of achaete-scute homolog 3 in Xenopus embryos converts ectodermal cells to a neural fate. *Genes Dev*. 8:1434-47

Van Halbeek H, Gerwig GJ, Vliegenthart JF, Smits HL, Van Kerkhof PJ, Kramer MF. 1983. Terminal alpha (1 leads to 4)-linked N-acetylglucosamine: a characteristic constituent of duodenal-gland mucous glycoproteins in rat and pig. A high-resolution 1H-NMR study. *Biochim Biophys Acta* 747: 107-16

Varki A. 1998. Factors controlling the glycosylation potential of the Golgi apparatus. *Trends Cell Biol* 8: 34-40

Voeltz, G.K., and W.A. Prinz. 2007. Sheets, ribbons and tubules - how organelles get their shape. *Nat Rev Mol Cell Biol*. 8:258-64

Waizenegger, T., T. Stan, W. Neupert, and D. Rapaport. 2003. Signal-anchor domains of proteins of the outer membrane of mitochondria: structural and functional characteristics. *J Biol Chem*. 278:42064-71

Walch-Solimena C, Novick P. 1999. The yeast phosphatidylinositol-4-OH kinase pik1 regulates secretion at the Golgi. *Nat Cell Biol* 1: 523-5

Wang H, Kouri G, Wollheim CB. 2005a. ER stress and SREBP-1 activation are implicated in beta-cell glucolipotoxicity. *J Cell Sci* 118: 3905-15

Wang Y, Satoh A, Warren G. 2005b. Mapping the functional domains of the Golgi stacking factor GRASP65. *J Biol Chem* 280: 4921-8

Wang, Y., J. Seemann, M. Pypaert, J. Shorter, and G. Warren. 2003. A direct role for GRASP65 as a mitotically regulated Golgi stacking factor. *Embo J*. 22:3279-90.

Wang YJ, Wang J, Sun HQ, Martinez M, Sun YX, et al. 2003. Phosphatidylinositol 4 phosphate regulates targeting of clathrin adaptor AP-1 complexes to the Golgi. *Cell* 114: 299-310

Ward, T.H., R.S. Polishchuk, S. Caplan, K. Hirschberg, and J. Lippincott-Schwartz. 2001. Maintenance of Golgi structure and function depends on the integrity of ER export. *J Cell Biol*. 155:557-70.

Watson P, Townley AK, Koka P, Palmer KJ, Stephens DJ. 2006. Sec16 defines endoplasmic reticulum exit sites and is required for secretory cargo export in mammalian cells. *Traffic* 7: 1678-87

Weisz OA, Rodriguez-Boulan E. 2009. Apical trafficking in epithelial cells: signals, clusters and motors. *J Cell Sci* 122: 4253-66

Wicky S, Schwarz H, Singer-Kruger B. 2004. Molecular interactions of yeast Neo1p, an essential member of the Drs2 family of aminophospholipid translocases, and its role in membrane trafficking within the endomembrane system. *Mol Cell Biol* 24: 7402-18

Xiang Y, Wang Y. 2010. GRASP55 and GRASP65 play complementary and essential roles in Golgi cisternal stacking. *J Cell Biol* 188: 237-51

Xu, X.Z., A. Choudhury, X. Li, and C. Montell. 1998. Coordination of an array of signaling proteins through homo- and heteromeric interactions between PDZ domains and target proteins. *J Cell Biol.* 142:545-55

Xu Y, Martin S, James DE, Hong W. 2002. GS15 forms a SNARE complex with syntaxin 5, GS28, and Ykt6 and is implicated in traffic in the early cisternae of the Golgi apparatus. *Mol Biol Cell* 13: 3493-507

Ye B, Zhang Y, Song W, Younger SH, Jan LY, Jan YN. 2007. Growing dendrites and axons differ in their reliance on the secretory pathway. *Cell* 130: 717-29

Yokoyama K, Suzuki M, Kawashima I, Karasawa K, Nojima S, et al. 1997. Changes in composition of newly synthesized sphingolipids of HeLa cells during the cell cycle -- suppression of sphingomyelin and higher-glycosphingolipid synthesis and accumulation of ceramide and glucosylceramide in mitotic cells. *Eur J Biochem* 249: 450-5

Yoshimura, S., K. Yoshioka, F.A. Barr, M. Lowe, K. Nakayama, S. Ohkuma, and N. Nakamura. 2005. Convergence of cell cycle regulation and growth factor signals on GRASP65. *J Biol Chem*. 280:23048-56

Yu RK, Bieberich E, Xia T, Zeng G. 2004. Regulation of ganglioside biosynthesis in the nervous system. *J Lipid Res* 45: 783-93

Zhang, Y., and J. Skolnick. 2004. Automated structure prediction of weakly homologous proteins on a genomic scale. *Proc Natl Acad Sci U S A*. 101:7594-9.